

# **The Influence of Specific Adenylyl Cyclase Isoform Expression on Antidepressant Response**

BY

JEFFREY SCHAPPI

B.S., University of Illinois at Urbana-Champaign, 1992

THESIS

Submitted as partial fulfillment of the requirements  
for the degree of Doctor of Philosophy in Physiology and Biophysics  
in the Graduate College of the  
University of Illinois at Chicago, 2017

Chicago, Illinois

Defense Committee:

Mrinalini Rao, Chair, Physiology and Biophysics  
Mark Rasenick, Advisor, Physiology and Biophysics  
Mark Brodie, Physiology and Biophysics  
Alessandro Guidotti, Psychiatry  
Sergey Popov, Physiology and Biophysics  
Aminah Pradhan, Psychiatry

## Acknowledgements

I would first like to thank my committee members, Drs. Rasenick, Rao, Brodie, Popov, Guidotti, and Pradhan, for their knowledge and advice through the years, but especially their patience.

Before returning to graduate school, I had been out of school for many years and the prospect of returning was daunting, to say the very least. I knew that I was interested in physiology, so I randomly picked a name off the department faculty list outside the physiology office and sought their advice. This was Dr. John Kennedy, whose support and advice got me back into school. To my great surprise and pleasure, the entire physiology faculty turned out to be cut from the same cloth and have been a pleasure to work with -- before starting, I had in my mind a fairly cold and sterile caricature of academia. I think I chose a very good department, and a great advisor, Mark Rasenick.

I have also met many great students, post docs, and staff. I would like to give a special thank you to all of my labmates through the years, whose company I appreciated daily for a multitude of reasons and with whom I am sharing quite a journey...Sia Koutsouris, Andrew Czysz, Harinder Singh, Nate Wray, Sam Erb, Tammy Tamayo, Natalie King, Aleks Krbanjevic, Bob Donati, Jiang-Zhou Yu, and Alex Jackson.

Finally, but not least, I would like to thank my mom and dad, David and Palmira Schappi, my aunt Dolly Malciauskas, and Jennifer Lurgio, Robert Lara III, and Mike Mancuso, who never wavered in their support. Thank you, everyone!

## Table of Contents

<b>CHAPTER 1: INTRODUCTION.....</b>	<b>1</b>
1.1 DEPRESSION .....	1
1.1.1 Introduction to depression.....	1
1.1.2 Treatment of depression .....	3
1.1.3 Methods to study depression.....	4
1.2 G PROTEINS AND SIGNALING THROUGH GPCRS .....	7
1.2.1 Heterotrimeric G proteins .....	7
1.2.2 G protein coupled receptors (GPCRs) .....	11
1.2.3 G proteins and depression .....	13
1.3 LIPID RAFTS .....	16
1.3.1 Lipid raft description.....	16
1.3.2 Study of lipid rafts.....	17
1.3.3 Lipid rafts and depression.....	18
1.4 CAMP SIGNALING .....	20
1.4.1 cAMP Overview.....	20
1.4.2 cAMP effectors .....	20
1.4.3 cAMP in depression.....	21
1.5 ADENYLYL CYCLASE.....	23
1.5.1 Adenylyl cyclase overview .....	23
1.5.2 Mammalian adenylyl cyclase structure and regulation.....	24
1.5.3 Adenylyl cyclase and mood disorders.....	28
1.6 MONOAMINE REUPTAKE TRANSPORTERS.....	31
1.6.1 Monoamine reuptake transporter structure and function .....	32
1.6.2 Monoamine reuptake transporter and mood disorders.....	34
1.7 ANTIDEPRESSANTS .....	35
1.7.1 Antidepressant history.....	35
1.7.2 Monoamine oxidase inhibitors .....	36
1.7.3 Tricyclic antidepressants and selective serotonin reuptake inhibitors.....	37
1.7.4 Selective membrane redistribution of $G_{\alpha_s}$ with antidepressant treatment.....	39
1.7.5 Membrane accumulation of antidepressants .....	40
1.7.6 HDAC6 inhibitors and ketamine as antidepressants .....	41
1.8 FLUORESCENCE RECOVERY AFTER PHOTBLEACHING (FRAP).....	43
1.8.1 FRAP background.....	43
1.8.2 Sample FRAP experiment and analysis.....	45
1.9 CELL LINES.....	50
1.9.1 C6 Glioma.....	50
1.9.2 HEK293.....	51
1.9.3 PC12 .....	52
1.9.4 COS7 .....	53
1.10 SPECIFIC AIMS.....	53
1.10.1 Aim 1: Identification and characterization of antidepressant responsive and nonresponsive cell lines.....	53
1.10.2 Aim2: Evaluate effect of SERT expression on antidepressant response of cell lines identified in Aim 1 .....	54
1.10.3 Aim 3: Evaluate effect of adenylyl cyclase isoform expression on antidepressant response of cell lines identified in Aim 1 .....	54
1.10.4 Aim 4: Development of an improved assay of antidepressant response via FRAP.....	54

<b>CHAPTER 2: MATERIALS AND METHODS.....</b>	<b>57</b>
2.1 CELL CULTURE AND DRUG TREATMENTS.....	57
2.2 EXPRESSION PLASMIDS .....	58
2.3 TRANSFECTION AND GENERATION OF STABLE/CLONAL CELL LINES.....	59
2.4 LIPID RAFT DENSITY GRADIENT PREPARATION .....	59
2.5 POLYACRYLAMIDE GEL ELECTROPHORESIS AND WESTERN BLOTTING .....	60
2.6 FLUORESCENCE RECOVERY AFTER PHOTOBLEACHING (FRAP).....	61
2.7 MEMBRANE ADENYLYL CYCLASE ACTIVITY ASSAY .....	66
2.8 CELL LINES: PROBLEMS AND SOLUTIONS.....	67
2.10 LIPID RAFT ANTIDEPRESSANT ACCUMULATION .....	69
2.10 STATISTICAL ANALYSIS .....	70
<b>CHAPTER 3: RESULTS .....</b>	<b>72</b>
3.1 IDENTIFICATION AND CHARACTERIZATION OF CELL LINES FOR FURTHER STUDY.....	72
3.1.1 <i>Membrane adenylyl cyclase assay results demonstrating effect on cAMP production in C6 glioma, PC12 pheochromocytoma, HEK293, and COS7 with antidepressant treatment.....</i>	<i>73</i>
3.1.2 <i>Characterization of altered lipid raft content of <math>G_{a_s}</math>, <math>G_{a_i}</math>, and <math>G_{a_q}</math> with antidepressant treatment in C6 glioma and HEK293. ....</i>	<i>81</i>
3.2 FRAP .....	86
3.2.1 <i>FRAP results of a variety of antidepressant and non-antidepressant drugs in C6 glioma ....</i>	<i>87</i>
3.2.2 <i>FRAP dose and time response with antidepressant treatment in C6 glioma .....</i>	<i>89</i>
3.2.3 <i>FRAP results of membrane disruption in C6 glioma with colchicine and methyl-<math>\beta</math>-cyclodextrin.....</i>	<i>91</i>
3.2.4 <i>FRAP results of GFP-<math>G_{a_i}</math> in C6 glioma contrasting antidepressant treatment and membrane disruption with colchicine and methyl-<math>\beta</math>-cyclodextrin .....</i>	<i>94</i>
3.2.5 <i>FRAP results in C6 glioma of fluorescent proteins of varied size and membrane anchoring</i>	<i>94</i>
3.2.6 <i>FRAP of GFP- <math>G_{a_s}</math> in C6 glioma demonstrating effect of ketamine and HDAC6 inhibitor tubastatin-A .....</i>	<i>98</i>
3.3 LACK OF SERT INFLUENCE IN ANTIDEPRESSANT RESPONSE.....	101
3.4 INFLUENCE OF ADENYLYL CYCLASE ISOFORM EXPRESSION ON ANTIDEPRESSANT RESPONSE .....	106
3.4.1 <i>NKY80 and calcium ion inhibition of adenylyl cyclase 5 and 6.....</i>	<i>106</i>
3.4.2 <i>Effect of adenylyl cyclase isoform expression on HEK293 antidepressant response.....</i>	<i>112</i>
3.4.3 <i>FRAP of fluorescent adenylyl cyclase isoforms in C6 glioma.....</i>	<i>118</i>
3.5 ACCUMULATION OF ANTIDEPRESSANTS IN LIPID RAFTS OF C6 GLIOMA AND HEK293 .....	120
<b>CHAPTER 4: DISCUSSION AND FUTURE DIRECTIONS .....</b>	<b>124</b>
<b>CHAPTER 5: CONCLUSION .....</b>	<b>139</b>
<b>WORKS CITED.....</b>	<b>143</b>
<b>VITA .....</b>	<b>157</b>
<b>COPYRIGHT .....</b>	<b>158</b>



## List of Tables and Figures

Table 1: Regulation and distribution of mammalian membrane adenylyl cyclase isoforms.....	22
Figure 1: G protein lipid anchors.....	10
Figure 2: G proteins and antidepressant effect.....	15
Figure 3: General structure of mammalian membrane adenylyl cyclase.....	27
Figure 4: C6 glioma stably expressing GFP-G $\alpha_s$ .....	48
Figure 5: General scheme of a FRAP experiment.....	49
Figure 6: Region of interest geometry and FRAP results.....	51
Figure 7: Setup of FRAP experiment.....	66
Figure 8: Production of cAMP in C6 glioma membranes.....	76
Figure 9: Production of cAMP in HEK293 membranes.....	79
Figure 10: Production of cAMP in PC12 membranes.....	80
Figure 11: Production of cAMP in COS7 membranes.....	82
Figure 12: Effects of escitalopram versus membrane disruptors upon lipid raft G protein content in C6 glioma and HEK293.....	86
Figure 13: Effect of membrane disruption on membrane cAMP production in C6 glioma and HEK293.....	87
Figure 14: FRAP results for a variety of antidepressant and non-antidepressant drugs in C6 glioma.....	90
Figure 15: Effects of different antidepressant doses on response of GFP-G $\alpha_s$ FRAP in C6 glioma .....	93
Figure 16: Effect of escitalopram treatment duration on GFP-G $\alpha_s$ FRAP in C6 glioma.....	95

Figure 17: Effect on FRAP of GFP- $G_{\alpha_s}$ in C6 glioma by membrane disruptors.....	96
Figure 18: Effect on FRAP of GFP- $G_{\alpha_i}$ in C6 glioma by antidepressants and membrane disruptors.....	98
Figure 19: Effect of size and membrane anchoring on FRAP of fluorescent proteins in C6 glioma.....	99
Figure 20: Dose and time dependence of response of GFP- $G_{\alpha_s}$ FRAP in C6 glioma....	102
Figure 21: GFP- $G_{\alpha_s}$ FRAP in C6 glioma comparing tubastatin-A and escitalopram....	103
Figure 22: Evaluation of hSERT expression on GFP- $G_{\alpha_s}$ FRAP in C6 glioma and HEK293.....	107
Figure 23: C6 glioma membrane cAMP production with AC5/6 inhibitors.....	111
Figure 24: HEK293 membrane cAMP production with AC5/6 inhibitor $Ca^{2+}$ .....	114
Figure 25: Effect of adenylyl cyclase isoform expression on FRAP of GFP- $G_{\alpha_s}$ in HEK293.....	117
Figure 26: Membrane expression of YFP-AC6 in C6 glioma.....	119
Figure 27: Effect of AC6 expression in HEK293 on antidepressant response.....	120
Figure 28: FRAP of varied fluorescent adenylyl cyclase isoforms in C6 glioma.....	122
Figure 29: Accumulation of antidepressant in lipid rafts of C6 glioma and HEK293..... .....	124
Figure 30: Reconceptualization of G protein antidepressant effect.....	134
Figure 31: Use of G protein acylation variants to evaluate the role of acylation in the antidepressant response.....	136
Figure 32: Cyclase specificity in the G protein antidepressant response. Why AC6?..... .....	139

## List of Abbreviations

A	Alanine
ANOVA	Analysis of variance
AC	Adenylyl cyclase
ADP	Adenine nucleotide diphosphate
AKAP	A-kinase anchoring protein
[AlF <sub>4</sub> ] <sup>-</sup>	Aluminum tetrafluoride anion
ATCC	American Type Culture Collection
ATP	Adenine nucleotide triphosphate
β <sub>2</sub>	Beta-2 adrenergic receptor
βγ	G protein betagamma subunit
BDNF	Brain derived neurotrophic factor
C6	C6 glioma cell line
cAMP	Cyclic adenosine monophosphate
cDNA	Complementary DNA
CFTR	Cystic fibrosis transmembrane conductance regulator
CHO	Chinese hamster ovary cell line
CNS	Central nervous system
COS7	COS7 cell line
CREB	cAMP response element binding protein
Da	Dalton
DAG	Diacylglycerol

DAT	Dopamine reuptake transporter
DBS	Deep brain stimulation
DMEM	Dulbecco's modified Eagle's medium
DNA	Deoxyribonucleic acid
DSM	Diagnostic and Statistical Manual of Mental Disorders
DTT	Dithiothreitol
ECT	Electroconvulsive therapy
EDTA	Ethylenediaminetetracetic acid
EGTA	Ethylene glycol-bis( $\beta$ -aminoethyl ether)-N,N,N',N'-tetraacetic acid
Epac	Exchange protein directly activated by cAMP
FACS	Fluorescence-activated cell sorting
FADS	Fatty acid desaturase
FRAP	Fluorescence recovery after photobleaching
FRET	Förster/fluorescent resonant energy transfer
G418	Geneticin
G $\alpha$	G protein alpha subunit
G $\alpha_s$	G protein alpha stimulatory subunit
G $\alpha_i$	G protein alpha inhibitory subunit
G $\alpha_q$	G protein alpha subunit activating PLC
GAP	GTPase activating protein
G $\beta\gamma$	G protein betagamma subunit
GC-MS	Gas Chromatography -Mass Spectrometry
GDNF	Glial cell derived neurotrophic factor

GDP	Guanine nucleotide diphosphate
GEF	Guanine exchange factors
GFAP	Glial fibrillary acidic protein
GFP	Green fluorescent protein
GPCR	G protein coupled receptor
GTP	Guanine nucleotide triphosphate
G $\gamma$	G protein gamma subunit
GWAS	Genome-wide association study
HEK293	Human embryonic kidney 293 cell line
HeLa	HeLa cell line
HEPES	4-(2-hydroxyethyl)-1-piperazineethanesulfonic acid
HRP	Horseradish peroxidase
5-HTTLPR	Serotonin transporter-linked polymorphic region
IBMX	3-isobutyl-1-methylxanthine
K	Lysine
kDa	Kilodalton
LeuT	Bacterial leucine transporter
M	Molar
mM	Milimolar
mAb	Monoclonal antibody
MAO	Monoamine oxidase
MAOI	Monoamine oxidase inhibitor
MAP	Microtubule-associated protein

M $\beta$ CD	Methyl- $\beta$ -cyclodextrin
MBCD	Methyl- $\beta$ -cyclodextrin
MDD	Major depressive disorder
MEM	Minimum essential medium
MgCl <sub>2</sub>	Magnesium chloride
NET	Norepinephrine reuptake transporter
NGF	Nerve growth factor
nM	Nanomolar
PBS	Phosphate buffered saline
PC12	Pheochromocytoma 12 cell line
PDE	Phosphodiesterase
PET	Positron emission tomography
PGE <sub>1</sub>	Prostaglandin E <sub>1</sub>
PGE <sub>2</sub>	Prostaglandin E <sub>2</sub>
PIP <sub>2</sub>	Phosphatidylinositol biphosphate
PKC	Protein kinase C
PLC	Phospholipase C
PPM	Parts per million
PTM	post-translational modifications
PVDF	Polyvinylidene fluoride
PKA	cAMP dependent protein kinase
PET	Positron emission tomography
RNA	Ribonucleic acid

RNA-seq	RNA sequencing
ROI	Region of interest
SCD1	Stearoyl-CoA desaturase-1
SEM	Standard error of the mean
SERT	Serotonin reuptake transporter
siRNA	Small interfering RNA
SLC	Sodium-dependent large solute carrier
SNRI	Selective norepinephrine reuptake inhibitor
SPR	Surface plasmon resonance
SSRI	Selective serotonin reuptake inhibitor
STAR*D	Sequenced Treatment Alternatives to Relieve Depression
TCA	Tricyclic antidepressant
TrkB	Tropomyosin receptor kinase B
TMS	Transcranial magnetic stimulation
TX-100	Triton X-100 detergent
TX-114	Triton X-114 detergent
$\mu$ M	Micromolar
wt	wild type

## Summary

Antidepressant drug development has stagnated and new targets are needed. The literature as a whole does not seem to widely consider the notion of antidepressant action in a way that is both non-canonical and significant or fundamental to the drug's mechanism.

Ostensibly, the major available drug classes act through targeting monoamine systems, but the monoamine hypothesis fails to explain many findings in depression and antidepressant effects: How, for example, do cells lacking reuptake transporters respond to antidepressants, and in a way that recapitulates the fundamental biochemical deviations seen in depression? Where are these drugs acting, and what factors determine one cell's response to antidepressant drugs vs. another cell's response?

A long-standing finding of the Rasenick laboratory describes an effect of antidepressant on G protein systems in vitro, in cell lines such as C6 glioma and PC12 pheochromocytoma, both neuroectodermal derivatives. These cell lines show a predictable response to a variety of commonly used antidepressant compounds and classes. However, not all cell lines, such as HEK293, show these responses. Specifically, the antidepressant-responsive cells show a redistribution of G protein  $G_{\alpha_s}$  from lipid raft to non-raft membrane fractions with increased functional coupling of  $G_{\alpha_s}$  and adenylyl cyclase, the reciprocal of changes observed in samples from depressed patients. This redistribution is not accompanied by a change in total membrane  $G_{\alpha_s}$  content. However,  $G_{\alpha_i}$  and  $G_{\alpha_q}$  are unaffected. Biochemically,



these changes are evidenced by increases in cAMP production compared to untreated controls, subsequent to stimulation with agonists of GPCR-mediated cAMP production. Yet, these cells do not express the serotonin reuptake transporter (SERT) or other monoamine reuptake transporters. It appears that the effect of antidepressants on G protein signaling is non-canonical and does not involve monoamine reuptake or other action at a reuptake transporter. The purpose of this study is to further examine contributors to this antidepressant response, with particular emphasis on cellular adenylyl cyclase isoform expression, to further understanding of antidepressants' mechanisms of action in the search for newer and better treatments.

## **Chapter 1: Introduction**

### **1.1 Depression**

#### **1.1.1 Introduction to depression**

Major depressive disorder (MDD -- henceforth referred to as depression), is a malady known since antiquity. The ancient Greeks considered depression to result from an excess of black bile, one of the four bodily humours, giving rise to the word melancholy (melan (black) + chol (bile)). Though many aspects of depression and antidepressant pharmacology have become better understood in the intervening years, no unifying hypothesis has emerged to explain the many disparate findings in the field.

Depression is commonly characterized by, but is not limited to, pervasive feelings of sadness or hopelessness. Lack of interest in pleasurable activities (anhedonia), sleep disturbances (both inability to sleep or increased sleeping), appetite changes (loss or gain of appetite), and psychomotor agitation or retardation, are also common symptoms of depression. Several of these symptoms reflect both ends of a behavioral spectrum (such as insomnia vs. hypersomnia), perhaps due to differences in underlying pathology. A clinical diagnosis of depression is made on the basis of criteria in the Diagnostic and Statistical Manual (DSM) of the American Psychiatric Association; patients meeting a certain number of criteria are considered to have depression.

In the United States, depression occurs with lifetime prevalence of 16% and 12-month incidence of almost 7%<sup>2</sup>. This translates to approximately 14 million Americans with depression per year, and 35 million over a lifetime<sup>3</sup>. In addition to the untold human cost of suffering, depression has a vast economic cost: in 2010, this number was nearly \$100 billion in the United States, with the majority attributed to the indirect workplace costs due to diminished productivity<sup>4</sup>. Furthermore, this is a problem that is growing, not improving. Depression is projected by the World Health Organization to represent the world's primary disease burden<sup>5</sup>. Clearly, increased attention to the development of new treatments is needed to address this situation.

The first modern conceptualization of depression came in the 1960s. J.J. Schildkraut distilled a number of studies implicating a deficiency of monoamine neurotransmitters in the pathogenesis of depression<sup>6</sup>. This was known as the Monoamine Hypothesis, which has guided depression psychopharmacology for the past 50 years. To this day, the vast majority of antidepressants clinically available are targeted to the monoamine systems, either through inhibition of breakdown or reuptake, in order to increase synaptic monoamine concentrations. Since then, drugs targeting other systems such as melatonergic and glutamatergic have also found use as antidepressants. Even drugs seemingly at odds with the tenets of the Monoamine Hypothesis, such as serotonin reuptake *enhancer* tianeptine, have found use in depression. These observations, however, do not suggest that the Monoamine Hypothesis is incorrect or that monoamines are not involved in the pathology of depression or its treatment; rather, that monoamines are a part of a much larger, complex puzzle, whose pieces slowly continue to be revealed.

No single brain region has been identified as a causative factor in the development of depression. Some regions prominently involved include prefrontal cortex and hippocampus, which are atrophied. In contrast, the amygdala, commonly viewed as a center of emotion, is hypertrophied, perhaps accounting for increased aggressiveness or anxiety in some cases of depression<sup>7</sup>. The hippocampus in particular is affected by increased circulating cortisol secondary to periods of stress resulting in reduction in volume, loss of dendritic spines, synapses, and glia (likewise, depression is a key feature of Cushing's disease). Antidepressants increase synaptogenesis and neurogenesis in the hippocampus, and restore hippocampal volume, and this neuroplasticity seems critical to the efficacy of antidepressants<sup>8</sup>. Others, however, have described antidepressant effects in the absence of neurogenesis<sup>9</sup>. Antidepressants also reverse the anatomic changes seen in the prefrontal cortex, but not the amygdala. Perhaps the lack of effect in the amygdala accounts in some part for the continued susceptibility to stress in depression relapses, and also a lessening of antidepressants' effects after multiple bouts of depression<sup>2</sup>.

### **1.1.2 Treatment of depression**

Depression is generally treated by antidepressant medication, psychotherapy, or a combination of the two. Both are comparably effective and combined are modestly more effective than either alone. DeRubeis et al. showed response rates (improvement of symptoms) of 58% for both medication and psychotherapy, and remission rates (absence of symptoms) of 46% for medication and 40% for psychotherapy<sup>10</sup>. Hollon et al. found medication plus psychotherapy versus medication alone at approximately 72% vs. 62% for response<sup>11</sup>. Results of the large NIMH STAR\*D study found response rates of approximately

50% and remission rates of approximately 30% for antidepressant citalopram<sup>12</sup>. These numbers are unlikely to be encouraging for the sufferer of depression<sup>13</sup>, and years of modern psychopharmacology have not improved the effectiveness of antidepressant medication, though safety has improved. Fortunately, failure of one medication does not mean that all medications will fail, and selection of a different drug often may result in successful treatment. Treatments such as electroconvulsive therapy (ECT) are also available. ECT is significantly more effective than antidepressant drugs, to a variable extent depending on the study, and generally shows a 20-30% increase in response rate<sup>14</sup>. Efficacy, however, is diminished in those who have previously failed to respond to antidepressant drugs<sup>12,15</sup>. ECT is further burdened with side effects such as memory loss, and the need for general anesthesia precludes its use as a first-line treatment for depression, despite its efficacy. For the above reasons, the discovery of new antidepressant mechanisms, targets, and drugs is a welcome development. Other non-pharmacological treatments include deep brain stimulation (DBS), transcranial magnetic stimulation (TMS) as well as neurofeedback with sensory stimulation<sup>16</sup>. DBS in particular is reserved for cases of treatment-resistant depression, as electrodes are implanted in the brain. One study reported a 40% response rate, with 20% remission, with DBS in treatment-resistant depression<sup>17</sup>, while a TMS study reported response and remission rates of approximately 25% and 15%<sup>18</sup>.

### **1.1.3 Methods to study depression**

While clinical research is performed on human subjects, most basic studies of depression and its treatment are done in rodent models, both for practical and ethical considerations.

Neither human knockdowns, nor humans expressing a modified form of a protein of interest, exist. This leaves animal models, which can be extensively manipulated. One must either use an animal model prone to depression, or “induce” a depressed state, generally through the application of stressors. This raises an important concern: can the brain of a rodent really recapitulate the workings of the human brain in any meaningful way? One cannot ask a mouse how he or she is feeling, necessitating inferences about the rodent’s “state of mind” through behavioral testing. Krishnan and Nestler elaborate a reasonable set of considerations in regards to the use of animal models<sup>19</sup>: 1) *Face validity* (does the test even make sense?) 2) *Etiological validity* (are the same causative factors involved?) and 3) *Pharmacological validity* (are the conditions treatable with the same drugs as in humans?).

The chronic mild stress paradigm is commonly used to induce a depressed phenotype<sup>20</sup>, subjecting animals to a variety of unpleasant conditions such as altered light/dark cycle, wet bedding, noise, or cage overcrowding for an extended period (weeks). Certain mutant rodent lines can also be utilized. Mice lacking K<sup>+</sup> channel TREK-1, for example, are resistant to the development of depression<sup>21</sup>. Consider the case of the serotonin reuptake transporter (SERT) knockout mice. In mouse lines CD-1 and 129S6/SvEv, SERT knockouts display a range of depressive behaviors<sup>22</sup>. In mouse line C57BL/6J, SERT knockouts did not display these depressed behaviors<sup>23</sup>. Thus, it is a combination of background as well as the particular genetic manipulation that determines behavioral characteristics of the rodent line.

Assessment of behavioral phenotype is done through a variety of tests reflecting different aspects of the experience of depression. Conceptually, in many of these tests, the less depressed or antidepressant treated mouse battles longer or demonstrates some kind of bravery absent in the comparison animals. In tail suspension and forced swim tests<sup>24</sup>, treated animals swim longer or struggle longer while hanging from their tail before giving up (in despair?). In a different approach, the elevated plus maze is shaped like a mathematical plus sign, with two open arms and two enclosed by walls. Here, the antidepressant treated mouse will spend more time in the unwall sections, while the “depressed” mouse will spend more time in the walled segments (seeking security?). This test is generally viewed as a test of anxiety-related behaviors<sup>25</sup>. Finally, the sucrose preference test is considered a test of anhedonia, the loss of interest in pleasurable things. Here, the antidepressant treated mouse will consume more sucrose than his depressed counterpart. Interestingly, while the swim, suspension, and elevated plus tests show differences shortly after antidepressant administration (within 90 minutes), sucrose preference requires a much longer period of treatment, up to 4 weeks<sup>26</sup>, suggesting that a different mechanism may be involved in restoration of hedonic behaviors. Other behaviors such as novelty-induced hypophagia (decreased feeding in strange settings) respond similarly.

Finally, primate models of depression have been used, and continue to see use. Such models have the benefit of a nervous system much closer to humans than that of rodents. Primates have been reported to experience depression related to their natural social experience and may reflect a process more similar to that which occurs in humans<sup>27</sup>.

Experiments in primates are expensive and carry a multitude of ethical concerns, limiting their use.

## **1.2 G Proteins and Signaling through GPCRs**

G proteins and the receptors whose signals they transduce, G protein coupled receptors (GPCRs), constitute the largest and most diverse mammalian signaling system. These receptors are utilized for the transduction of hormonal, neurotransmitter, visual, gustatory, and olfactory signals. While estimates vary depending on the source, humans express in excess of 800 GPCRs<sup>28</sup>, many of which recognize various odorant molecules; animals more dependent on sense of smell express an even greater repertoire of odorant receptors, in excess of 1000<sup>29,30</sup>. As a practical matter, G proteins and GPCRs are of great clinical significance, with estimates of 30-50% of current drugs targeted at this system<sup>31</sup>.

### **1.2.1 Heterotrimeric G proteins**

The role of many GPCRs remains unidentified and these are termed “orphan receptors.” These may be functionally vestigial, or may simply have an undiscovered function. One particularly interesting example of the latter case is seen in GPR30, now termed GPER<sup>32</sup>. This previously orphaned GPCR was found to be a transmembrane receptor for estrogen. This is unusual because steroid hormones were previously thought to act exclusively through soluble receptors which when bound acted directly upon transcription in the nucleus. Many other orphan GPCRs exist. Some have identified function (e.g. GPR56



regulates development in the cerebral cortex) but as yet lack an identifiable agonist. Much is likely yet to be revealed about the range of GPCR functions.

Despite the large number of GPCRs and G proteins, they can be systematically classified on the basis of their function. Heterotrimeric G proteins, so-named because of their association with GTP upon activation by a GPCR, consist of an alpha, beta, and gamma subunit. Alpha subunits are further subdivided based on their function:  $G\alpha_s$  and  $G\alpha_i$  stimulate and inhibit adenylyl cyclase respectively, and are most closely associated with cAMP signaling.  $G\alpha_q$  activation stimulates phospholipase C activity, which cleaves membrane phospholipid  $PIP_2$  into membrane diacylglycerol and  $IP_3$ , releaser of intracellular  $Ca^{2+}$  stores.  $G\alpha_{12/13}$  acts upon actin dynamics in growth and development. Alpha subunits associate with the tightly bound beta and gamma subunits often considered singly as “betagamma.” After activation of the heterotrimer, betagamma subunits also participate in signaling, such as in betagamma activation of  $K^+$  channels after activation of muscarinic acetylcholine receptors<sup>33</sup>.

These subunits interact with the plasma membrane through both protein-protein interaction as well as lipid anchoring.  $G\alpha$  subunits contain a labile, post-translational N-terminal palmitoyl lipid anchor ( $G\alpha_i$  is additionally myristoylated;  $G\alpha_q$  is dually palmitoylated), while the gamma subunit of betagamma contains a C-terminal farnesyl or geranylgeranyl lipid anchor which is not removable under physiologic conditions<sup>29</sup>. These G proteins and their acylations are depicted in Figure 1. Numerous isoforms of the subunits exist, with 16  $\alpha$ , 5  $\beta$ , and 12  $\gamma$  isoforms presently identified; these are not all expressed in

every cell, not all subunit combinations are actually able to form, and the functional significance of isoform combinations is not well-understood{Hillenbrand:2015ia}. Expression of these lipid anchors is required for G protein localization to the cell membrane and lipid rafts{Moffett:2000ty}<sup>36</sup>.

An additional class of small, cytosolic G proteins exists which are activated by varied signals and act upon varied effectors. Examples of these include members of the Ras superfamily. These are not activated by GPCRs and do not act upon the same targets as heterotrimeric G proteins. Though they are activated by, and hydrolyze GTP, they are a functionally separate class<sup>37</sup>.

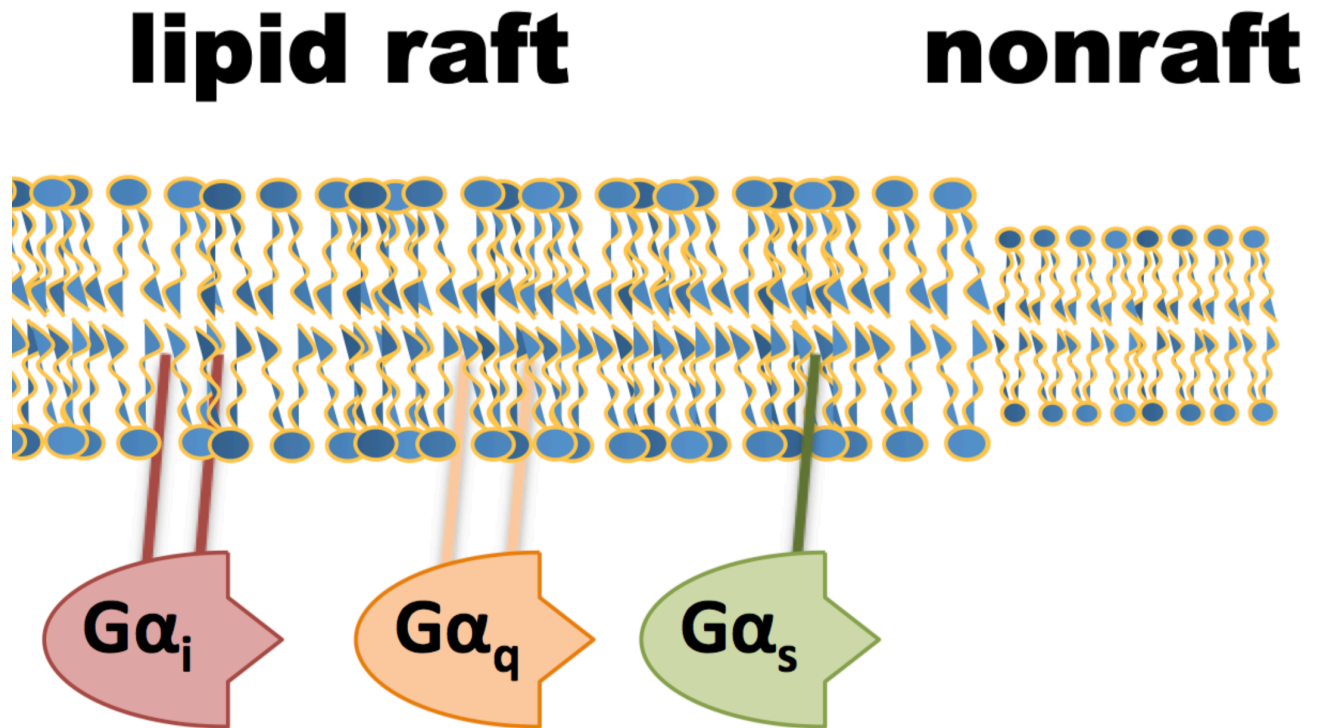


**Figure 1: G protein lipid anchors**

G proteins require post-translational acylation to establish proper targeting to lipid rafts/cell membrane, and are primarily localized in lipid rafts. Nonacylated variants are not targeted to the membrane, but instead are primarily cytosolic.  $G\alpha_s$  is singly palmitoylated (16-carbon saturated chain), while  $G\alpha_q$  is dually palmitoylated.  $G\alpha_i$  is palmitoylated and myristoylated (14-carbon saturated chain).

### 1.2.2 G protein coupled receptors (GPCRs)

GPCRs are transmembrane receptors for a wide variety of signals, as mentioned above. Their structure consists of an extracellular N-terminus followed by seven transmembrane segments. Upon binding by ligand, a particular receptor conformation is stabilized which acts effectively as guanine nucleotide exchange factor (GEF) for  $G\alpha$  subunits. The ligand-bound receptor now catalyzes the exchange of GTP for GDP within alpha subunits, leaving the alpha subunit in the active form. Thus activated, the alpha and betagamma subunits are free to interact with various effectors as described above. The intrinsic GTPase activity of alpha subunits allows the subunit to convert itself to the inactive, GDP-bound form and terminate signaling. The termination of signaling by  $G\alpha$  GTPase can be accelerated by the action of a protein class known as GTPase activating proteins, or GAPs. The steps of G protein activation and inactivation also illustrate a classic example in physiology and medicine, as cholera and pertussis symptoms stem from disruptions to these actions. Cholera toxin ADP-ribosylates  $G\alpha_s$  subunits, inhibiting their self-inactivating function, and resulting in increased cAMP production (important in both pathologies)<sup>38</sup>. Pertussis toxin ADP-ribosylates  $G\alpha_i$  subunits, preventing their activation by the receptor, effectively preventing their activation, and promoting cAMP accumulation<sup>39</sup>. In the case of cholera, increased cAMP production leads to PKA phosphorylation of the cystic fibrosis transmembrane conductance regulator (CFTR) channel, leading to efflux of chloride ion and water from intestinal epithelia, and significant diarrhea<sup>38</sup>. The precise mechanism of increased cAMP in the pathology of pertussis is not currently known<sup>33,40</sup>.

After  $G\alpha$  subunit inactivation, the cycle is complete and the subunits and receptor are free to repeat the process. A fairly standard textbook depiction of GPCR and G protein interaction suggests that a GPCR activated by its ligand then “attracts” a GDP-bound heterotrimeric G protein complex in the next step of the cycle. This notion has been challenged by numerous studies demonstrating a phenomenon of “precoupling,” wherein an inactive GDP-bound heterotrimer is physically associated with its associated receptor prior to ligand binding<sup>41-43</sup>. Furthermore, it is not clear whether after activation, alpha and betagamma subunits undergo a literal physical separation, a rearrangement, or some other change in association<sup>44</sup>.

In addition to inactivation of G proteins, signaling control is also implemented by the cell at the level of the GPCR. After binding of ligand to receptor, the active GPCR conformation now presents sites subject to phosphorylation by GPCR kinases, or GRKs. Once phosphorylated, these sites on the GPCR bind arrestins, which inhibit further signaling in two ways. First, GPCR-G protein interaction is sterically blocked. Second, arrestins interact with clathrin and other components of the receptor-mediated endocytosis process, promoting internalization of the GPCR and preventing further signaling<sup>45,46</sup>.

Finally, another deviation from signaling dogma is illustrated by the example of functional selectivity, also known as biased agonism. In this circumstance, the typical process of G protein/GPCR signaling is altered by the agonist itself. A  $\beta_2$  adrenergic receptor, for example, normally couples with  $G\alpha_s$  and promotes the production of cAMP through  $G\alpha_s$  interaction with adenylyl cyclase subsequent to stimulation with epinephrine or

norepinephrine. A different agonist could instead stabilize a receptor confirmation that no longer couples with  $G\alpha_s$ , instead preferably coupling with  $\beta$ -arrestin for internalization, or even another class of G protein<sup>47</sup>. The ability to utilize this receptor manipulation is of great interest clinically.

### 1.2.3 G proteins and depression

Changes in G protein signaling are well known in depression and antidepressant action, and have been the focus of the Rasenick lab for many years, both in human samples and in cellular models. In an early study in humans utilizing brain tissue from suicide victims, Cowburn et al., noted the curious finding that membranes prepared from frontal cortex of suicide victims showed decreased production of cAMP in response to various agonists, with no change in total membrane  $G\alpha_s$  or  $G\alpha_i$  content<sup>48</sup>. A similar latter study by Donati et al. again examined the membrane content of  $G\alpha_s$  in suicide victims, but in lipid rafts instead of total membrane. In this case, a difference was found between suicide and control subjects in cortex and cerebellum: although total membrane  $G\alpha_s$  was unchanged between suicide and control samples, the suicide samples showed increased amounts of  $G\alpha_s$  in lipid raft membrane fraction, where  $G\alpha_s$  is less able to activate adenylyl cyclase to produce cAMP<sup>49</sup>. While  $G\alpha_i$  was not tested in this study,  $G\alpha_q$  was found to be unchanged between groups.

In contrast, antidepressant treatment has shown the opposite effect, increasing cAMP production. In one of the earliest studies of the topic, Menkes et al. demonstrated in antidepressant treated rats, four different tricyclic antidepressants tested increased cAMP

production from rat brain cortex and hippocampal membranes after chronic (15-22d) antidepressant treatment<sup>50</sup>. Electroconvulsive therapy (ECT) also enhanced cAMP production, perhaps an early indication of the wide range of depression therapies that would later be found to converge on  $G\alpha_s$  signaling. Studies from the Rasenick lab (unpublished) by Sia Koutsouris in human peripheral cells such as platelets also show a similar change, relocation of  $G\alpha_s$  from membrane raft to non-raft with antidepressant treatment, and could constitute a circulating biomarker of antidepressant response.

Finally, these antidepressant effects are also seen in certain cell lines, but not others. C6 glioma, a rat cell line, responds similarly to antidepressant drug treatment, with a selective redistribution of  $G\alpha_s$  (but not other G proteins) from raft into non-raft membrane domains and a concomitant increase in agonist-stimulated cAMP production. This effect of  $G\alpha_s$  redistribution occurs in a dose- and time-dependent fashion<sup>51</sup>. HEK293, a human kidney cell line, does not show this response to antidepressant treatment. The differences between responsive and nonresponsive cell lines are to this point unknown, and constitute the focus of the present study. This phenomenon is schematically depicted in Figure 2.

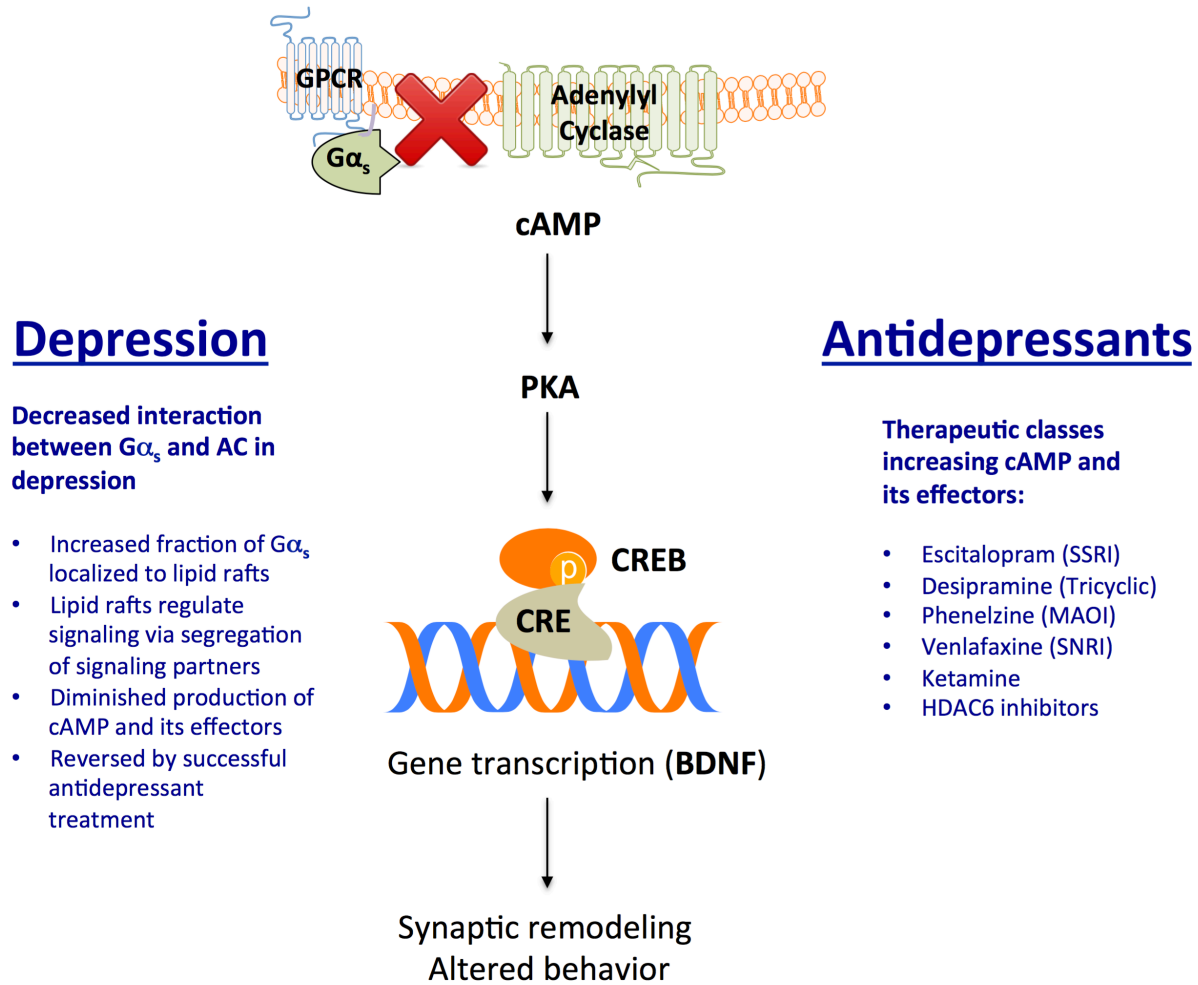


**Figure 2: G proteins and antidepressant effect**

In depression, an increased fraction of  $G\alpha_s$  is localized to lipid rafts. Under these conditions,  $G\alpha_s$  has decreased functional coupling with adenylyl cyclase resulting in diminished production of cAMP and its downstream effectors such as neurotrophin BDNF. These changes are reversed by all antidepressant classes tested, as well as non-pharmacologic treatments such as electroconvulsive therapy (ECT).



### 1.3 Lipid Rafts

The initial “fluid mosaic” model of the cell membrane provided by Singer and Nicholson in 1972 describes a lipid bilayer in which protein components can diffuse freely and even specifically eschews the notion of a membrane ordered on a scale any larger than that needed for the sequential apposition of electron transport chain proteins, as an example<sup>52</sup>. Since that time, a picture of membrane structure and function far more complex has emerged, including a regulatory role for the membrane in signaling. Continued membrane research soon identified regions of the membrane that tended to cluster under conditions of lowered temperature<sup>53</sup> and within a more fluid lipid milieu<sup>54</sup>, specific association of membrane lipids based on chain length<sup>55</sup>, and a number of other indicators of membrane order<sup>56</sup> far in excess of that initially envisioned by Sanger and Nicholson.

#### 1.3.1 Lipid raft description

Lipid rafts are domains of the plasma membrane, described as regions high in cholesterol and sphingolipids, enhanced in microtubular anchoring, with lipids of longer chain length and greater saturation, ranging from 10-200nm in size<sup>57</sup> and experimentally as regions resistant to solubilization by detergent Triton-X100. These domains are enriched in proteins modified via palmitoyl- and glycosylphosphatidylinositol (GPI) anchors, and the relative enrichment of certain proteins and exclusion of others is thought to underlie a role for lipid rafts in the regulation of signaling<sup>58</sup>. Indeed, examples of both lipid raft potentiation<sup>59</sup> and inhibition<sup>57</sup> of signaling cascades have been demonstrated. The phenomenon of membrane  $G\alpha_s$  redistribution in response to antidepressant treatment

described in this study is another such example; here, lipid rafts seem to inhibit the interaction between  $G\alpha_s$  and its effector adenylyl cyclase.

Two important raft scaffolding proteins are caveolins, which organizes invaginated “caveolar” or cave-like rafts, and flotilins, which form non-invaginated or planar lipid rafts<sup>60</sup>. While caveolae are known to participate in endocytosis, the differential roles of these two classes are not well understood. Other proteins of relevance to this study with known raft associations are adenylyl cyclases:  $Ca^{2+}$  regulated cyclases (1,3,8 and 5,6) are considered primarily raft-localized, while others are non-raft localized<sup>61-63</sup>. While proteins can be targeted to rafts via a lipid anchor or through protein-protein interaction, the targeting of larger transmembrane proteins is unclear. Transmembrane proteins are able to slow the diffusion and induce ordering of nearby proteins and lipids<sup>64</sup>, leaving open the question: which molecular species is organizing which?

### **1.3.2 Study of lipid rafts**

Various methods commonly used to study lipid raft function in living cells include raft disruption through microtubular destabilization with colchicine or cholesterol sequestration with methyl- $\beta$ -cyclodextrin. Membrane fractions containing lipid rafts can be isolated by sequential detergent extractions (rafts are insoluble in Triton X-100 but soluble in Triton X-114) or via density (sucrose) gradient fractionation. The use of cholesterol sequestration was found in one study to inhibit normal turnover of membrane phospholipid phosphatidylinositol biphosphate ( $PIP_2$ )<sup>65</sup>; therefore if one is studying a phenomenon affected by membrane  $PIP_2$  content rather than exclusively by lipid raft

structure, results and interpretation could be affected. Detergent extractions also have inherent problems, as a protein weakly associated could be unexpectedly solubilized. Likewise, a protein with microtubular anchoring could escape solubilization<sup>66</sup>. For these reasons, it is likely wise to study rafts through a combination of complementary techniques, rather than relying on any single technique.

Methods are also available for studying rafts in situ. The use of cholera toxin B, which associates with lipid rafts and can be labeled with a fluorescent tag, is well established. This can be used in the context of Förster/fluorescent resonant energy transfer (FRET) with another labeled protein to demonstrate close association (1-10nm) and joint residence in lipid raft domains. In this study, a technique was developed and utilized to study protein localization with respect to lipid rafts, based on differing lateral membrane mobility in vs. outside of rafts, and is fully discussed later in this paper.

### **1.3.3 Lipid rafts and depression**

The involvement of lipid rafts in the pathology of depression with respect to G protein signaling has been discussed previously in this paper. Evidence also implicates lipid rafts themselves in the mechanism of antidepressant action, though the mechanism remains unclear. Eisensamer et al. demonstrated accumulation of antidepressant and antipsychotic drugs in lipid rafts in HEK293<sup>66</sup>. In this study, lipid raft membrane fractions were collected via sucrose density centrifugation and exposed to antidepressant or antipsychotic drugs. Drug content of samples was then determined by ultraviolet absorbance. Antidepressants of various classes were found to accumulate: SSRI (fluoxetine), tricyclic (desipramine), and

several atypical antidepressants (mirtazapine, reboxetine). Monoamine oxidase inhibitor moclobemide, however, did not accumulate. All antipsychotics tested (fluphenazine, haloperidol, risperidone, clozapine) accumulated in lipid rafts<sup>67</sup>.

Recently, in a more sensitive and perhaps more physiologically relevant approach, Erb et al. examined accumulation of antidepressant and antipsychotic drugs in lipid raft membrane fractions in C6 glioma cells. In this study, cells were first treated for three days with drug, followed by sucrose gradient fractionation and isolation of lipid rafts. Rafts were then analyzed for drug content via GC/MS. In this case, robust raft accumulation of monoamine oxidase inhibitor (phenelzine) and SSRI (fluoxetine, escitalopram) was found, but three tricyclics tested (amitriptyline, desipramine, imipramine) accumulated to a much lesser extent. Citalopram stereoisomer *R*-citalopram did not accumulate. Antipsychotic drugs (aripiprazole, olanzapine) did not accumulate; these drugs were included because of their occasional adjunctive use in depression<sup>68</sup>.

It is difficult if not impossible to compare the two studies directly. In *Eisensamer*, the exposure to antidepressants was non-physiologic and in a cell line known to be unresponsive to antidepressants (HEK293), at least with respect to G protein signaling. In contrast, *Erb* utilized cells known to respond to antidepressant drugs (C6 glioma), and the cells were treated over a period of days of normal growth.

## 1.4 cAMP signaling

### 1.4.1 cAMP Overview

Cyclic adenosine monophosphate or cAMP is an important signaling molecule throughout the tree of life, from bacteria to slime molds to mammals. In mammals, cAMP is a key second messenger, transducing the signal of various hormones and neurotransmitters. Stimulation of a GPCR coupled to  $G\alpha_s$  activates the G protein, which is then able to stimulate the production of cAMP by adenylyl cyclase. The cAMP produced may then transmit its signal to another molecule, or it may be hydrolyzed by a phosphodiesterase (PDE) into adenosine monophosphate (AMP). Eleven classes of phosphodiesterases are presently identified, with some acting exclusively on cAMP (PDEs 4,7,8), some exclusively on cGMP (PDEs 5,6,9), and some acting on both (PDEs 1,2,3,10,11)<sup>69</sup>.

### 1.4.2 cAMP effectors

Protein kinase A (PKA) is an important effector of cAMP. Binding of cAMP to PKA's regulatory subunits liberates PKA's catalytic subunits and allows phosphorylation of a wide range of targets, from transcription factors to ion channels. One phosphorylation target particularly important in depression is the cAMP response element binding protein (CREB). After phosphorylation, CREB acts as a transcription factor for numerous proteins. One such protein is brain derived neurotrophic factor (BDNF), an important neurotrophin discussed below. Another target of cAMP is exchange protein directly activated by cAMP, or Epac. Epac acts as an exchange factor for GTP in small G proteins of the Rap subfamily of Ras<sup>70,71</sup>. Epac has also found great use as the foundation of a cAMP sensor based on FRET. Dually

modified with a FRET pair, binding of cAMP induces a conformational change in the Epac molecule which alters the FRET signal, indicating the presence of cAMP{Ponsioen:2004bj, Klarenbeek:2015kd}.

### 1.4.3 cAMP in depression

Cellular events significantly delayed in onset may reflect the activation of transcriptional pathways, with the time delay representing the period required for synthesis and action of various effectors. One such pathway with numerous downstream effectors is the cAMP/PKA pathway; alterations in cAMP signaling and cAMP's downstream effectors are commonly found in mood disorders, including depression{Blendy:2006bs}<sup>74,75</sup>. These changes are seen in varied cell types. Studies of lymphocytes from depressed patients have shown alterations in cAMP signaling compared to non-depressed controls. Specifically, these cells displayed smaller increases in cAMP in response to agonists of  $\beta$ -adrenergic, GPCR/G-protein-mediated cAMP production compared to controls<sup>76</sup>. Notably, the decreased GPCR/G-protein signaling is not accounted for by a decrease in receptor number or sensitivity<sup>48</sup>. More recently, differences have been shown in  $G\alpha_s$  localization in brain tissue of depressed patients post-suicide compared to controls. These samples showed an increased localization of  $G\alpha_s$  in lipid raft membrane fractions, where it may be less able to activate adenylyl cyclase production of cAMP<sup>49</sup>. Studies in rat brain membranes have shown increased adenylyl cyclase activity (cAMP production) in response to chronic treatment with a variety of antidepressants, as well as in response to ECT, or electroconvulsive treatment, a non-pharmacologic treatment for depression<sup>77,78</sup>. Likewise,

studies of platelet membranes as well as leukocytes from depressed humans have shown a similar increase in adenylyl cyclase activity subsequent to antidepressant treatment <sup>79</sup>.

More recently, studies such as positron emission tomography(PET) in human subjects have demonstrated directly the changes in brain cAMP in depression and with successful antidepressant treatment. These studies utilized <sup>11</sup>C-labelled cAMP phosphodiesterase PDE4 inhibitor rolipram to measure activity of PDE4, which is activated by cellular cAMP levels via PKA phosphorylation. PDE4 thus activated binds increased amounts of rolipram, which is detectable in PET via its <sup>11</sup>C label. Briefly, depressed subjects evidenced decreased binding of labeled rolipram, indicating decreased cAMP levels (approximately 20% decrease in total brain cAMP, consistent across 10 regions measured)<sup>80</sup>. Treatment with antidepressant (SSRIs citalopram, escitalopram, or sertraline) increased cAMP levels by approximately 12% across these same brain regions<sup>81-83</sup>. Together, these two studies represent the most direct demonstrations in human subjects of cAMP changes in depression and with antidepressant treatment.

The consequences of diminished cAMP signaling in depression are multifold and stem from the decreased expression of cAMP's effectors. In particular, BDNF expression is reduced. This is widely seen in animal models of depression. Strategies to create a depressed phenotype in rodents (various chronic stressors) result in decreased expression of BDNF mRNA and protein<sup>84</sup>. Exogenous glucocorticoids depress BDNF production, and endogenous cortisol production is increased by stressors<sup>85</sup>. Antidepressant treatment reverses the decrease in BDNF production secondary to glucocorticoid treatment<sup>86</sup> as well

as stress models<sup>87</sup>. Chronic (21 day) but not acute (1 day) treatment with a variety of classes of antidepressant drugs (tricyclic, SSRI, MAOI) increase BDNF expression in rodents<sup>88</sup>. Electroconvulsive therapy increased BDNF production in rodents after a single treatment<sup>89</sup>. Finally, increased production of BDNF appears to be a critical mediator of antidepressant effects. The increase of cellular cAMP alone after antidepressant treatment is not sufficient to produce antidepressant effects: mice with knocked-out forebrain BDNF expression show a significant attenuation of antidepressant effect in behavioral tests<sup>90</sup>.

## **1.5 Adenylyl Cyclase**

### **1.5.1 Adenylyl cyclase overview**

Adenylyl cyclases catalyze the cyclization of ATP into second messenger 3',5'-cyclic adenosine monophosphate (cAMP) and pyrophosphate anion. Multiple classes of adenylyl cyclase enzymes exist in both prokaryotic and eukaryotic cells, in bacteria, animals, and even plants. Structure, mechanism, function, and regulation are quite different among these classes.

Adenylyl cyclases can be broadly grouped into six classes based on their diversity of structure. Most of these (classes 1,2,4,5,6) are bacterial enzymes. Notably, class 2 adenylyl cyclases are of clinical importance due to their role in bacterial virulence. Examples of



these include anthrax edema factor and pertussis CyaA toxins. These are secreted by bacteria and incorporated into a host cell, mediating the virulence of these microorganisms through increased cAMP production<sup>91</sup>. These are far more catalytically active (1000x) than class 3 adenylyl cyclases<sup>92</sup>, transmembrane proteins expressed in mammalian cells, yeast, and some bacteria<sup>93</sup>. Mammalian cells also express a soluble adenylyl cyclase regulated by bicarbonate, most commonly associated with signaling roles in sperm<sup>90</sup>. Class 4 cyclases are the smallest known at ~19kD, and are present in bacteria including *Yersinia pestis*<sup>94</sup>. Plants also utilize cAMP signaling, but few plant cyclases have been identified<sup>95</sup>. One such cyclase identified is expressed in the pollen of *Zea mays* (corn)<sup>96</sup>. Henceforth, discussion of adenylyl cyclases will be limited to the mammalian, membrane-bound types, class 3. These class 3 adenylyl cyclases are comprised of 9 isoforms, discussed in the next section.

### **1.5.2 Mammalian adenylyl cyclase structure and regulation**

Mammalian (class 3) adenylyl cyclases represent a large, diversely localized and regulated group of enzymes (Table 1). The membrane adenylyl cyclases (AC types 1-9) share a common structure, depicted in Figure 3, with significant homology in transmembrane and catalytic regions, and greater divergence in the N-terminal region, and range in size from approximately 120-140kD {Sadana:2009kq}.

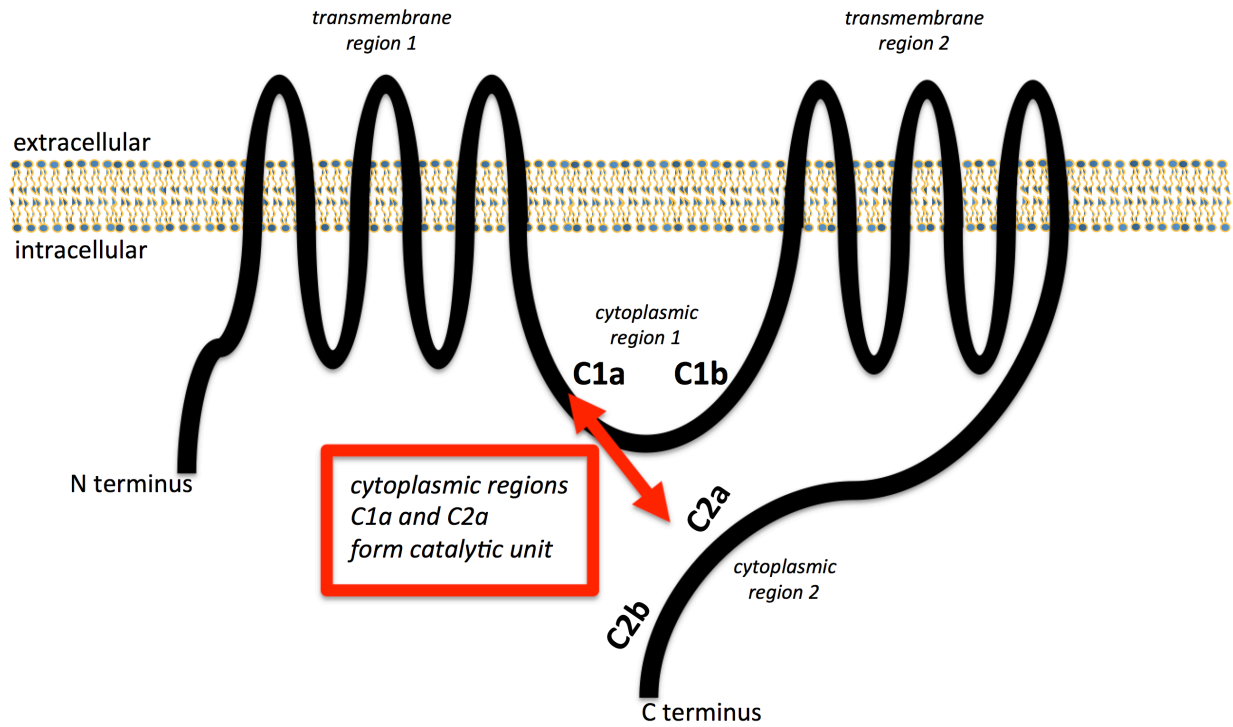
AC isoform	G $\alpha$ protein stimulation	G $\alpha$ protein inhibition	Ca <sup>2+</sup> regulation	Comments
AC1,AC3,AC8	G $\alpha_s$	G $\alpha_i$	Ca <sup>2+</sup> /calmodulin	Ca <sup>2+</sup> /calmodulin stimulated
AC5,AC6	G $\alpha_s$	G $\alpha_i$	Ca <sup>2+</sup>	Ca <sup>2+</sup> inhibited
AC2,AC4,AC7	G $\alpha_s$			
AC9	G $\alpha_s$			

AC isoform	Tissues with prominent expression of isoform
AC1	brain, adrenal, kidney
AC2	brain, skeletal muscle, testis
AC3	testis, ovary, colon, primary cilia
AC4	heart, lung, spleen, testis, ovary
AC5	heart, brain, adrenal, kidney, testis, ovary
AC6	heart, brain, adrenal, kidney, testis, ovary
AC7	heart, lung, liver, pancreas, spleen, colon
AC8	brain, pancreas, testis
AC9	widespread

**Table 1: Regulation and distribution of mammalian membrane adenylyl cyclase isoforms**

Key regulators of adenylyl cyclase isoforms are shown in the upper panel of Table while distribution is shown in the lower panel<sup>97,99</sup>. Note, AC3 may be less sensitive to activation by Ca<sup>2+</sup>/calmodulin than are AC1 or AC8 (*Halls ML and Cooper, DM. Regulation by Ca<sup>2+</sup>-Signaling Pathways of Adenylyl Cyclases. Cold Spring Harb Perspect Biol. 2011 Jan; 3(1): a004143.*)



**Figure 3: General structure of mammalian membrane adenylyl cyclase**

Mammalian membrane adenylyl cyclase isoforms share a common structure of 12 transmembrane segments, constituted as two sets of 6 segments each followed by two large intracellular regions (C1 & C2), which combine to create the catalytic unit of the enzyme<sup>97</sup>.

The diversity of adenylyl cyclase isoforms and their regulation suggests a diversity of function mediated by differential associations of adenylyl cyclase isoforms with other varied cellular components. Indeed, various studies have begun to reveal these associations. The calcium-regulated adenylyl cyclases (isoforms 1,3,5,6 and 8), for example, are predominantly localized to membrane lipid rafts, while those not regulated by calcium (isoforms 4,7, and 9) are not <sup>101</sup>. Calcium-inhibited isoforms (AC5,6) are inhibited by action at a high-affinity  $\text{Ca}^{2+}$  binding site which is sensitive to  $\text{Ca}^{2+}$  concentrations in the low/sub-micromolar, or physiologic, range. All cyclase isoforms are inhibited by supraphysiologic  $\text{Ca}^{2+}$  concentrations via competition with  $\text{Mg}^{2+}$  associated with ATP at the cyclase's catalytic "P-site", the site of ATP binding<sup>97</sup>.

Isoforms stimulated by physiologic  $\text{Ca}^{2+}$  increases (AC1,3,8) act through  $\text{Ca}^{2+}$ - calmodulin interaction with cyclase, rather than  $\text{Ca}^{2+}$  alone. Furthermore, the calcium regulation of raft-associated adenylyl cyclase isoforms (specifically, regulation via store-operated or capacitative calcium entry) is dependent on the residence of the cyclase in lipid rafts; disturbance of this localization by cholesterol depletion or other means abolishes this particular mode of regulation <sup>102-104</sup>.

Adenylyl cyclases are also regulated via various protein interactions, particularly G protein subunits and protein kinases. While all isoforms are subject to stimulation by  $\text{G}\alpha_s$ , only  $\text{Ca}^{2+}$  -regulated isoforms are inhibited by  $\text{G}\alpha_i$ . G protein  $\beta\gamma$  units can be stimulatory or inhibitory, depending on the cyclase isoform in question. Likewise, phosphorylation by

protein kinases A and C can be stimulatory or inhibitory, depending on both cyclase and kinase isoform.

Another emerging example of cyclase isoform regulation is residence in and regulation by specific and segregated microdomains, addressing the question: how can a cell respond with specificity to different agonists that share the same effectors, such as cAMP and pKA? This was first observed by Buxton and Bunton, who noted different responses in cardiomyocytes subjected to isoproterenol and PGE<sub>1</sub>, both agonists acting through G $\alpha_s$ -coupled GPCRs<sup>105</sup>. Others noted the co-purification of PKA with microtubules as well as microtubule associated protein MAP2, the first “A kinase anchoring protein,” or AKAP, identified<sup>106,107</sup>. Numerous additional AKAPs have been identified, including AKAP 79, which exerts an inhibitory influence on adenylyl cyclase by anchoring protein kinase A near its target (here, adenylyl cyclase) and phosphorylating a specific residue on the cyclase<sup>108</sup>. AKAP79 is targeted to lipid rafts via palmitoylation, and inhibition of AKAP79 function or its lipid raft targeting abolishes its regulatory function<sup>109</sup>. A picture has emerged of cAMP signaling through specific microdomains or signalosomes, with specific receptors, effectors, and phosphodiesterases brought into association by specific AKAPs, with resulting compartmentalization of signaling<sup>110</sup>.

### **1.5.3 Adenylyl cyclase and mood disorders**

Variations in adenylyl cyclase isoform expression have been associated with mood disorders, particularly depression. Krishnan et al. examined the effect of knockouts in mice

of  $\text{Ca}^{2+}$  regulated cyclase isoforms (double knockouts of AC1&8, both stimulated by  $\text{Ca}^{2+}$ -calmodulin vs. knockout of AC5,  $\text{Ca}^{2+}$  inhibited isoform)<sup>111</sup>, which are highly expressed in the limbic system. Mice with AC5 knockdown displayed an anxiolytic/antidepressant phenotype in behavioral assays, while AC1/8 knockout mice displayed behaviors indicating increased anxiety, lethargy, and decreased sucrose consumption (anhedonia). Neither transgenic mouse showed changes in anatomical regions measured (hippocampus). Regional differences in BDNF production were also noted. While the AC5 knockout mouse (“antidepressant” phenotype) showed *decreased* production of BDNF and its receptor TrkB in amygdala, these were unchanged in hippocampus and nucleus accumbens. AC1/8 knockouts showed no change in BDNF in these regions, but showed *increased* expression of TrkB in nucleus accumbens. These changes are, in a sense, opposite of what might be expected based on a simple model of BDNF and depression. Clearly, regional differences in these pathways seem to exist and complicate the notion of increased BDNF signaling equating to an antidepressant phenotype.

The role of AC3 in depression has also been evaluated in AC3 knockout mice by Chen et al<sup>112</sup>. In this study, three different mouse AC3 knockouts were studied: global constitutive, global inducible, and forebrain-specific knockouts of AC3. AC3 knockouts demonstrated increased depressive behaviors in a range of behavioral tests. Hippocampal size and activity was also reduced in AC3 knockout mice, compared to controls. Learning and memory were disturbed. Sleep disturbances of increased REM sleep was also noted in both global knockouts; increased REM sleep is characteristic of sleep changes noted in depression in human subjects<sup>113</sup>. Interestingly, AC3 is primarily expressed in, and is used

as a marker of, primary cilia both in brain and elsewhere<sup>114,115</sup>. The primary cilium's role is still elusive and has traditionally been associated with development and cell division<sup>116</sup>. It is unclear at this point how disturbances in ciliary AC3 signaling produce the range of effects seen in this study.

Human data on adenylyl cyclase in depression are limited to postmortem and genome-wide association studies (GWAS). One GWAS identified AC3 as a significant target<sup>117</sup>, though other studies have not corroborated this finding<sup>118</sup>. Human postmortem studies of brain from depressed suicide victims by Reisch et al.<sup>119</sup> examined the expression and catalytic activity of adenylyl cyclase 1, 4, and 5/6 in these patients. Only AC4 expression was altered (diminished) compared to controls. Cyclase activity (cAMP production) in response to forskolin was also diminished in the depressed subjects. Joeyen-Waldorf et al.<sup>120</sup> have shown increased expression of AC7 in both serotonin transporter (SERT) knockout mice, which have a depressed phenotype, and depressed human postmortem brain samples. Hines et al.<sup>121</sup> contrasted mouse models overexpressing AC7 vs. heterozygous knockdowns of AC7 and revealed a sexual dimorphism with respect to AC7 and depression. The mice overexpressing AC7 showed a depressed behavioral phenotype compared to wild type controls, while the heterozygous knockdowns showed an antidepressant phenotype. These phenotypes were, however, only observed in female mice; no changes were observed in the corresponding male subjects. Furthermore, the authors associated in humans a particular AC7 tetranucleotide polymorphism in the 3' UTR of AC7 with depression, but only in female subjects.

It is not currently possible to assign a unified model of action to the above cyclase findings with respect to depression. Rather, these examples together illustrate the complexity of these systems in both disease and health. In the particular case of AC7, one might be tempted to ascribe a cause and effect relationship: In Hines et al.<sup>121</sup>, opposite manipulations of AC7 expression produced opposite effects on behavioral phenotype (but only in females). In Joeyen-Waldorf et al.<sup>120</sup>, SERT was knocked down, producing a depressed phenotype with an accompanying increase in AC7 expression. In the first case, AC7 manipulation was the cause; in the second case perhaps an effect. At this point, it is perhaps best to describe the relationships between adenylyl cyclase isoforms and depression as a statistical association, rather than attempt to link these varied observations mechanistically.

## **1.6 Monoamine Reuptake Transporters**

After release of monoamine neurotransmitters (such as serotonin, dopamine, norepinephrine) into the synapse by the presynaptic neuron, the same neurotransmitters are reclaimed whole by the presynaptic cell through the action of reuptake transporters. This is in contrast to the case of acetylcholine, which is enzymatically degraded into choline and acetate in the synapse through the action of acetylcholinesterase. Reuptake transporters are a molecular target of the largest classes of antidepressant drugs (SSRI,



tricyclics) as well as stimulant drugs such as amphetamine and cocaine (though these drugs have additional mechanisms of action).

### **1.6.1 Monoamine reuptake transporter structure and function**

Reuptake transporters for serotonin (SERT), norepinephrine (NET), and dopamine (DAT) are large (approximately 620 amino acids) proteins with 12 transmembrane segments and cytosolic N- and C- termini, expressing a high degree of homology to one another<sup>122</sup>, particularly in transmembrane regions<sup>123</sup>. Furthermore, these are highly conserved among species with rat and human SERT showing 92% sequence homology<sup>124</sup>. All are members of the sodium-dependent large solute carrier family (SLC6), as is bacterial leucine transporter LeuT, which had been crystallized and widely studied in the context of antidepressant binding and mechanism.

Monoamine reuptake transporters utilize the cell's sodium concentration gradient to cotransport sodium, chloride, and a specific monoamine, and are therefore indirectly powered by membrane  $\text{Na}^+/\text{K}^+/\text{ATPase}$  activity. In the case of SERT and NET, one  $\text{Na}^+$  and one  $\text{Cl}^-$  ion are cotransported with each substrate molecule<sup>122</sup>. In the case of DAT, two  $\text{Na}^+$  ions are transported with one  $\text{Cl}^-$  ion, causing a depolarizing current. This current secondary to DAT activity has been linked to activation of voltage-gated  $\text{Ca}^{2+}$  channels; the significance of this function is not known<sup>125</sup>.

Crystallization and other studies have identified binding sites through which antidepressants regulate and inhibit the function of reuptake transporters. LeuT and SERT

have demonstrated at least two binding sites: a high-affinity primary or orthosteric site, and a lower affinity secondary or allosteric site<sup>126,127</sup>. In the case of SERT, a wide variety of antidepressants bind and inhibit transporter function through the primary site, while escitalopram (an antidepressant extensively used in this thesis) binds additional sites with unknown significance, perhaps modulating affinity to the primary site. *R*-citalopram may also bind a site on SERT, inhibiting escitalopram binding at its primary site<sup>128</sup>. Analysis of the crystal structure of desipramine-bound LeuT showed that desipramine binds and restricts the movement of a gating structure by inducing ionic bond formation between particular regions of the transporter<sup>129</sup>. Experimentally, mutagenized transporter variants resistant to the effects of antidepressants have been developed and are discussed in the “Results” section.

Antidepressants differ in their affinity to a particular reuptake transporter. Consider the following (all affinity values given as  $K_i$ )s<sup>127</sup>:

**Escitalopram: SERT ~1 nM/NET 7800 nM/DAT 27,400 nM**

**Paroxetine: SERT 0.07- 0.2 nM/NET 40-85 nM/DAT 490 nM**

Both antidepressants are selective for serotonin and classed among SSRIs. Paroxetine has greater affinity for SERT, while escitalopram has greater selectivity for SERT.

Escitalopram’s profound selectivity for SERT over NET and DAT was a factor in its inclusion in this study, along with its clinical significance. Desipramine, in contrast, demonstrates the following affinities<sup>122</sup>:

**Desipramine: SERT 61 nM/NET 4 nM/DAT 78,720 nM**

Thus, desipramine inhibits both SERT and NET and clinically relevant antidepressant concentrations (commonly in submicromolar range), but does not act at DAT. This dual affinity for SERT and NET, with varying relative activity at the two, is typical of tricyclic antidepressants.

### **1.6.2 Monoamine reuptake transporter and mood disorders**

Finally, reuptake transporters themselves have been implicated in mood disorders. Mice lacking SERT demonstrate behaviors considered characteristic of a depressed or anxious phenotype<sup>130,131</sup>. This is non-intuitive, as pharmacological inhibitors of SERT, namely antidepressants, relieve depression and anxiety. One possible explanation of this observation is that these mice have lacked SERT function throughout development, and their nervous system has developed abnormally, with effects on behavior as noted above. Inducible knockouts would be useful in this regard, and at least one model has been created. Tryptophan hydroxylase is required in the synthesis of serotonin from tryptophan, and is considered a marker of serotonergic cells. This model utilizes a Cre-lox system controlled by the tryptophan hydroxylase promoter, limiting expression to serotonergic cells. Thus, SERT activity can be ablated at later stage, controlled by the experimenter<sup>132</sup>. This model has not been widely used to this point.

Particular variants in the promoter region of the SERT gene, termed 5-HTTLPR, are also associated with increased depression and anxiety in human subjects<sup>133</sup>. This promoter region is polymorphic and variants are commonly classed as “long” or short”, with effects on SERT expression and function. The long variant of this promoter region causes increased transcription of SERT mRNA<sup>134</sup>, while the short variant is typically associated with increased anxiety and depression<sup>135</sup>. However, in Long, et al.<sup>136</sup>, Han Chinese expressing the short variant displayed increased anxiety as well as reduced functional connectivity between the prefrontal cortex and the amygdala. At least 10 sub-variants of the long and short promoter variants have been identified<sup>137</sup>, and research actively continues in this area. A comprehensive understanding of 5-HTTLPR variations in mood disorders, though, has not been achieved.

## **1.7 Antidepressants**

### **1.7.1 Antidepressant history**

The discovery of modern antidepressant drugs was serendipitous, arising out of research on isoniazid and iproniazid, hydrazine derivatives of isonicotinic acid, as antitubercular agents. Researchers noticed that patients treated with these drugs experienced a pronounced elevation of mood compared to controls<sup>138,139</sup>. Iproniazid was soon identified as an inhibitor of monoamine oxidase, and commercialized on the basis of its antidepressant effects, ushering in the era of the monoamine hypothesis<sup>140</sup>. Though

microdialysis studies have shown increases in extracellular monoamine neurotransmitter in response to antidepressant treatment <sup>141-143</sup>, no studies to date have demonstrated a synaptic deficiency of neurotransmitter *per se* in either depressed patients or animal models of depression. Antidepressants are commonly used not only in the treatment of depression, but anxiety-spectrum disorders as well, including obsessive-compulsive disorder. It should be noted that the efficacy of antidepressants in these disorders does not necessarily imply a common pathophysiological basis; nor does it necessarily imply a common mechanism of drug action.

### **1.7.2 Monoamine oxidase inhibitors**

Monoamine oxidase inhibitors (MAOIs), the first clinical class of antidepressant available, act through inhibition of mitochondrial enzyme monoamine oxidase (MAO). Monoamine neurotransmitters including serotonin, norepinephrine, and dopamine are oxidatively deaminated by MAO. These drugs elevate presynaptic monoamine content by inhibiting their degradation after reuptake by monoamine reuptake transporters (SERT, NET, DAT). This increases presynaptic neurons' content of monoamines, making increased neurotransmitter available for release upon stimulation. MAO is expressed as two isoforms, MAO-A and MAO-B, both of which are expressed in the brain. Peripherally, MAO-B is expressed in platelets while MAO-A is expressed in liver and intestine; MAO-A inhibition is thought to be primarily responsible for antidepressant effects of MAOIs<sup>144</sup>. The era of MAOIs, which began in the 1950s, was short lived (though they remain in regular use) due to two factors: toxicity and the development of the next class of antidepressants, tricyclics. The toxicity of MAOIs stemmed from their tendency to precipitate hypertensive crises due

to inhibition of dietary trace amine tyramine, found in a variety of foods. Furthermore, hydrazine-derived MAOIs (iproniazid, isocarboxazid, phenelzine) were found to cause hepatotoxicity<sup>140</sup>. Though safer MAOIs were developed (reversible MAO-A inhibitors, MAO-B inhibitor selegiline for Parkinson's disease), their use in depression was quickly supplanted by tricyclics.

### **1.7.3 Tricyclic antidepressants and selective serotonin reuptake inhibitors**

The 1950s was in many ways an awakening of modern psychopharmacology.

Contemporaneously with the development of MAOIs, researchers identified the first antipsychotic compound, chlorpromazine (Thorazine). Study into derivatives of the three-ringed chlorpromazine structure ultimately produced a series of tricyclic compounds (TCA) whose clinical efficacy was not directed towards psychosis, but depression. While MAOIs increased presynaptic neurotransmitter content via inhibition of metabolism, tricyclics were found to act through inhibition of presynaptic monoamine reuptake transporters for norepinephrine and serotonin (NET and SERT) with a variable specificity between the two. The net effect of this inhibition is an increase in the amount of neurotransmitter available at the synaptic cleft. Some well-known tricyclics include imipramine, desipramine, and amitriptyline. While these compounds were no more efficacious overall than MAOIs, they have an improved side effect profile. Despite their improved safety, tricyclics are still lethal in overdose due to cardiac effects, a clear problem in depressed patients who may use them to commit suicide. Nonetheless, tricyclics reigned through the 1980s<sup>145</sup>.

Continued study of monoamines in depression in the 1960s and 1970s led to the observation that certain tricyclics had greater specificity for norepinephrine or serotonin and further, that serotonin might be more responsible for the mood elevating effects of antidepressants<sup>146-148</sup>. Derivatives of diphenhydramine (Benadryl), in particular LY110140 (later termed fluoxetine (Prozac)) and its oxalate salt LY82816 were identified as having greater than 100x selectivity for serotonin reuptake vs. norepinephrine reuptake<sup>149-151</sup>. These and other serotonin-selective reuptake compounds like sertraline (Zoloft) and paroxetine (Paxil) were studied throughout the 1980s and were released in the 1990s as the first selective serotonin reuptake inhibitors (SSRIs), quickly achieving clinical popularity. As in the shift from MAOIs to tricyclics, SSRIs were no more efficacious as a class than their predecessors. SSRIs do, however, have a much-improved side effect and safety profile, and are unlikely to cause death in overdose. Improved safety is likely one of the reasons for the widespread popularity of this class. In the case of escitalopram, the availability of a single enantiomer of citalopram (escitalopram—Lexapro) provided a compound that could be introduced in lower doses, avoiding some of the common problems (anorgasmia, nausea) associated with SSRIs. Additionally, drugs classed as serotonin-norepinephrine inhibitors (SNRIs) such as venlafaxine (Effexor) as well as triple reuptake inhibitors (SERT, NET, and DAT inhibition) such as nefazodone (Serzone) are in clinical use.

Functionally, these drugs (reuptake inhibitors) rapidly increase concentrations of monoamine neurotransmitters at the synapse. Single doses of fluoxetine in rodents at 10mg/kg cause approximately 50% inhibition of serotonin reuptake with minimal effects

on norepinephrine reuptake, sustained up to 24 hours after dosing<sup>149,151</sup>. Effects on standard behavioral tests of antidepressant effect such as forced swim, tail suspension, or novelty-induced hypophagia show significant and characteristic antidepressant effects within 30 minutes<sup>152</sup>, although other behaviors like increased sucrose preference require longer treatment (20+ days) to evolve<sup>25</sup>.

The increased availability of neurotransmitter at the synapse promotes increased signaling at both pre- and post-synaptic sites. The post-synaptic membrane contains receptors appropriate to the pre-synaptic neuron with which it synapses (serotonin, norepinephrine, or dopamine), while the pre-synaptic membrane contains autoreceptors which inhibit release of neurotransmitter. In noradrenergic neurons, this autoregulation is achieved through  $\alpha_2$ -adrenoreceptors while 5-HT<sub>1A</sub> and 5-HT<sub>1B</sub> serotonin receptors mediate this inhibition in serotonergic neurons. Paradoxically, elevated synaptic neurotransmitter concentrations produced by reuptake inhibition has a sustained inhibitory effect on further neurotransmitter release by the pre-synaptic neuron<sup>153,154</sup> and suggests the possibility of drugs targeted at autoreceptor inhibition to further enhance neurotransmitter concentration in the synapse. Despite the inhibition of neurotransmitter release, the net effect of reuptake inhibition is to increase synaptic neurotransmitter availability.

#### **1.7.4 Selective membrane redistribution of G<sub>αs</sub> with antidepressant treatment**

The Rasenick laboratory has studied for many years the effect of antidepressants on G protein systems in immortalized cell lines such as C6 glioma. These cells display a predictable response to a variety of commonly used antidepressant compounds acting at



SERT, with nanomolar affinity<sup>155</sup>. However, not all cell line types show these responses. Antidepressant-responsive cells show a redistribution of  $G\alpha_s$  from lipid raft to non-raft membrane fractions with increased functional coupling of  $G\alpha_s$  and adenylyl cyclase, the reciprocal of changes observed in samples from depressed patients. This redistribution is not accompanied by a change in total membrane  $G\alpha_s$  content<sup>156</sup>. Biochemically, these changes are evidenced by increases in cAMP production compared to untreated controls, subsequent to stimulation with agonists of GPCR-mediated cAMP production, as well as direct activators of adenylyl cyclase and  $G\alpha_s$ <sup>50,157</sup>. Yet, these cells do not express SERT or other monoamine reuptake transporters<sup>67</sup>, suggesting that monoamine-targeted antidepressants act at a site or sites other than reuptake transporters.

### 1.7.5 Membrane accumulation of antidepressants

Furthering this idea, recent work by the Rasenick lab has demonstrated that a variety of antidepressants of differing classes (MAOI, SSRI) accumulate in membrane lipid rafts in living C6 glioma cells, in excess of their oil/water partitioning characteristics.

Accumulation of tricyclic antidepressants imipramine and amitriptyline, however, was much less<sup>67</sup>. This study extended the previous work of others who examined accumulation of antidepressant in isolated membranes<sup>66</sup>. Particularly notable was the finding that while escitalopram accumulates in lipid rafts, *R*-citalopram does not, despite their similar lipid solubility. The membrane accumulation of antidepressant despite low oil-water partitioning, and the peculiar lack of *R*-citalopram accumulation suggest a specific membrane target or targets able to bind antidepressants. Again, as these cells do not express SERT or other reuptake transporters, this target is not a reuptake transporter. It is

presently unclear how the accumulation of antidepressants in lipid raft relates to their mechanism of action.

### **1.7.6 HDAC6 inhibitors and ketamine as antidepressants**

While the above antidepressants act on monoamine signaling (in addition to their effect on G proteins), as do most antidepressant drugs released in the era of modern psychopharmacology, other drug classes not linked to monoamine metabolism or trafficking are now under study and in limited clinical use. Two such drugs/classes are histone deacetylase (HDAC) 6 inhibitors, as well as the common anesthetic drug ketamine; both are currently under study by members of the Rasenick laboratory.

HDACs, a family of 11 related enzymes, inhibit transcription via deacetylation of N-terminal histone lysine residues, promoting the condensation of chromatin in the nucleus<sup>158</sup>, while HDAC inhibition has the opposite effect. Inhibition of numerous HDAC isoforms has produced an antidepressant effect in animal models, and numerous and varied changes in HDAC expression are seen in depression<sup>159</sup>. Hobara et al., for example, examined blood samples of mood disorder patients and found elevated mRNA for HDAC2 in MDD, with normalization of mRNA after successful treatment and remission<sup>160</sup>. In contrast, Covington et al. showed in a social defeat model of depression in mice a decrease in HDAC2 mRNA<sup>161</sup>; these opposite findings could be related to the nature of the sample (blood vs. specific brain region).

Specific inhibition of HDAC6 has received recent attention in the treatment of depression. In the case of HDAC6, “HDAC” is effectively a misnomer as this isoform is primarily cytosolic, acting as a deacetylase for variety of cytosolic proteins, notably tubulin/microtubules<sup>162,163</sup>. The interaction between G proteins, including  $G\alpha_s$ , and tubulin/microtubules is well-established and described by Schappi et al.<sup>164</sup>. The interplay between tubulin acetylation and lipid raft content of  $G\alpha_s$  is currently under study in the Rasenick laboratory.

Ketamine is an anesthetic widely used both in clinical and research settings. Its canonical mechanism of action involves inhibition of glutamate’s NMDA receptor, binding a site inside the channel also acted upon by phencyclidine (PCP), another inhibitor of the NMDA channel<sup>165</sup>, producing an unusual “dissociative anesthesia.” Ketamine’s antidepressant properties have been under study since at least the early 1990s and are markedly different than those of traditional antidepressants with respect to the timing of therapeutic effects: while reuptake inhibitors require 4-12 weeks of treatment, ketamine’s effects are nearly instantaneous and persist for 1-2 weeks after a single dose<sup>166</sup>. This rapid action is obviously desirable, and ketamine is now widely-researched in the context of depression.

Despite many studies, no accepted mechanism of action exists to explain ketamine’s antidepressant effects. Autry et al. suggested that ketamine’s antidepressant effects are due to increased expression of neurotrophic factor BDNF, occurring through increased BDNF mRNA translation<sup>167</sup>. Their model suggests that inhibition of  $Ca^{2+}$  influx through the NMDA channel depresses the inhibitory activity of  $Ca^{2+}$ -calmodulin dependent elongation

factor 2 (EF2) kinase. This loss of inhibition then allows increased EF2 activity and increased BDNF synthesis. The Duman group has suggested activation of the mTOR pathway by ketamine, though this has not been widely replicated, and recently has implicated GABA<sub>A</sub> receptors in the process. Blockade of GABA<sub>A</sub> receptors inhibited the release of BDNF subsequent to ketamine exposure in primary neuronal cultures<sup>168</sup>. Zanos et al. demonstrated in mice that ketamine's antidepressant effects are mediated through its *N*-demethylated metabolites, and furthermore, that these effects are independent of action at the NMDA receptor<sup>169</sup>. This is somewhat analogous to the phenomenon under study in this thesis, in that the drug's antidepressant effect does not seem to involve its canonical mechanism of action. Again, further study is required, and ketamine is currently a very active area of research.

## **1.8 Fluorescence recovery after photobleaching (FRAP)**

### **1.8.1 FRAP background**

The technique of FRAP aims to assess the lateral mobility of proteins in the plasma membrane via analysis of the speed at which a photobleached region of fluorescent tagged proteins recovers fluorescence. Although the technique has gained popularity in the past two decades, particularly in the 2000s<sup>170</sup>, the basic technique was established and in use by the 1970s<sup>171-173</sup>. Although fluorescent proteins and confocal microscopy were not yet

available, proteins of interest were labeled with rhodamine or fluorescein isothiocyanate (FITC) and viewed through a fluorescence microscope.

Particle diffusion in general depends on a variety of factors including temperature, viscosity of the medium, and particle size (Stokes-Einstein equation). In the case of a protein in a membrane, other factors restrict the diffusion of a given protein, such as protein-protein interactions with other membrane proteins or cytoskeleton<sup>174</sup>. In FRAP analysis, mobility is indicated by the half-time of recovery, which is the time required for 50% recovery of fluorescence intensity; this is the primary parameter of analysis considered in this paper. A longer half-time reflects lower or slower mobility, while a shorter half-time reflects greater or faster mobility.

Experimentally, one must have a fluorescent-labeled protein properly expressing in a cell of interest. Other considerations include heating of the sample by the laser, which could alter mobility characteristics. This is limited by the use of very brief (millisecond) exposures to the bleaching pulse. Photoswitching of fluorophores can also occur after bleaching; this is a spontaneous reversion of the bleached form of the fluorophore to the fluorescent form through a molecular rearrangement. Photobleached green fluorescent protein and its variants will revert to a fluorescent state with a low (~15% or less) probability. This effect could complicate analysis since recovery includes reactivating fluorophores, instead of reflecting only newly diffusing fluorophores. This is mitigated by the practice of comparing samples under identical conditions, which should show the same degree of photoswitching<sup>175</sup>. In the present study, the GFP-  $G\alpha_s$  construct used was created

by the Rasenick laboratory and is fully described in Yu, et al.<sup>176</sup> and is depicted in Figure 4. It utilizes an internal, rather than a terminal, GFP tag, and is membrane localized normally, and activates adenylyl cyclase in the same manner as wild type  $G\alpha_s$ . The GFP portion of the construct was further modified with A206K mutation, which prevents aggregation of GFP molecules<sup>177</sup>.

### 1.8.2 Sample FRAP experiment and analysis

Figure 5 shows the general scheme of a FRAP experiment. A selected region of interest is bleached, and recovery of fluorescence (though never a complete recovery) occurs over a period of time. The “normalized recovery” vertical axis reflects light intensity measured by the microscope. Thus, one sees a given initial intensity, followed by an immediate drop in intensity (bleaching), followed by a gradual return of intensity as new fluorescent GFP-  $G\alpha_s$  molecules diffuse into the bleached region. In this graph (Figure 5b), note that the recovery of control (no drug) cells is nearly superimposed on the recovery of *R*-citalopram (inactive stereoisomer of escitalopram). This indicates that the rate of recovery of fluorescence is nearly identical in both cases. In contrast, the recovery of escitalopram-treated cells is less steep. This indicates a slower recovery of fluorescence. In practice, this presentation of data is somewhat cumbersome, so a single number is derived from each curve to describe the process. This value is the half-time of recovery, and all FRAP data henceforth are presented in this format.

As a point of clarification, it is important to note the significance of the numbers produced by the FRAP assay. FRAP is “qualitatively quantitative”. Although a number is ultimately

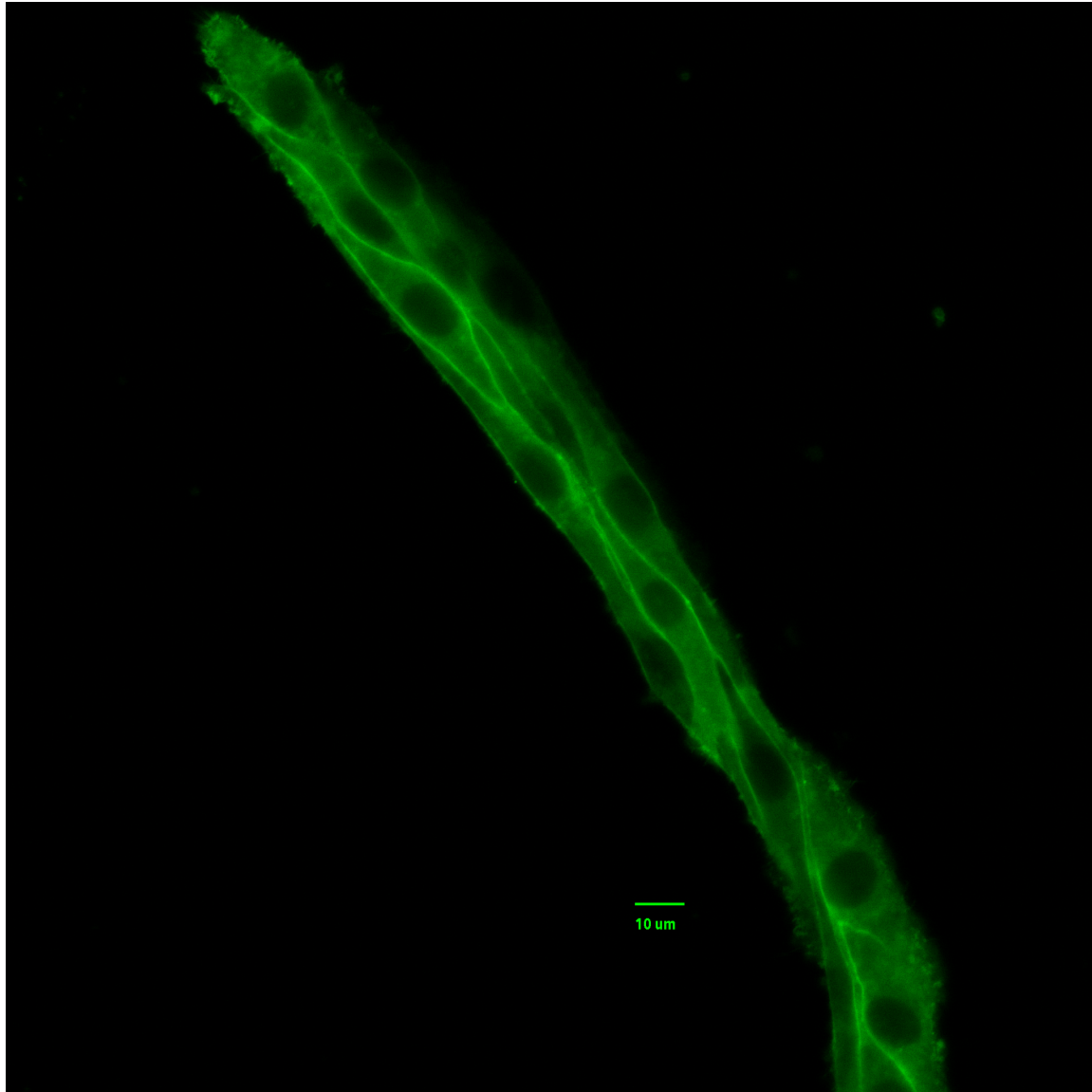


**Figure 4: C6 glioma stably expressing GFP-G $\alpha_s$**

C6 glioma express GFP-G $\alpha_s$  over the entire plasma membrane in a slightly patchy distribution. All cells do not show equal fluorescence due to microscope focus.

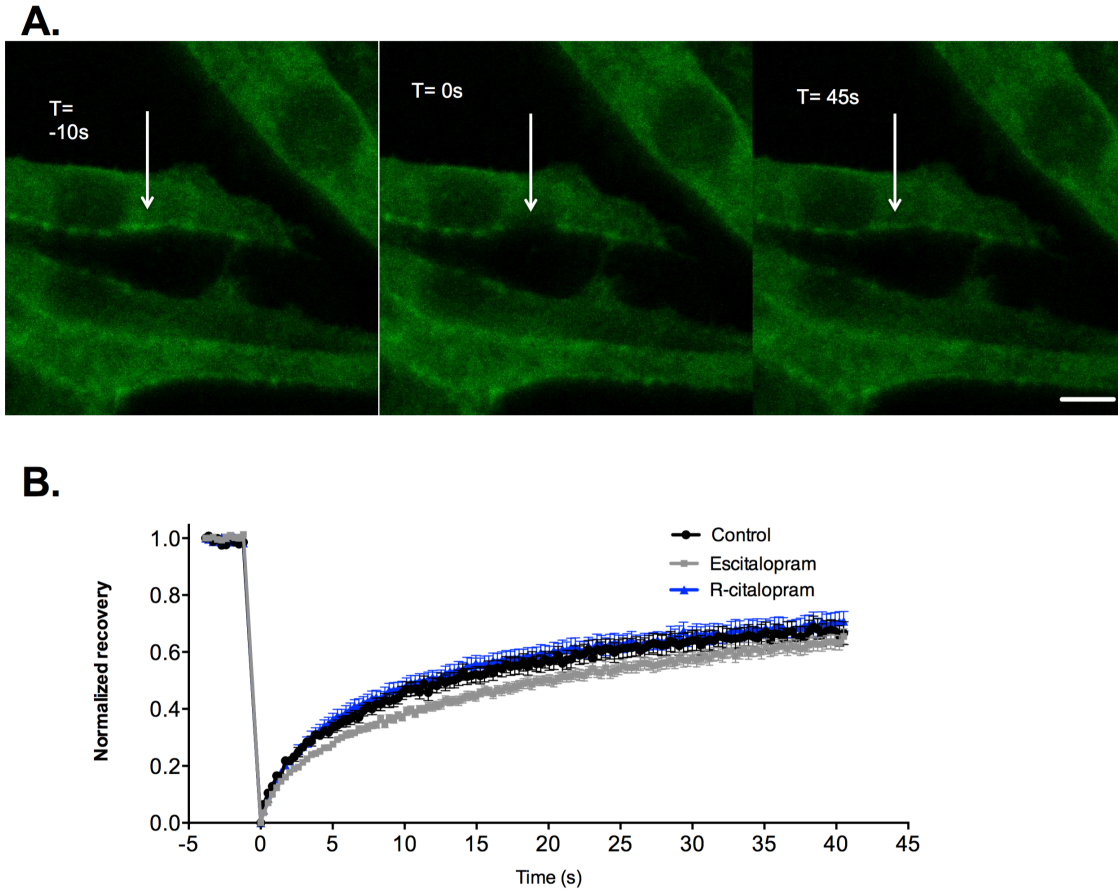


**Figure 5: General scheme of a FRAP experiment**

(a) C6 glioma expressing GFP- $G\alpha_s$  before photobleaching, immediately post-photobleaching, and after recovery of fluorescence.

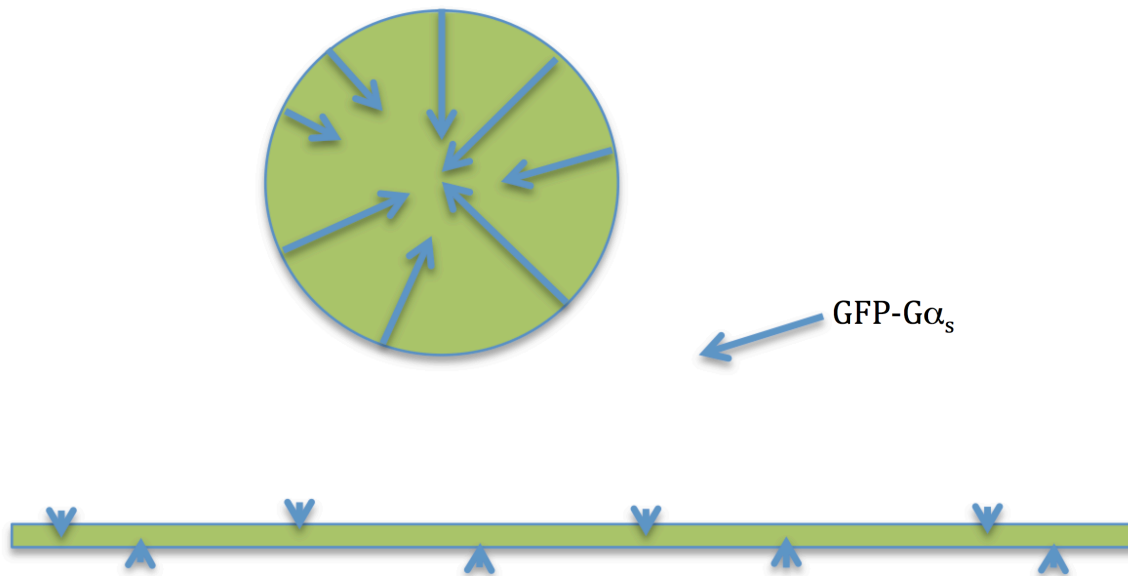
(b) FRAP recovery of C6 glioma expressing GFP- $G\alpha_s$  under three treatment conditions. Recovery is less rapid for escitalopram treatment.



generated (the half-time of recovery) by the analysis software, this value has no intrinsic significance. Furthermore, the same sample analyzed by two different microscope systems, even identical systems from the same manufacturer, will likely give different results due to subtle variations in the light path. For this reason, it is important that comparisons are all done on the same microscope system; this is true of the data in this thesis. As illustration of the utility of the half-time of recovery, consider the following thought experiment (Figure 6): a fluorescent protein is studied by FRAP under two differing conditions. A membrane region of equal area is photobleached in both, but the geometry of the bleached region differs in the two cases.

In the first, a circular region is bleached. This configuration would maximize the distance for new fluorescent molecules to diffuse into the bleached region. In the other case, a long, thin rectangular region of equal area is bleached. New fluorescent molecules would have far less distance to diffuse and a much lower half-time of recovery would be recorded. As a theoretical extreme, a nearly infinitely long rectangle of the same area would recover its fluorescence nearly instantaneously. In the cases of both the circular and rectangular regions, the same area is being bleached, and the same number of molecules is involved. Yet, drastically different half-time numbers would be obtained, and both would accurately reflect the specifics of the experimental conditions. Because of the above, one could not use half-time of recovery to make any claim about the stoichiometry of the phenomenon observed; a 10% change in half-time after drug treatment does not suggest or correspond to an effect upon 10% of the protein under consideration, for example.

Region 1: longer diffusion paths (slower)



Region 2: shorter diffusion paths (faster)

**Figure 6: Region of interest geometry and FRAP results**

Thought experiment contrasting FRAP of regions of equal area with differing geometry. Though equal numbers of fluorophore molecules must diffuse to restore fluorescence in both cases, recovery would be much faster in the thin rectangle (Region 2) compared to the circle (region 1), because molecules have a much shorter distance to travel.

## 1.9 Cell lines

### 1.9.1 C6 Glioma

C6 glioma cells were developed in 1968 by Benda, et al. and further characterized by Schmidek, et al. at Massachusetts General Hospital<sup>178,179</sup>. Outbred Wistar rats were injected with the tumorigenic alkylating agent n-nitrosomethylurea, and subsequent CNS tumors which developed were removed and studied; tumor “6” provided the cells which constitute the C6 glioma cell line and was described as a grade 2 astrocytoma (glial cell/astrocyte origin), a histologically mid-grade tumor. Tumors produced in vivo by the administration of C6 glioma cells in rat models are more severe grade 3/4 astrocytomas<sup>180</sup>.

C6 glioma is described by American Type Culture Collection (ATCC) as having fibroblast morphology. The cells are generally spindly, though pleomorphic. Glial fibrillary acidic protein (GFAP), a structural intermediate filament protein characteristic of glial cells (though also produced in non-neural cell types such as kidney and testis<sup>181,182</sup>), is produced. An intracellular S100 protein, characteristic of neural crest-derived tissue, is found in C6 glioma and cycles through each passage, increasing with cell confluency and decreasing after passage<sup>178,183</sup>. S100 proteins are acidic, Ca<sup>2+</sup> regulated EF-hand containing proteins with varied roles. C6 have been differentiated neurally<sup>184</sup> and glially<sup>185,186</sup> and are well-accepted as a cell line of neural origin.

### 1.9.2 HEK293

HEK293 (Human Embryonic Kidney) are a well-known and widely-used cell line, second to HeLa in general biological usage and second in use to CHO (Chinese hamster ovary) in pharmaceutical production<sup>187</sup>. This line was created in 1973 from aborted human kidney tissue infected with sheared adenovirus 5 DNA<sup>188</sup>. Expression of adenoviral E1a/E1b proteins immortalize the cell by driving cell cycle progression and inhibiting apoptosis<sup>189</sup>. Numerous variants of HEK293 for specialized applications have been developed, such as HEK293T/HEK293FT for rapid cell growth and protein expression, and HEK293S for growth in suspension. HEK293 and its common variants have recently been characterized and sequenced: HEK293 are pseudotriploid, and apparently female, as no Y-chromosomal sequences were detected in any of the variants<sup>187</sup>. The study also examined the stability of the HEK293 genome over a period of seven passages in HEK293T. While the HEK293 variants significantly diverged both in genome content and gene expression, these factors were quite stable over seven passages within a given variant (here, HEK293T). Thus, while HEK293T diverged somewhat over a period of seven passages, the initial and seventh passage cells were more similar to each other, than they were to HEK293S, for example. The authors note, however, that the ability to generate these variants in response to assorted selection techniques suggests a particular genetic flexibility in HEK293 cells, and that a culture of HEK293 cells is likely to be genomically heterogeneous. Cell line stability and consistency is an issue of general concern in cell culture.

Finally, HEK293 were initially prepared from a crude homogenate of embryonic kidney, which would be expected to contain a variety of cell types: kidney stroma, tubules,

developing vasculature, and neural tissue. One study found the expression of several neurofilament proteins (neural intermediate filament/cytoskeletal components) in HEK293<sup>190</sup>. The authors also created independently several human and rodent embryonic kidney lines via transformation with adenovirus 5 and 12. Many, though not all of the lines created, also express various neurofilament proteins; the authors posit that perhaps adenovirus preferentially transforms neural cell types and that HEK293 are of neural origin. Nonetheless, HEK293 are most widely regarded and accepted as being of kidney tubular epithelial origin.

### **1.9.3 PC12**

Like C6 glioma, PC12 pheochromocytoma are a rat-derived cell line from a tumor of neural origin. PC12 were initially isolated from rat pheochromocytoma, a catecholamine secreting tumor of the adrenal medulla. Under nerve growth factor (NGF) stimulation, the cells develop a neural phenotype with neurite extensions as well as electrical excitability, and are often used as a model of neurons. Under dexamethasone stimulation, the cells develop an adrenal medulla chromaffin cell-like phenotype, the putative origin of the PC12 cell line itself<sup>191,192</sup>. PC12 produce, store in vesicles, and secrete dopamine and norepinephrine. Even under dexamethasone-stimulated differentiation into chromaffin-like cells, though, they do not produce epinephrine, as phenylethanolamine-N-methyltransferase (PNMT) is not expressed, preventing the conversion of norepinephrine to epinephrine<sup>192</sup>. PC12 do not express adrenergic receptors, and are not responsive to stimulation by catecholamines<sup>193</sup>.

#### **1.9.4 COS7**

Unlike PC12, but similar to HEK293, COS7 were created from African Green Monkey kidney tissue in successive transformations by the Rous sarcoma virus (RSV) and simian vacuolating virus (SV40) <sup>194,195</sup>. These cells have fibroblast morphology and are often used as a model of such; they are also commonly used in general studies of cellular signaling and other cellular phenomena.

### **1.10 Specific Aims**

Antidepressant drugs have been used for nearly 70 years, but remain incompletely understood. This study seeks to better understand antidepressant action, particularly their effect on G proteins, through study of cells that respond to antidepressants compared to cells which do not.

#### **1.10.1 Aim 1: Identification and characterization of antidepressant responsive and nonresponsive cell lines**

Cells having a clear G protein antidepressant response or lack of response must be identified for study, and the nature of their response with respect to G proteins must be characterized. Cells should not express SERT (or other reuptake transporters), as this study will evaluate actions independent of monoamine transporters.

### **1.10.2 Aim2: Evaluate effect of SERT expression on antidepressant response of cell lines identified in Aim 1**

The antidepressant response under study is thought to occur independent of SERT, a canonical antidepressant target. This study will examine how the expression of SERT affects this response, both in antidepressant responsive and non-responsive cell types. Cells that do not express SERT or other reuptake transporters will be utilized, and their antidepressant response compared to that of versions transgenically expressing SERT.

### **1.10.3 Aim 3: Evaluate effect of adenylyl cyclase isoform expression on antidepressant response of cell lines identified in Aim 1**

The antidepressant response under study involves increased production of cAMP secondary to altered G protein localization enhancing  $G\alpha_s$  coupling with adenylyl cyclase. Investigation thus far has focused primarily on the involvement of  $G\alpha_s$  in this process. This study will examine the role of adenylyl cyclase in this interaction; specifically, does expression of specific adenylyl cyclase isoforms factor into this response?

### **1.10.4 Aim 4: Development of an improved assay of antidepressant response via FRAP**

The Rasenick laboratory sought to develop a higher throughput assay of antidepressant response. Over the course of this study, I collaborated in the development of a new assay of antidepressant response utilizing the FRAP technique.







## **Chapter 2: Materials and Methods**

### **2.1 Cell Culture and Drug Treatments**

C6 glioma and HEK293 cell lines were obtained from American Type Culture Collection (ATCC, Manassas, VA). C6 glioma, COS7, and PC12 pheochromocytoma cells were cultured in Dulbecco's modified Eagle's medium (DMEM), 4.5 g of glucose/L, 10% newborn calf serum (Hyclone Laboratories, Logan, UT). HEK293 were cultured in Minimum Essential Medium (MEM) also including 10% fetal calf serum (Hyclone Laboratories, Logan, UT) as above. Both DMEM and MEM used were Gibco brand (ThermoFisher, Waltham, MA) or Mediatech (Corning, Manassas, VA). Media for initial experiments with adenylyl cyclase assays included 100 mg/ml (1%) penicillin and streptomycin. For subsequent experiments, antibiotic treatment was not used. This was done to prevent any minor contaminations from going unnoticed. No deleterious effects on cell culture, such as increased frequency of contamination, were noted after discontinuation of antibiotic prophylaxis. C6 and HEK293 cell lines used throughout this study were also tested for mycoplasma contamination according to manufacturer's instructions with MycoAlert™ Mycoplasma Detection Kit (Lonza, Walkersville, MD). No cells tested positive for mycoplasma contamination.

All cells were grown at 37°C in a humidified 5% CO<sub>2</sub> environment. The cells were generally treated with 10µM antidepressants, for three days or as otherwise specified in the Results section. In all cases, cell media and drug were changed daily. Drug treatments had no observable deleterious effects on cell growth or morphology.

Escitalopram and *R*-citalopram were gifts from Lundbeck (Copenhagen, Denmark). Venlafaxine and sertraline were gifts from Pfizer (New York, NY). Desipramine hydrochloride, reserpine, tianeptine sodium salt, and bupropion hydrochloride were obtained from Tocris Bioscience, Ellisville, MO. Lithium chloride, chlorpromazine hydrochloride, fluoxetine hydrochloride, d-amphetamine sulfate, imipramine hydrochloride, phenelzine sulfate, olanzapine, haloperidol, diazepam, imipramine hydrochloride, colchicine, and M $\beta$ CD were obtained from Sigma-Aldrich (St. Louis, MO).

## 2.2 Expression Plasmids

The primary fluorescent construct, GFP-G $\alpha_s$  used in this study was developed in the Rasenick laboratory and is described in Yu et al.<sup>176</sup>. GFP-G $\alpha_s$  A206K was developed by Andrew Czysz with Stratagene Quick-change mutagenesis kit using the Rasenick laboratory's previous GFP-G $\alpha_s$  construct as a template<sup>176</sup>. This mutation is widely used and was implemented based upon the work of Zacharias et al.<sup>177</sup>. Substitution of lysine for alanine at the 206 position of GFP prevents aggregation of GFP and poor membrane expression of the construct, as well as decreased cell viability. Other plasmids used include adenylyl cyclase constructs (AC2,3,6 and fluorescent variants) supplied by the laboratory of Carmen Dessauer (University of Texas at Houston) and Dermot Cooper (AC8)(University of Cambridge, England).

### **2.3 Transfection and generation of stable/clonal cell lines**

All transfections were performed via the Neon Transfection System (Invotrogen/ThermoFisher, Waltham, MA) according to the manufacturer's protocol. Transfections were done using 5-10 $\mu$ g of plasmid DNA per million cells. Post transfection, cells were grown in flasks with cell-appropriate media containing G418 (Sigma, St. Louis MO) 1mg/mL for at least three passages to select for transfected cells (plasmids utilized generally carried G418 resistance). The clonal C6 GFP-G $\alpha_s$  line used throughout the FRAP experiments was obtained through fluorescence-activated cell sorting (FACS) at the UIC Research Resources Center (RRC) flow cytometry service. The expressed GFP-G $\alpha_s$  construct retains its native ability to bind GTP as well as activate adenylyl cyclase<sup>176</sup>. For experiments using HEK293 expressing GFP-G $\alpha_s$ , the same transfection procedure was used, but clonal cell lines were not created via FACS. In this case, G418-selected stable, but not clonal, cells were used. The results obtained were consistent from experiment to experiment, suggesting no additional benefit would be gained from the lengthy FACS/clonal selection process. C6 and HEK293 expressing adenylyl cyclase isoforms were created similarly as stable, but not clonal, lines. C6 glioma and HEK293 stably expressing hSERT were obtained from the laboratory of Susan Amara (University of Pittsburgh, currently NIMH).

### **2.4 Lipid Raft Density Gradient Preparation**

After drug treatment, cells were washed and harvested in ice-cold phosphate-buffered saline (PBS) by Mediatech (Corning, Manassas, VA). Cells were lysed in buffer containing 10

mM HEPES, 150 mM 30 NaCl, 0.25M sucrose, 1 mM DTT, protease inhibitor cocktail, pH 7.4. The buffer also contained 1% TX-100 (Sigma, St. Louis, MO) to solubilize non-raft membrane fractions. Cells were homogenized with 10 strokes of a Potter-Elvehjem homogenizer. Cell homogenates were mixed with equal volumes of 80% sucrose in HEPES buffer to form 40% sucrose and placed in Beckman Ultra-Clear ultracentrifuge tubes. Sucrose gradients were made by carefully layering 30, 15, and 5% sucrose over the homogenate. The tubes were then centrifuged at 100,000 x g for overnight (>16 hours) in an SW55 rotor (Beckman, Palo Alto, CA). Cloudy bands between the 15 and 30% sucrose layers contain lipid raft material and these were carefully suctioned from the tube, pelleted, and resuspended in HEPES buffer for protein estimation via Bradford assay or NanoDrop (ThermoFisher, Waltham, MA) prior to western blotting. For each sample, a portion of whole cell lysate was also reserved to determine total cellular content of proteins of interest.

## **2.5 Polyacrylamide Gel Electrophoresis and Western Blotting**

After protein estimation as described above, equal amounts of protein were loaded in lanes of Bio-Rad Stain-Free gels (Bio-Rad, Hercules, CA). These gels contain a proprietary fluorescent compound which labels tryptophan residues in the sample. After electrophoresis, gels were imaged under fluorescence in a Bio-Rad ChemiDoc. This procedure allows visualization and quantification of the total protein banding pattern per lane. Thus, later normalization for protein loading of western blot results is based on the

total lane protein content. This obviates the need to run a second western blot to normalize results to a particular cellular protein such as actin. After electrophoresis, gels were transferred to Immobilon-P PVDF membranes (EMD Millipore, Billerica, MA). Membranes were blocked with 5% nonfat dry milk in TBS-T (10 mM Tris-HCl, 159 mM NaCl, and 0.1% Tween 20, pH 7.4) for 1 h. After blocking, membranes were thrice washed with TBS-T and incubated at 4°C with primary antibody until the next day. Membranes were then thrice washed with TBS-T and incubated with secondary antibody as appropriate [HRP-linked anti-mouse antibody IgG F(ab')<sub>2</sub> or HRP-linked anti-rabbit antibody IgG F(ab')<sub>2</sub>] (Jackson ImmunoResearch, West Grove, PA) for 1 hr at room temperature, thrice washed in TBS-T, and developed with ECL Luminata Forte reagent (Millipore, Billerica, MA). Bio-Rad ChemiDoc (Bio-Rad, Hercules, CA) system was used to image membranes, which were then quantified with Bio-Rad ImageLab 5.2.1 software (Bio-Rad, Hercules, CA). Anti-G $\alpha_s$  antibody was obtained from NeuroMab (Davis, CA). Anti-G $\alpha_i$  and anti-G $\alpha_q$  antibodies were obtained from Santa Cruz Biotechnology (Dallas, TX).

## **2.6 Fluorescence recovery after photobleaching (FRAP)**

Cell lines expressing fluorescent-tagged proteins of interest were grown and treated with drug in glass-bottom microscope dishes. One hour prior to imaging, media was replaced with phenol red-free media containing a lower amount of serum (2.5% newborn calf serum). This was done to wash out drug (to demonstrate effects are chronic, not acute responses to the presence of drug) as well as eliminate extraneous sources of background fluorescence (phenol red, various serum components). Cells were imaged at 37°C

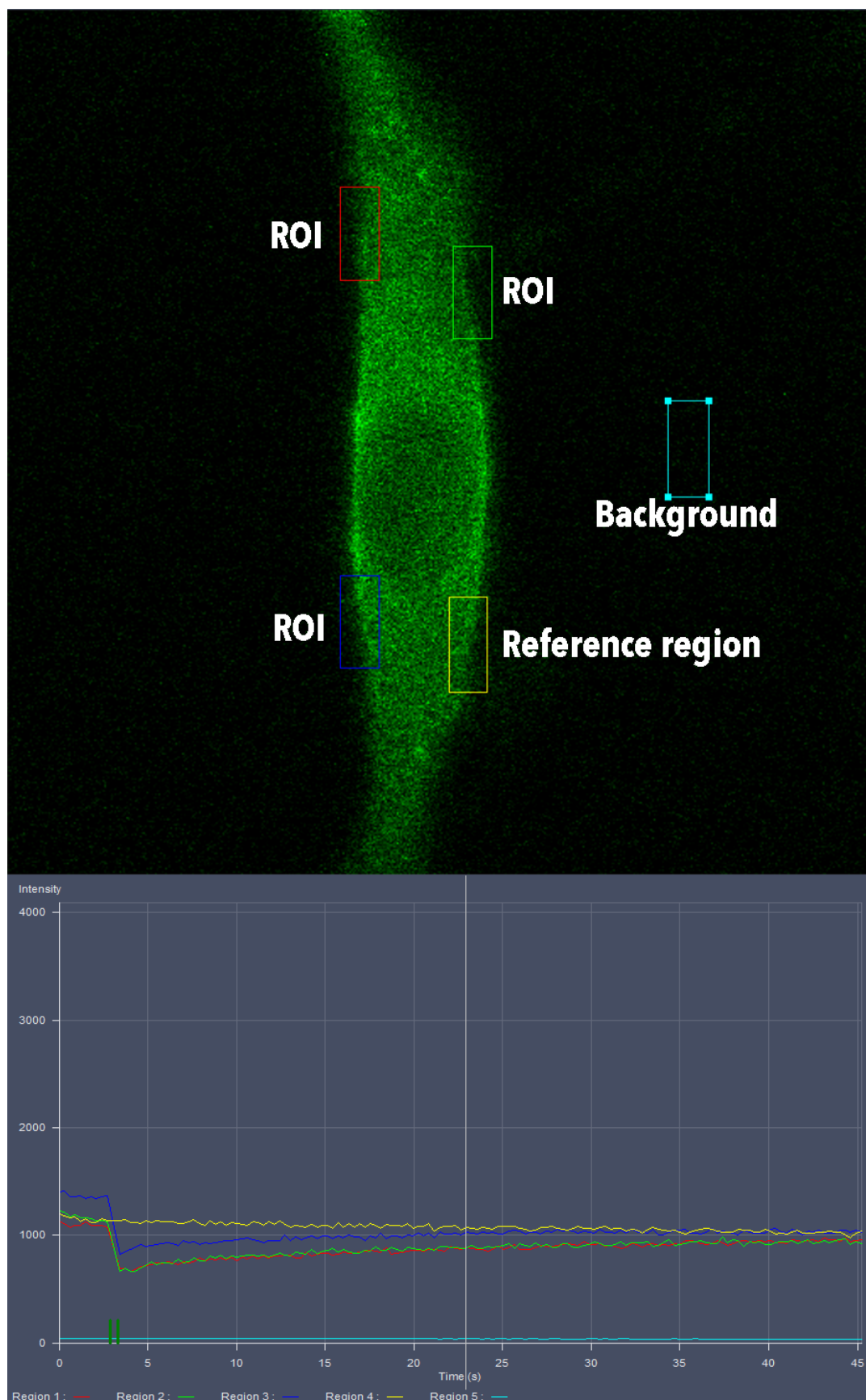
maintained by Pecon heated stage insert in a Zeiss LSM 710 confocal microscope. Images were obtained at 512x512 resolution with open confocal pinhole; this allowed fast imaging and maximum signal while minimizing unwanted photobleaching. For each region imaged, 150 images separated by 300ms were collected to capture the process of photobleaching and gradual recovery of fluorescence. Half-time to recovery was calculated by the FRAP module of the Zeiss Zen microscope software, including adjustment of values to account for background intensity as well as overall photobleaching. For each cell imaged, three test regions of interest of 23 x 55 pixels were tested; this was generally the largest number that could be practically tested due to the size of the field. Each region of interest generates one “data point,” as referenced in the results section. At 400x on the Zeiss 710 microscope system, these regions of interest are 2.3 $\mu$ m x 5.5 $\mu$ m; as lipid rafts range from 10-200nm<sup>56</sup>, the regions of interest are not limited to raft or nonraft, but contain a mixture of both domains. Thus, these FRAP experiments do not measure the mobility of GFP-G $\alpha_s$  in raft or nonraft specifically; instead, net membrane mobility is measured, incorporating raft and nonraft regions. Regions at the “edge” of the cell are selected because of greatly increased signal/noise ratio in this area. Other groups have used more central regions of interest<sup>174</sup>, while others have extended the technique to nonmembrane soluble proteins such as nuclear actin<sup>196</sup> or even structural proteins such as sarcomeric protein CapZ<sup>197</sup>. These are non-typical applications of FRAP and perhaps reflect a versatility of the FRAP technique in assessing protein turnover in nonmembrane environments.

Figure 7 (top panel) shows the setup of a FRAP experiment. The green, red, and dark blue regions are regions of interest selected by the experimenter, which will be photobleached

and measured for return of fluorescence. The yellow region is a reference region, which is not bleached, but measured to correct for general photobleaching, which is factored into the analysis of the regions of interest. Fluorescence can widely vary over the field of view, and it is important to select a reference region of comparable intensity to the regions of interest. In my experience, this greatly increases the consistency of the data. The Zeiss Zen software FRAP component allows selection of this region in real time, so intensities can be matched. Finally, the light blue region represents background fluorescence and is generally of low intensity, and is also factored into the analysis of regions of interest.

Figure 7 (lower panel) shows the typical progress of a FRAP experiment, from initial pre-bleaching conditions through recovery. Note all regions begin at a similar intensity (excepting background reading). The yellow line represents the reference region, which is not bleached but generally decays in intensity due to background photobleaching. The green, red, and dark blue lines represent the regions of interest. These show a sharp initial decrease due to strong photobleaching at full laser power, and gradual recovery, finally nearly reaching the intensity of the reference region. The recovery is never complete, due to an “immobile fraction” of fluorophore, which does not recover on the time scale of the experiment. There is presently no accepted physical interpretation for this consistent finding in FRAP experiments. From each of these recovery curves, various quantifications can be made. These FRAP experiments utilize the half-time of recovery, as it has shown itself to be a consistent indicator of antidepressant response as assessed by GFP-G $\alpha_s$





**Figure 7: Setup of FRAP experiment**

Regions of interest (ROIs) are selected for bleaching, along with an unbleached reference region to assess background photobleaching, as well as a background region. After bleaching, indicated by dual green vertical lines on the graph, regions of interest rapidly lose fluorescence, which returns over the course of the experiment due to diffusion of unbleached GFP- $G\alpha_s$  molecules into the bleached region. Colored lines on the graph reflect regions selected above.

mobility. Other factors, particularly immobile fraction, have shown no consistency with regard to antidepressant effect or lack thereof, and are not considered in this thesis.

## **2.7 Membrane Adenylyl Cyclase Activity Assay**

Membranes for adenylyl cyclase activity after drug treatment were obtained by lysing cells in buffer (10 mM HEPES, 150 mM 30 NaCl, 0.25M sucrose, 1 mM DTT, protease inhibitor cocktail, pH 7.4) with 10 strokes of a Potter-Elvehjem homogenizer. An initial low speed spin of 1000xg for 10 minutes was used to remove the nuclear fraction. This was followed by a higher speed spin of 1000,000xg for 30 minutes in a table top ultracentrifuge to pellet cell membranes. Adenylyl cyclase assays were done according to the method of Salomon<sup>198</sup>. Cell pellets were resuspended in buffer (15mM HEPES buffer, 1x protease inhibitor cocktail, pH 7.5) and protein content estimated by Bradford assay. From these protein values, 25 µg of membranes were added to a reaction mixture containing 15 mM HEPES, 0.05 mM ATP, 2.5 µCi/ml [<sup>32</sup>P]ATP, 5 mM MgCl<sub>2</sub>, 1 mM EGTA, 1 mM DTT, 0.05 mM cAMP, 0.01 mM GTP, 0.25 mg/ml bovine serum albumin, 0.5 mM 3-isobutyl-1-methylxanthine (IBMX), 0.5 mg/ml creatine phosphate, and 0.14 mg/ml creatine phosphokinase at pH 7.5. For experiments with NKY80 inhibition, NKY80 was included in the reaction cocktail at a concentration of 10µM. For experiments with Ca<sup>2+</sup> inhibition, final reaction cocktail concentration of 0.8mM was used to achieve a final concentration of 0.2µM (due to EGTA chelation of Ca<sup>2+</sup>), calculated by Maxchelator program. Reactions were run at 30°C per assay protocol. Generated cAMP is separated from ATP by sequential

Dowex and alumina columns. Key components of this mixture include phosphodiesterase inhibitor IBMX to prevent hydrolysis of the generated cAMP, as well as nucleotide triphosphate regeneration system of creatine phosphate and creatine phosphokinase. This regeneration system allows minimal starting concentrations of ATP, which must be separated from cAMP in the final two-column step. Without regeneration, larger starting amounts of ATP would be required and could affect the final column separations of cAMP from ATP. Before column separation, a known amount of [<sup>3</sup>H]cAMP was also added to each sample to measure recovery of cAMP through the columns. Quantitation of cAMP was determined by liquid scintillation counting and mathematical analysis. All samples were assayed in triplicate.

## **2.8 Cell lines: Problems and solutions**

One issue consistently observed was an inverse relationship between C6 glioma cell density/confluence and the ability to detect a change by any of the above techniques in G protein localization subsequent to antidepressant treatment. It is difficult to state a precise percentage confluency at which the antidepressant effect is lost or not detected, but as cells exceed approximately 75% coverage of the flask or dish in which they are grown and treated, the effect becomes undetectable. The earliest characterizations of the C6 glioma cell line noted the cyclical increase and decrease of astrocytic S100 protein with each growth and passage of the cells; as cells became more confluent, S100 protein increases, and decreases again after passage<sup>178</sup>. Several classes of S100 proteins have been shown to cause destabilization and disassembly of microtubules<sup>199</sup>. Thus, the effect of increased confluence and S100 expression could decrease microtubule stability. This could cause an

effect similar to the result of microtubule-disrupting colchicine treatment presented in Section 3.1.2., in which the effect of raft disrupting treatments colchicine and methyl- $\beta$ -cyclodextrin is tested. Those data demonstrate that either treatment causes a nonselective exodus of G proteins from lipid raft into nonraft domains. If increased expression of S100 proteins causes a destabilization of microtubules similar to the effect of colchicine, then all experimental groups including the control would experience a loss of G proteins, particularly  $G\alpha_s$ , from lipid rafts. This condition would obscure any differences between experimental groups and present itself as a “loss” of antidepressant effect. The loss of the cells’ ability to demonstrate an antidepressant effect is not permanent, and should be returned to baseline with the next passage, ostensibly because of the decreased expression of S100 proteins. This problem can be avoided by avoiding overly confluent cell conditions during treatment and keeping confluency to less than approximately 75%.

A second, and quite vexing, problem also occurred with the clonal C6 glioma GFP-  $G\alpha_s$  cell line used for FRAP experiments. The cell line was originally established by electroporation, G418 selection, and cell sorting by Andrew Czysz as described above. At the time, numerous aliquots of these cells were frozen down for future use. Within two years of their creation, the cells began to lose fluorescence, rendering them too dim for proper imaging and FRAP, save the occasional appearance of a brighter cell. The dimness was in excess of that which could be compensated by increased laser power during microscopy, as the ratio of signal to noise decreases rapidly under such conditions. Frozen stocks were similarly affected. Extensive attempts to recreate the cell line were made both via electroporation and transfection reagents, varying a wide range of parameters for both.

New C6 glioma cells were ordered from ATCC. The GFP-  $G\alpha_s$  plasmid was regrown and sequenced for its GFP- $G\alpha_s$  component, as we considered that perhaps a mutation had occurred resulting in poor GFP expression or folding; the proper sequence was detected. None of these steps resolved the problem of GFP-  $G\alpha_s$  expression in C6 glioma: although the cells rapidly gained G418 resistance as expected, they remained dim and unusable. Contemporaneous testing of the plasmid in HEK293, however, continued to demonstrate the expected results of the plasmid: clear and bright membrane expression. This dramatically showed the progress of this project, and was not effectively resolved at the time. Since the completion of the experiments in this thesis, our GFP-  $G\alpha_s$  construct was recreated in a baculovirus vector by Montana Molecular (Bozeman, MT). This virus produces clear and bright membrane expression of GFP-  $G\alpha_s$ , and has restored the efficiency of FRAP experiments. The cause of the original problem was never determined. It may be the case that the original sorting procedure simply captured an “ideal” cell through serendipity, though this does not explain the loss of fluorescence from frozen stocks. As a result of this experience, I would hesitate to stubbornly invest such time again in a consistently fruitless endeavor. If an experiment consistently fails, one may have to adopt a dramatically different approach; in this case, use of a new expression vector was required and could have been tried sooner.

## **2.10 Lipid raft antidepressant accumulation**

These methods are extensive and fully discussed in Erb, et al.<sup>67</sup>.

### **2.10 Statistical Analysis**

All experiments were performed at least three times. Data were analyzed for statistical significance using Student's t or a one-way ANOVA followed by Tukey test for post hoc multiple comparisons of means as appropriate and as described in figure legends. Values of  $p < 0.05$  indicate significance. Analysis was done with Graphpad Prism 6.0 and 7.0 software.





## Chapter 3: Results

### 3.1 Identification and characterization of cell lines for further study

In the first set of experiments, cell lines suitable for this study were sought. The cells selected must display either a clear response, or a clear lack of response to antidepressant treatment with respect to G protein membrane redistribution and cAMP production. Cells must also lack SERT, as the antidepressant response in question is believed to be independent of antidepressant action at reuptake transporters. Though the Rasenick laboratory has traditionally utilized C6 glioma as a cellular model of positive antidepressant response<sup>50</sup>, no comprehensive index exists detailing these characteristics in commonly available cell lines, and cell lines meeting all these criteria will be determined experimentally. Furthermore, the entire G protein family response to antidepressant treatment in a variety of cell lines had not been characterized.

The initial experiments performed used the measure of membrane cAMP production in response to various agonists as indication of drug response. Cells were grown in flasks, treated with antidepressant for three days (the traditional time point used by the laboratory), harvested by scraping, lysed, and membranes pelleted by high-speed centrifugation (45k x g, 30 mins). These pellets were resuspended and assayed for cAMP production by the method of Salomon<sup>198</sup>(described in Materials and Methods).

### 3.1.1 Membrane adenylyl cyclase assay results demonstrating effect on cAMP production in C6 glioma, PC12 pheochromocytoma, HEK293, and COS7 with antidepressant treatment

Figure 8 shows the results in C6 glioma. In this and the three following figures, cAMP generation is compared in membranes from untreated cells versus cells treated for three days with 10 $\mu$ M escitalopram. Membranes were assayed at baseline (vehicle) or in the presence of agonist (10 $\mu$ M isoproterenol, 10mM NaF+20 $\mu$ M AlCl<sub>3</sub> (active as aluminum tetrafluoride anion [AlF<sub>4</sub>]<sup>-1</sup>), or 100 $\mu$ M forskolin). The data show modestly increased cAMP production (trend) at baseline, and significant increases in response to agonist stimulation, in membranes from cells treated with escitalopram compared to untreated cells.

Isoproterenol, a nonselective  $\beta$  receptor agonist, demonstrates activity through the full signaling pathway of agonist (isoproterenol) > receptor (here,  $\beta_2$  adrenergic receptor) > transducer (activated G protein) > effector (adenylyl cyclase) > second messenger (cAMP).

Forskolin is a strong, but not maximal, activator of adenylyl cyclase at the concentration used (100 $\mu$ M), as escitalopram treatment increased cAMP production in forskolin-agonized membranes. Fluoride as [AlF<sub>4</sub>]<sup>-1</sup> is an activator of G proteins, substituting for the third/gamma phosphate in GDP-bound (inactive) G proteins<sup>200</sup>. A nonhydrolyzable GTP analog such as GTP $\gamma$ S could also have been used for this purpose.

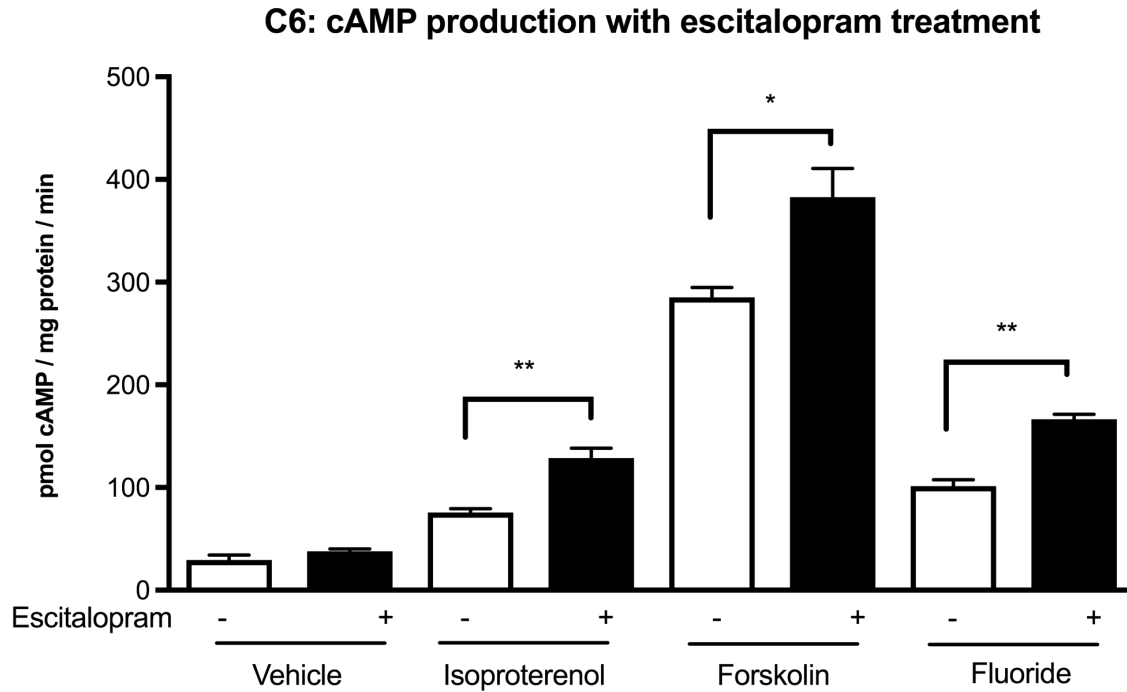


**Figure 8: Production of cAMP in C6 glioma membranes**

C6 glioma were treated in flasks for 3 days with vehicle (water) or 10 $\mu$ M escitalopram. Membranes were prepared and assayed for cAMP production as described in Materials & Methods. Membranes from cells treated with escitalopram demonstrate increased cAMP production in response to agonist compared to cells that were not treated with escitalopram. Agonists used were 10 $\mu$ M isoproterenol, 100 $\mu$ M forskolin or 10mM NaF+20 $\mu$ M AlCl<sub>3</sub> (active as aluminum tetrafluoride anion [AlF<sub>4</sub>]<sup>-1</sup>). Data from 3 similar experiments were analyzed by one-way ANOVA followed by Tukey test for post hoc multiple comparisons of means (control versus treatment, \*p < 0.05, \*\* p < 0.01) and are presented as mean +/- SEM.

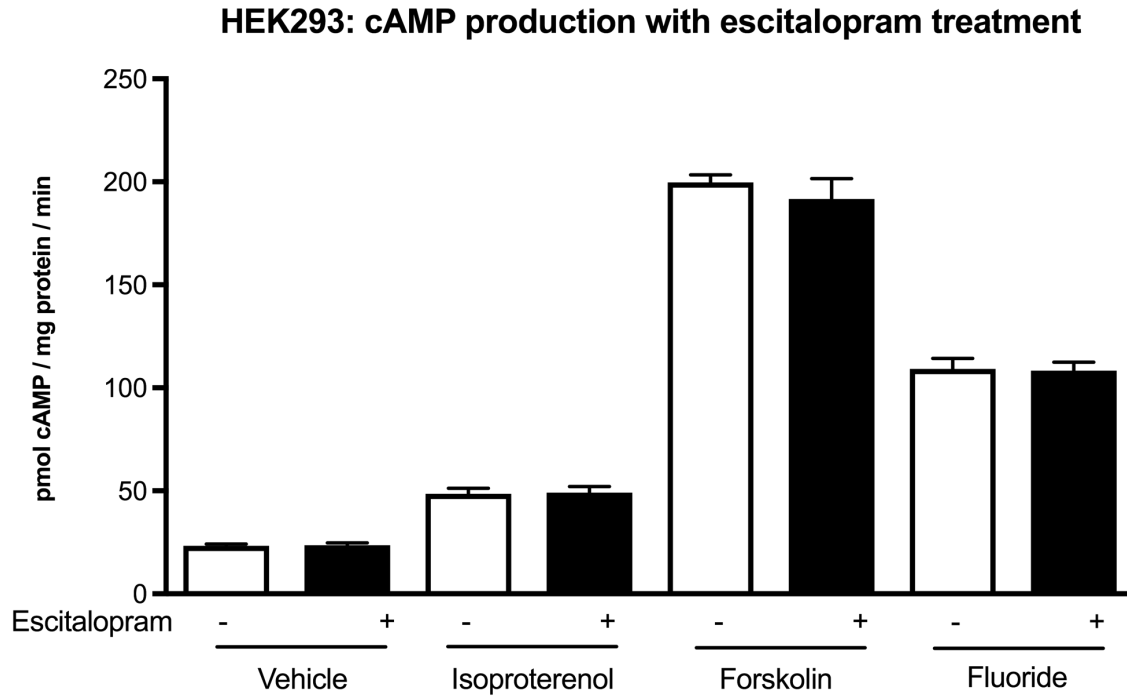
The Rasenick laboratory's past body of work has consistently shown both in vivo and in responsive cell lines that compounds with human antidepressant activity result in a redistribution of G protein  $G\alpha_s$  from raft into nonraftmembrane fractions. Total cellular G protein is unchanged, suggesting the phenomenon reflects altered cellular membrane distribution of  $G\alpha_s$ . Also seen is an increased immunoprecipitation of cyclase by  $G\alpha_s$  and increased production of cAMP<sup>50,156,201</sup>. Thus, the lab's working model of this phenomenon describes an exodus of  $G\alpha_s$  from lipid raft into nonraft membrane fractions, followed by increased functional coupling between  $G\alpha_s$  and its effector adenylyl cyclase, resulting in increased production of cAMP.

In this light, the results of Figure 8 can be interpreted as follows: membranes from cells treated with escitalopram show increased production of cAMP in response to agonist due to increased coupling of  $G\alpha_s$  and adenylyl cyclase. In the case of baseline cAMP production (vehicle) little difference is seen between groups, though escitalopram treated samples are slightly greater. While no added agonist is present, GPCRs still have a basal level of activity<sup>202</sup> and promote cAMP production. With a much larger number of trials (higher "N") this comparison would likely show significance as well. In the case of isoproterenol,  $\beta_2$ -receptors are more fully activated and the difference in cAMP production becomes significant, reflecting the increased activity through this signaling pathway due the increased coupling between receptor and adenylyl cyclase. Forskolin, in contrast, strongly and directly activates adenylyl cyclase. It does not, however, maximally activate cyclase. Forskolin has increased affinity for  $G\alpha_s$  – adenylyl cyclase complexes (and labeled forskolin has been used experimentally to detect these complexes) compared to cyclase alone<sup>203</sup>.

This is reflected in the assay results seen with forskolin. While forskolin alone produces strong activation of adenylyl cyclase, the increased association of  $G\alpha_s$  with adenylyl cyclase in antidepressant treated samples results in even greater activation of cyclase and resultant cAMP production. Finally, fluoride activation of  $G\alpha_s$  reflects the same trend: increased amounts of  $G\alpha_s$  are available to couple with adenylyl cyclase in antidepressant treated samples, and increased generation of cAMP is observed.

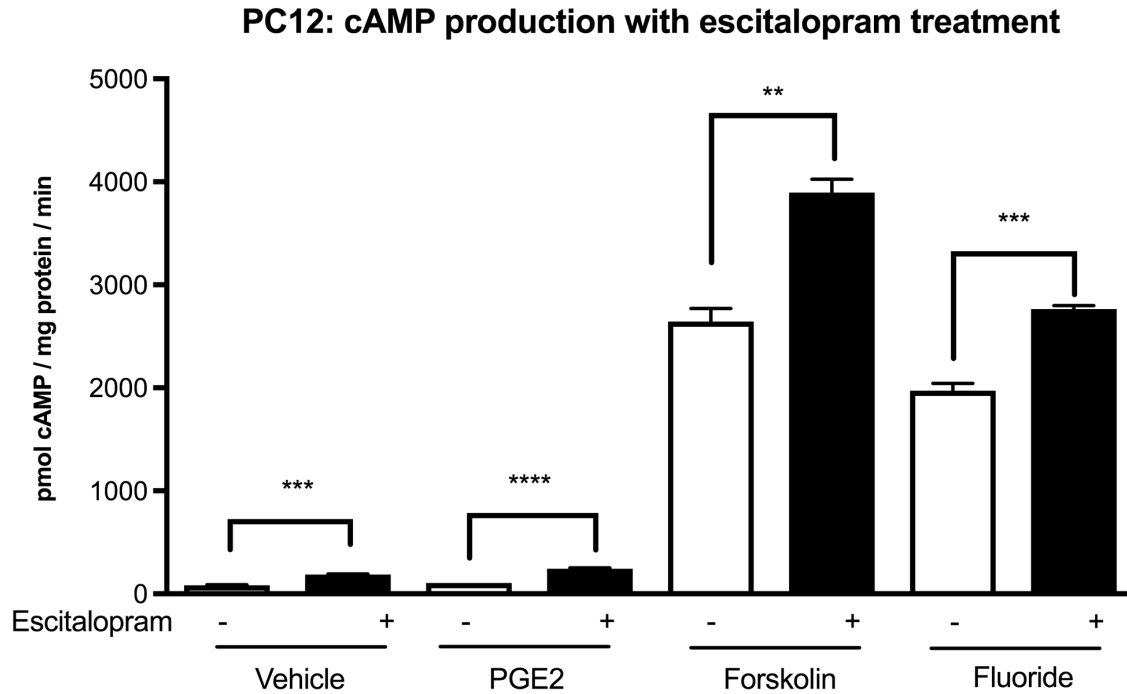
Figure 9 shows analogous experiments as Figure 8, now in HEK293. HEK293 do not show the same response to antidepressant treatment seen in C6 glioma. No statistical difference between antidepressant treated and untreated samples is seen for any agonist. This suggests that unlike the case with C6 glioma, redistribution of G protein  $G\alpha_s$  does not occur in HEK293 in response to antidepressant treatment.

Figure 10 shows experiments analogous to the above in PC12 pheochromocytoma cells. Prostaglandin E2 (PGE2) is used in place of isoproterenol, as PC12 do not express  $\beta$  receptors (a reasonable practice for cells of a catecholamine-secreting tumor!). The results are qualitatively similar to those obtained in C6 glioma: antidepressant treated samples show increased production of cAMP in response to all agonists used. One notable difference is the magnitude of effect. While C6, HEK293, and PC12 show roughly similar levels of cAMP production for vehicle and isoproterenol/PGE2, forskolin and fluoride stimulated cAMP production are dramatically (20-40x) higher than that seen in C6 or HEK293. Forskolin and fluoride act distal to the GPCR/G protein complex. Regulated, receptor-mediated production of cAMP is similar in all three cell types, but the large



**Figure 9: Production of cAMP in HEK293 membranes**

HEK293 were treated in flasks for 3 days with vehicle (water) or 10 $\mu$ M escitalopram. Membranes from cells treated with escitalopram no not demonstrate increased cAMP production in response to agonist compared to cells that were not treated with escitalopram. Agonists used were 10 $\mu$ M isoproterenol, 100 $\mu$ M forskolin or 10mM NaF+20 $\mu$ M AlCl<sub>3</sub> (active as aluminum tetrafluoride anion [AlF<sub>4</sub>]<sup>-1</sup>). Data from 4 similar experiments were analyzed by one-way ANOVA followed by Tukey test for post hoc multiple comparisons of means and are presented as mean +/- SEM.



**Figure 10: Production of cAMP in PC12 membranes**

PC12 were treated in flasks for 3 days with vehicle (water) or 10 $\mu$ M escitalopram. Membranes were prepared and assayed for cAMP production as described in Materials & Methods. Membranes from cells treated with escitalopram demonstrate increased cAMP production in response to agonist as well as at baseline compared to cells that were not treated with escitalopram. Agonists used were 10 $\mu$ M PGE2, 100 $\mu$ M forskolin or 10mM NaF+20 $\mu$ M AlCl<sub>3</sub> (active as aluminum tetrafluoride anion [AlF<sub>4</sub>]<sup>-1</sup>). Data from 3 similar experiments were analyzed by one-way ANOVA followed by Tukey test for post hoc multiple comparisons of means (control versus treatment, \*\* p < 0.01, \*\*\* p < 0.001, \*\*\*\* p < 0.0001) and are presented as mean +/- SEM.

increase in cAMP production as a result of **direct** activation of adenylyl cyclase with forskolin may reflect a significantly increased expression of adenylyl cyclase in PC12 or perhaps the absence of some regulator present in C6 and HEK293. The results with fluoride are similarly increased and reflect non-receptor mediated  $G\alpha_s$  activation of adenylyl cyclase; again, this suggests either increased expression of adenylyl cyclase in PC12 or absence of a regulator expressed in C6 or HEK293. One simple way to explore this would be to probe for total cyclase on a western blot using a pan-cyclase antibody. Additionally, the dramatically higher amounts of cAMP produced in PC12 membranes also demonstrate and confirm the flexibility of the cyclase assay: in no cases is the assay “maxed out” in terms of cAMP production. If this were the case, differences between groups could be masked by the inability of the assay setup to accurately reflect cAMP production. For reasons described below, PC12 cells were not ultimately used in this work, and no further examination of PC12 was done.

Finally, Figure 11 shows the results of membrane cyclase activity in COS7 cells. Similar to HEK293, and unlike C6 and PC12, membranes from COS7 cells treated with escitalopram do not produce increased amounts of cAMP in response to agonist stimulation.

In summary, this set of experiment demonstrates that membranes from C6 glioma and PC12 pheochromocytoma generate increased amounts of cAMP in response to escitalopram treatment, but HEK293 and COS7 do not. Not all cells respond in the same fashion same to antidepressant stimulation, with respect to effects on G protein signaling and cAMP production. As one aim of this study was to bridge the gap of understanding



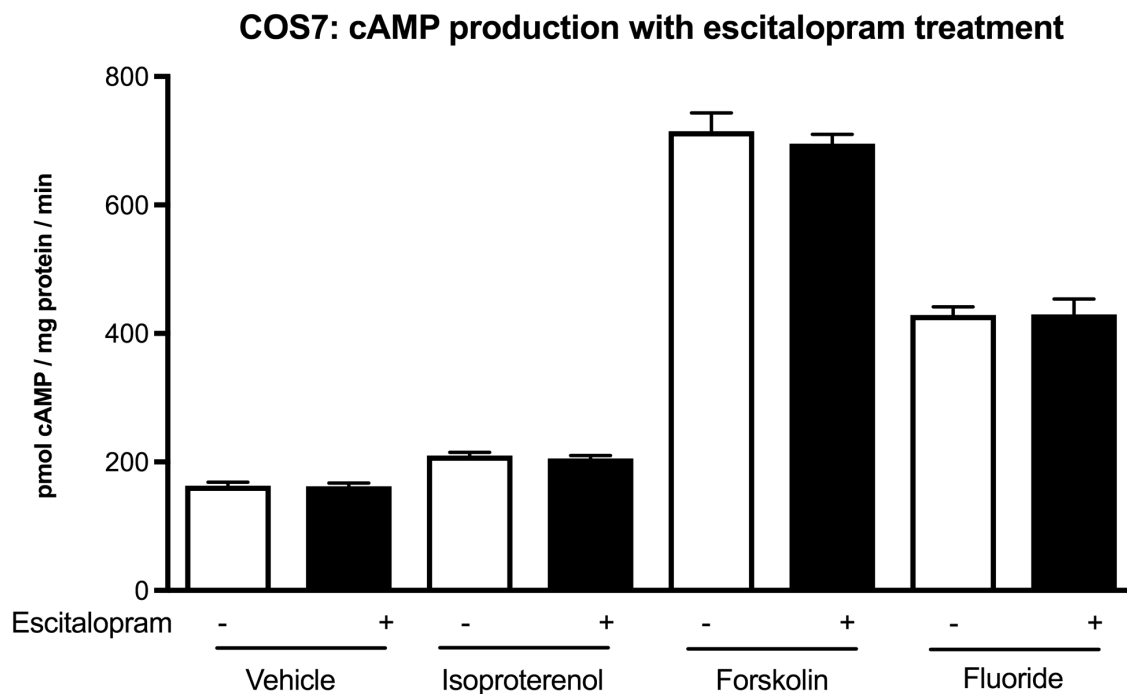


**Figure 11: Production of cAMP in COS7 membranes**

COS7 were treated in flasks for 3 days with vehicle (water) or 10 $\mu$ M escitalopram. Membranes from cells treated with escitalopram do not demonstrate increased cAMP production in response to agonist compared to cells that were not treated with escitalopram. Agonists used were 10 $\mu$ M isoproterenol, 100 $\mu$ M forskolin or 10mM NaF+20 $\mu$ M AlCl<sub>3</sub> (active as aluminum tetrafluoride anion [AlF<sub>4</sub>]<sup>-1</sup>). Data from 3 similar experiments were analyzed by one-way ANOVA followed by Tukey test for post hoc multiple comparisons of means and are presented as mean  $\pm$  SEM.

between antidepressant responsive and non-responsive cells, C6 glioma (responsive) and HEK293 (non-responsive) were chosen for further study. All cell lines considered are well-known and widely used. C6 glioma have been used successfully in the Rasenick laboratory for two decades and were chosen the example of a responsive cell line, while HEK293 were chosen as the example of a non-responsive cell line. One particular issue shared by COS7 and PC12 made them difficult to use. Both consistently required high seeding densities in order to grow, but then grew relatively fast, and were sloughing off the flask by day two of a three day treatment. Though media was changed daily, the continual presence of dying cells in culture could have unexpected effects, and these two cell lines were rejected.

It is tempting to view the drug response pattern observed thus far as neural vs. non-neural: here, the two neural-derived cell lines showed such a response, while the non-neural cell lines did not. This conceptualization is somewhat of a red herring. Our laboratory has examined (unpublished) other cell types, particularly various blood cells (red blood cells, platelets, lymphocytes) which are mesodermal derivatives<sup>204</sup> and clearly non-neural. These cell types all show changes in G protein membrane distribution in depression and in response to antidepressant treatment that are analogous to what is observed in the responsive cell lines used in this study. Therefore, the phenomenon is perhaps better characterized as responsive vs. non-responsive cell types.

### **3.1.2 Characterization of altered lipid raft content of $G_{\alpha_s}$ , $G_{\alpha_i}$ , and $G_{\alpha_q}$ with antidepressant treatment in C6 glioma and HEK293.**

C6 glioma and HEK293 were next examined for their response in membrane disposition of G proteins  $G_{\alpha_s}$ ,  $G_{\alpha_i}$ , and  $G_{\alpha_q}$  after three days of antidepressant drug treatment.  $G_{\alpha_s}$  and  $G_{\alpha_i}$

both directly regulate adenylyl cyclase, with obvious implications on cAMP signaling which is known to be diminished in depression.  $G\alpha_q$  is not known to directly regulate adenylyl cyclase, though it differentially regulates various cyclase isoforms through protein kinase C (PKC) activation<sup>205</sup>.  $G\alpha_{12/13}$  were not examined in this study. This class of G proteins is known to regulate various cellular processes such as differentiation and motility through actions on the actin and microtubular cytoskeleton<sup>164</sup>, but has not been implicated in depression or the regulation of cyclase activity and are not further discussed in this study.

Experimentally, cells were treated with 10 $\mu$ M escitalopram, 10 $\mu$ M *R*-citalopram or vehicle (water) for three days in flasks, harvested by scraping, lysed, and processed by sucrose density gradient centrifugation to obtain lipid raft membrane fractions. Lipid raft and was then western blotted for G protein content. Escitalopram was used as antidepressant because of its past successful use in our laboratory<sup>50</sup> as well as escitalopram's particular selectivity for SERT inhibition over other reuptake transporters compared to other commonly used antidepressants<sup>127</sup>. *R*-citalopram, the therapeutically inactive isomer of escitalopram, was used as a negative control. Furthermore, to assess the possibility that antidepressant compounds are acting on cell membrane or G proteins in a general, non-targeted fashion, colchicine (1 $\mu$ M, 30 min treatment) and methyl- $\beta$ -cyclodextrin (MBCD) (10mM, 30 min treatment) were used as positive controls of "membrane disruption" on G protein disposition. Treatment with membrane disrupting agents was done immediately prior to harvest. These are known to disrupt lipid raft structure through microtubule destabilization and cholesterol sequestration, respectively, and affect signaling regulated

through lipid raft domains<sup>206,207</sup>. Assays of membrane cyclase activity were also performed on C6 and HEK293 subjected to membrane disrupting treatment.

Figure 12 shows the results of the membrane fractionation experiments. In both C6 glioma and HEK293, all three G proteins examined,  $G\alpha_s$ ,  $G\alpha_i$ , and  $G\alpha_q$ , were liberated from lipid rafts by the nonspecific membrane disruptors colchicine and MBCD. No G proteins in either cell type were mobilized by *R*-citalopram treatment. The effects of escitalopram were a striking contrast to those obtained from membrane disrupting agents: only  $G\alpha_s$  was liberated from lipid rafts, and only in C6 glioma.

The results of membrane cyclase activity in cells subjected to membrane disrupting treatment also contrasted those obtained in cells treated with escitalopram. Figure 13 shows these results. After membrane disruption with colchicine or MBCD prior to cell collection and membrane isolation, both C6 glioma and HEK293 show an “antidepressant-like” enhancement of cAMP production in response to agonist. Compare this result to the effect of escitalopram treatment in these cell types (Figures 8 & 9). In the case of escitalopram treatment, only C6 glioma cAMP production was affected; escitalopram had no effect on HEK293.

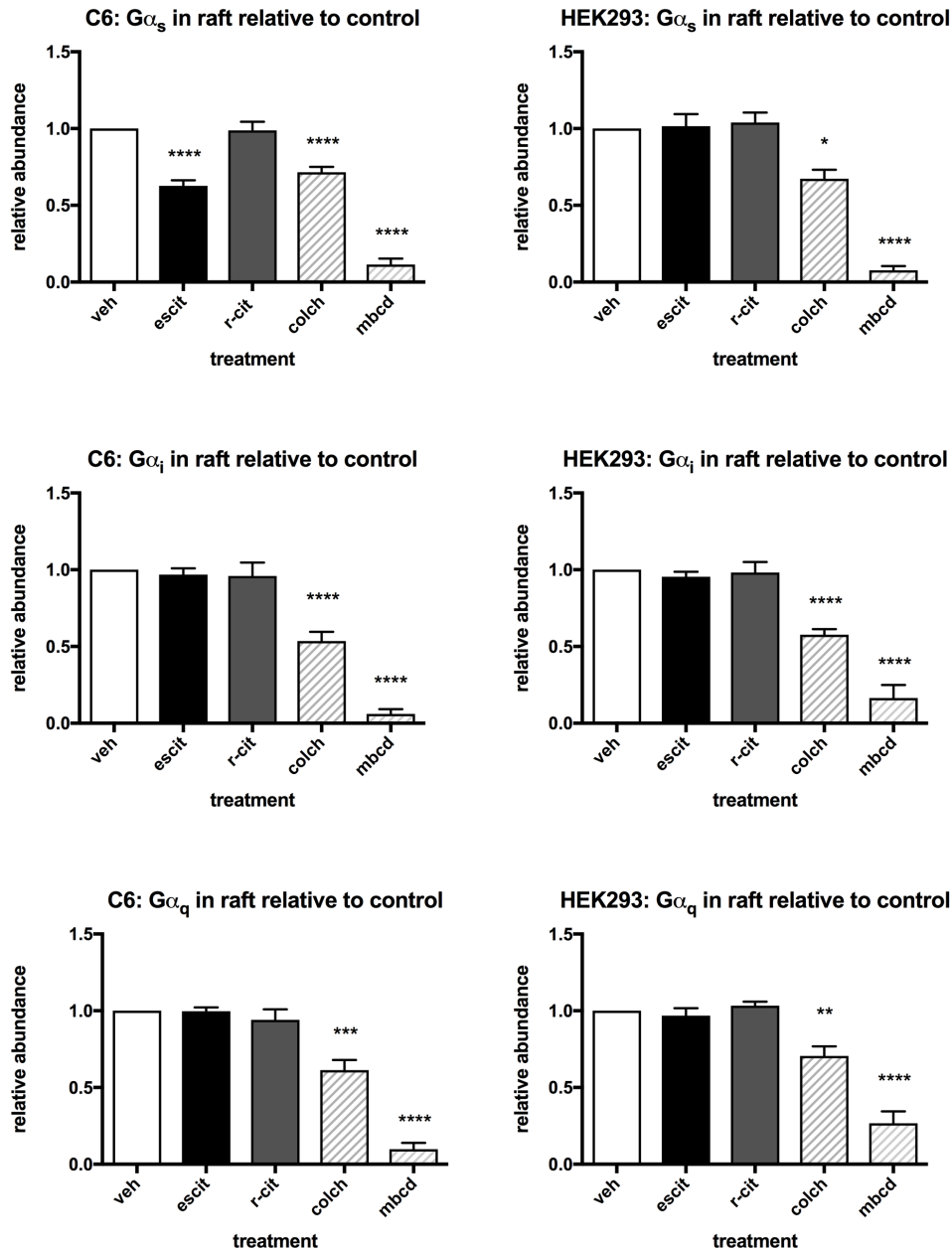


**Figure 12: Effects of escitalopram versus membrane disruptors upon lipid raft G protein content in C6 glioma and HEK293**

Membrane lipid rafts were prepared as described in Methods & Materials from cells treated with 10 $\mu$ M escitalopram, 10 $\mu$ M *R*-citalopram, or vehicle (water) and immunoblotted with quantification for G protein content. For disruptors, cells were grown for three days as was vehicle group, but treated immediately prior to harvest with either colchicine (1 $\mu$ M, 30 minutes) or mbccl (methyl- $\beta$ -cyclodextrin, 10mM, 30 min treatment). While G proteins in both cell types are lost nonselectively from lipid raft in response to disruptors, escitalopram specifically targets G $\alpha_s$  in C6 glioma. *R*-citalopram affects neither cell type. Data from 3-7 similar experiments were analyzed by one-way ANOVA (control versus treatment, \*\*  $p < 0.01$ , \*\*\*  $p < 0.001$ , \*\*\*\*  $p < 0.0001$ ) followed by Tukey test for post hoc multiple comparisons of means and are presented as mean  $\pm$  SEM.

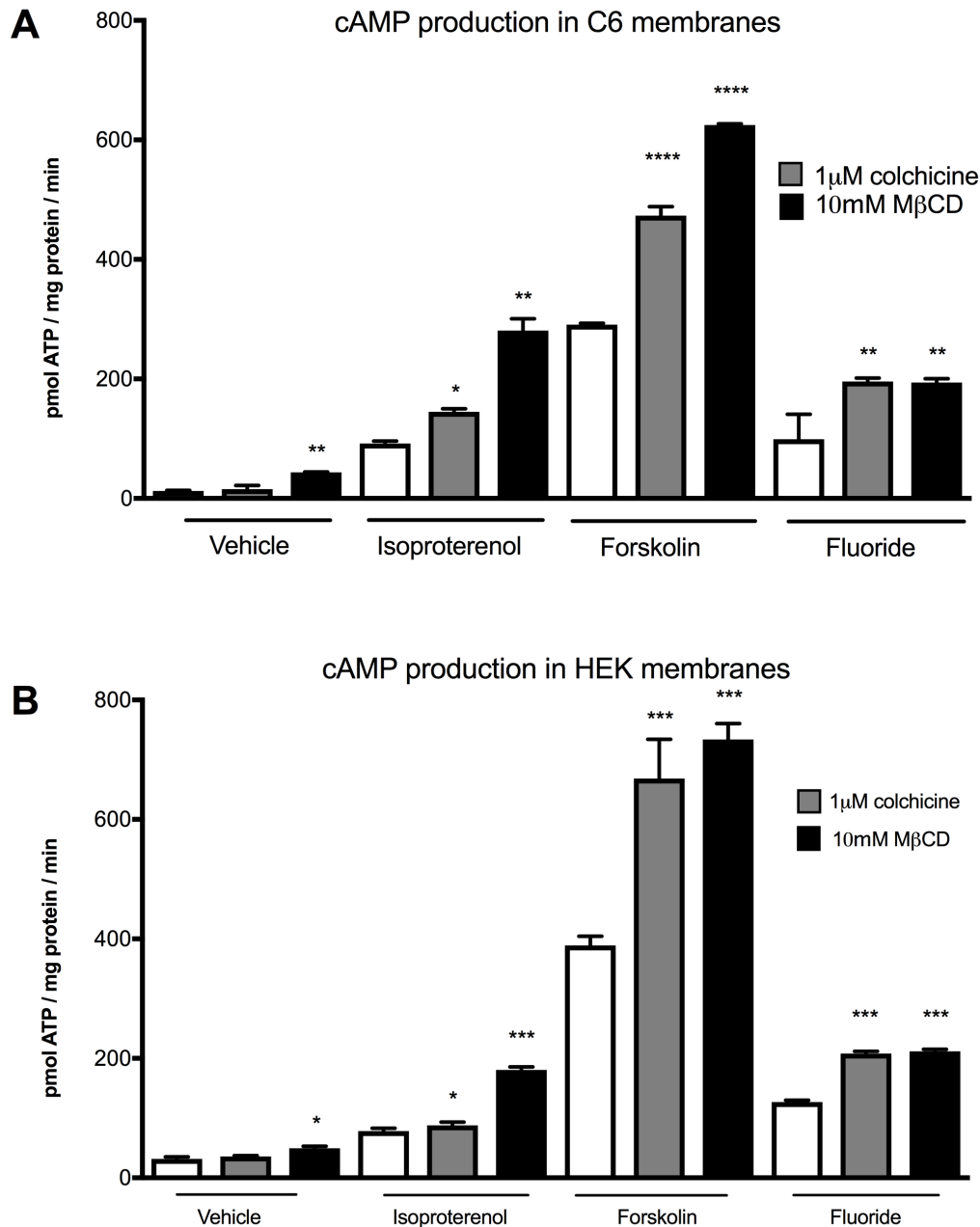


**Figure 13: Effect of membrane disruption on membrane cAMP production in C6 glioma and HEK293**

Cells were grown in flasks and harvested as described in Materials & Methods. Immediately prior to harvest cells were treated with either colchicine (1mM, 30 minutes) or MbCD (methyl- $\beta$ -cyclodextrin, 10mM, 30 min treatment). Either treatment caused an increased production of cAMP in membranes from both (A) C6 glioma and (B) HEK293. Agonists used were 10mM isoproterenol, 100mM forskolin or 10mM NaF+20mM AlCl<sub>3</sub> (active as aluminum tetrafluoride anion [AlF<sub>4</sub>]<sup>-1</sup>). Data from 3 similar experiments were analyzed by one-way ANOVA followed by Tukey test for post hoc multiple comparisons of means (control versus treatment, \*p < 0.05, \*\* p < 0.01) and are presented as mean +/- SEM.

Together, the preceding data demonstrate the following: Changes in membrane G protein distribution with antidepressant treatment are specific for  $G\alpha_s$  and only in certain cell types (C6 glioma), and do not reflect a general disruption of G protein localization.

Antidepressants (here, escitalopram) promote a selective redistribution of  $G\alpha_s$  out of lipid rafts, but not other G proteins. Furthermore, this effect is independent of action at SERT, the canonical target of escitalopram, as C6 glioma do not express SERT or other reuptake transporters (SERT is further explored in a later results section).

### 3.2 FRAP

Over the course of the previous experiments, I developed a new assay for antidepressant response in collaboration with Andrew Czysz, of the Rasenick laboratory. The data presented thus far were obtained via very reliable, but very slow, low-throughput techniques requiring large amounts of starting material. Consider, for example, the data demonstrating the differential mobilization of G proteins after antidepressant treatment (Figure 9). For each condition, three T-150 flasks are required to produce enough lipid raft material to analyze. Cells must be harvested, lysed, set up as sucrose density gradients, and centrifuged at high speed over night. Several days of work lead up to the extraction of lipid rafts, and several more for the western blot process. Because the centrifuge rotor can accommodate six samples, many experiments were done with six conditions. Experiments requiring 18 flasks per trial and daily media changes consume supplies and incubator space at an alarming rate. For the cyclase assays, the specifics are different, but the

procedure is similarly labor-intensive and low-throughput. This makes the investigation of current or prospective new antidepressant compounds extremely difficult.

Fluorescence recovery after photobleaching (FRAP) utilizes fluorescence microscopy and mathematical analysis to quantitatively assess lateral plasma membrane mobility of fluorescent-tagged proteins of interest. We reasoned that because  $G\alpha_s$  changes its membrane localization and protein associations (such as increased cyclase association) subsequent to antidepressant treatment, its mobility in the plasma membrane as assessed by FRAP may be affected in a predictable way. If so, this could serve as a new way to determine response to antidepressant drugs. In contrast to the above techniques, the cells are grown and treated in small, special glass-bottom microscope dishes. After the drug treatment period, no further preparation is required; the cells are ready to view via confocal microscopy. Because of this, FRAP is the “cleanest” technique and is essentially a window into the living cell, and a vastly higher-throughput assay. The following sets of experiments demonstrate that FRAP is consistent with all past measures of antidepressant response, and even allows for determination of small changes previously inaccessible to detection.

### **3.2.1 FRAP results of a variety of antidepressant and non-antidepressant drugs in C6 glioma**

Figure 14 shows FRAP results from a variety of antidepressants, from different classes, contrasted to *R*-citalopram and several additional non-antidepressant



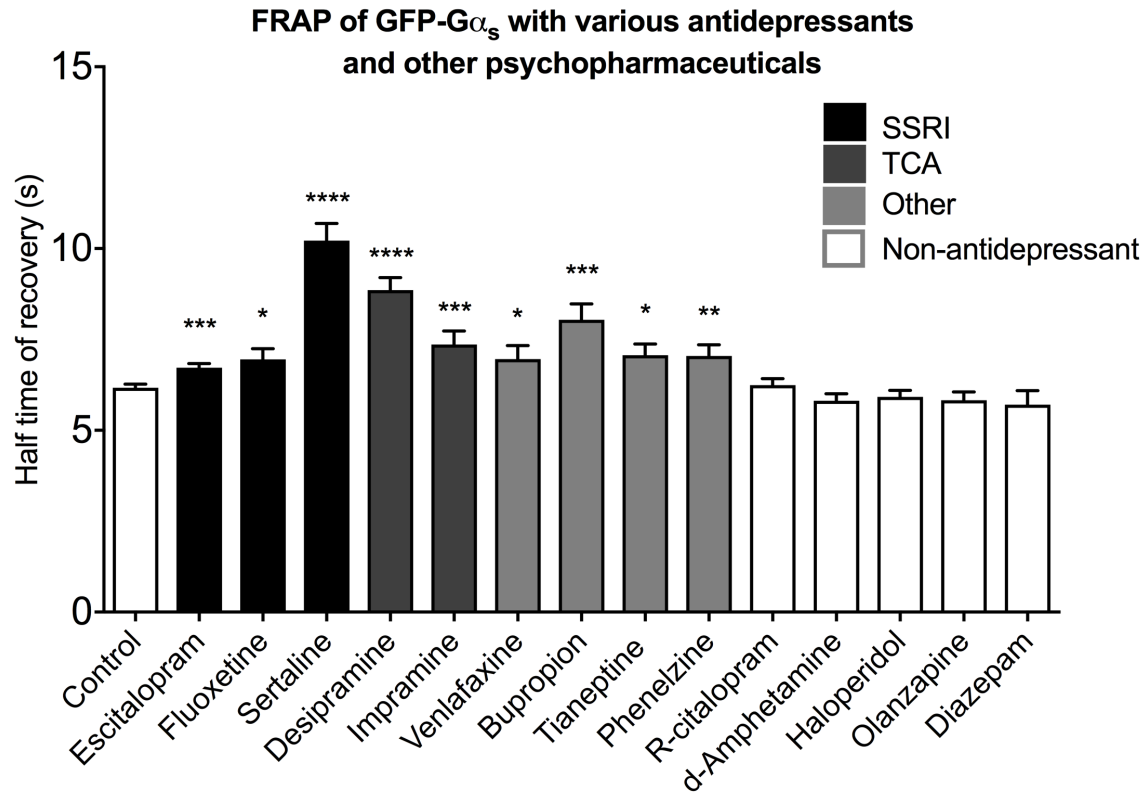


**Figure 14: FRAP results for a variety of antidepressant and non-antidepressant drugs in C6 glioma**

C6 glioma stably expressing GFP- $G\alpha_s$  were grown in glass bottom microscope dishes and treated for 3 days with the indicated compounds at 10 $\mu$ M concentration. Half-time to FRAP recovery is increased by a variety of antidepressant compounds from several classes, but not by *R*-citalopram or non-antidepressant drugs. Data were obtained from 20-300 data points depending on drug and were analyzed by one-way ANOVA (control versus treatment, \*  $p < 0.05$ , \*\*  $p < 0.01$ , \*\*\*  $p < 0.001$ , \*\*\*\*  $p < 0.0001$ ) followed by Tukey test for post hoc multiple comparisons of means and are presented as mean  $\pm$  SEM.

psychopharmaceuticals after three-day antidepressant treatment. While clinically efficacious antidepressants significantly increase half-time to recovery of GFP-  $G\alpha_s$ , neither inactive isomer *R*-citalopram nor non-antidepressant compounds affect this value. These data indicate that lateral membrane mobility of GFP-  $G\alpha_s$  is slowed by “chronic” treatment with drugs showing clinical antidepressant activity, but not by drugs without antidepressant activity. Note: the data in this figure were obtained jointly by Andrew Czysz and this author for publication as Czysz et al.<sup>208</sup>.

### 3.2.2 FRAP dose and time response with antidepressant treatment in C6 glioma

Figure 15 shows dose responses in C6 glioma of GFP-  $G\alpha_s$  FRAP. The data show a response to even 50nM with three days of treatment for two antidepressants of different classes, SSRI (escitalopram) and tricyclic (desipramine). This addresses an important concern with our experimental approach and the potential clinical utility of this G protein effect in determining response to antidepressant treatment. While clinically effective plasma escitalopram concentrations are in the range of 100-200nM<sup>209</sup>, the Rasenick laboratory has traditionally used 10 $\mu$ M concentration for all antidepressants. This concentration generally produces a maximal effect on G protein localization without apparent effect on cell viability. However, the disparity of these values needs to be addressed. Though antidepressants are known to accumulate at the synapse, it could be that the 10 $\mu$ M antidepressant treatment exerts its effects in a non-physiological fashion and is not relevant to what occurs at actual clinical dosages. Furthermore, if this G protein effect is to be useful in a clinical assay, it must actually occur at clinically relevant drug concentrations;

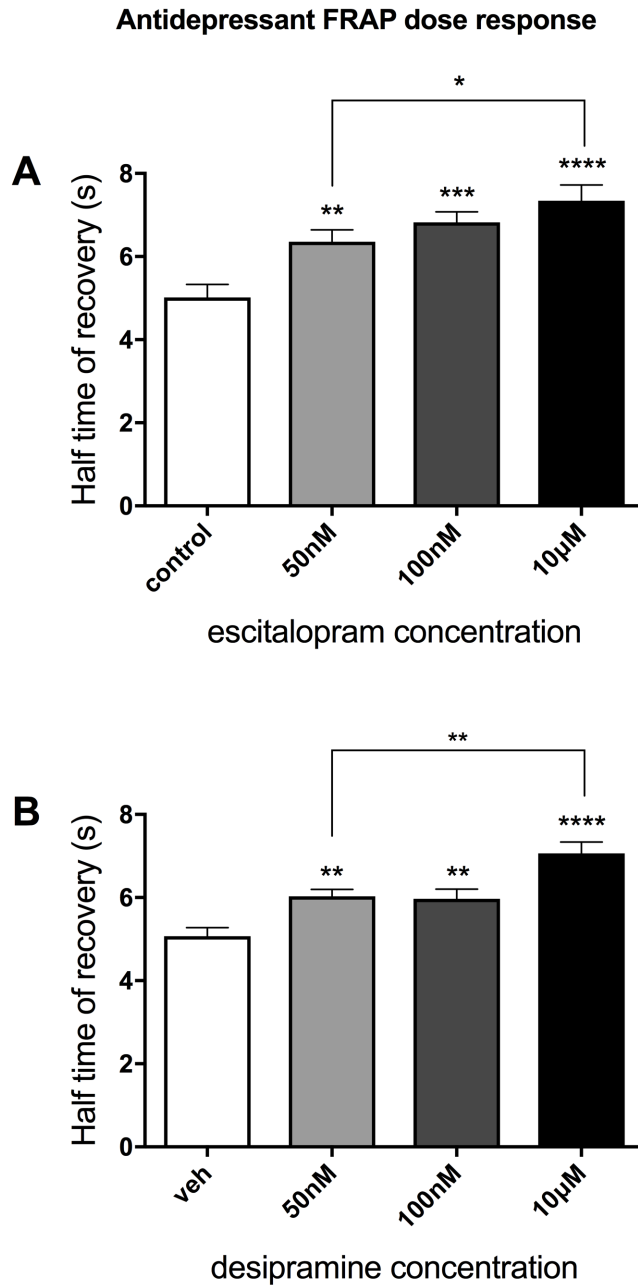


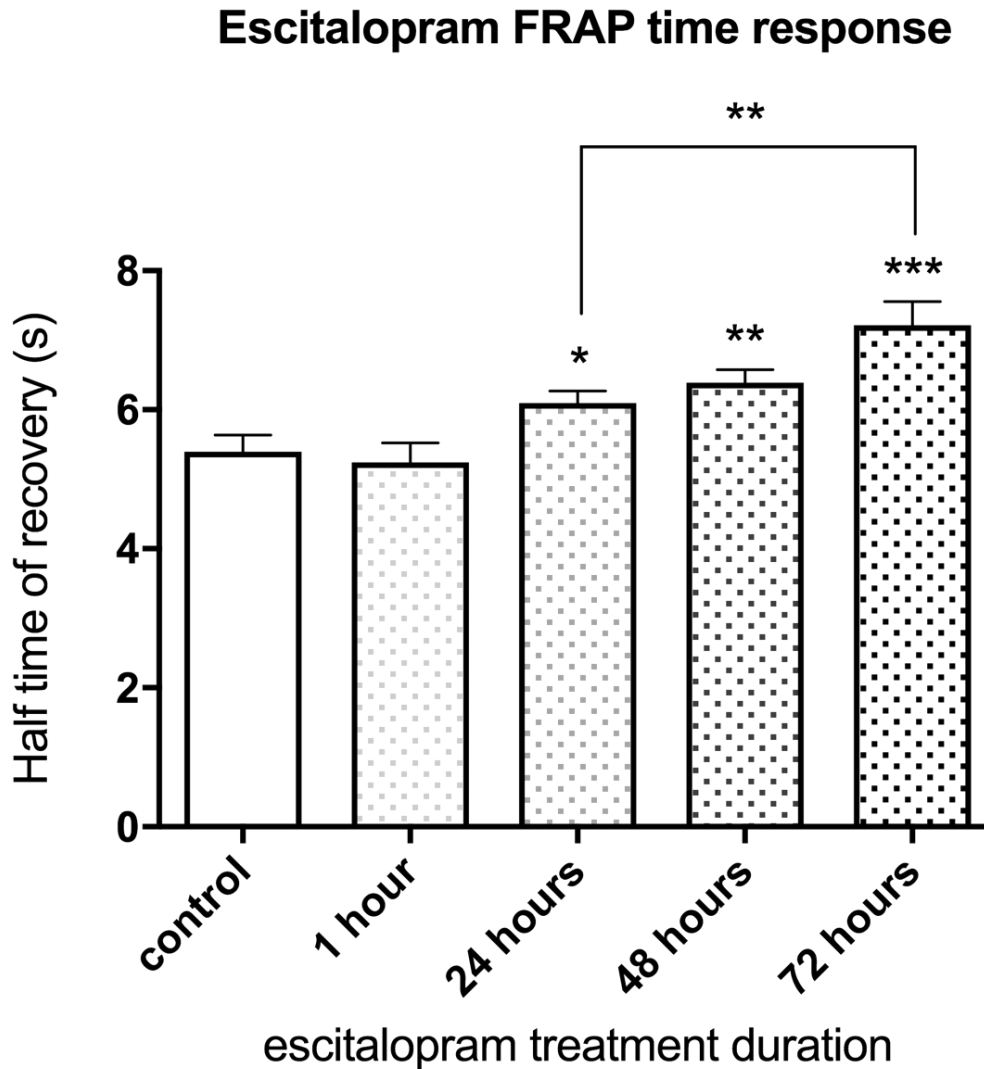
**Figure 15: Effects of different antidepressant doses on response of GFP- $G\alpha_s$  FRAP in C6 glioma**

C6 glioma stably expressing GFP- $G\alpha_s$  were grown in glass bottom microscope dishes and treated for 3 days with either (A) escitalopram or (B) desipramine at the indicated concentrations. Effect on FRAP recovery is observed at concentrations down to 50nM for both drugs. Data were obtained from 30-70 data points depending on drug and were analyzed by one-way ANOVA (control versus treatment, \*  $p < 0.05$ , \*\*  $p < 0.01$ , \*\*\*  $p < 0.001$ , \*\*\*\*  $p < 0.0001$ ) followed by Tukey test for post hoc multiple comparisons of means and are presented as mean  $\pm$  SEM.

such a test would likely use peripheral (blood) cells, which “experience” the range of plasma concentrations noted above. Both questions are answered by this experiment: clinically relevant drug concentrations slow GFP-  $G\alpha_s$  FRAP recovery, and the effect of escitalopram or desipramine down to 50nM is detectable by the FRAP assay. Past experiments using older techniques (sucrose gradient membrane fractionation) have only demonstrated significant escitalopram effects down to 1 $\mu$ M escitalopram<sup>50</sup>, a 20x higher concentration. The time-response data (Figure 16) are also consistent with past data, and show a time-dependent increase over a three day treatment period<sup>50</sup>, with response detected within one day but no acute response at one hour.

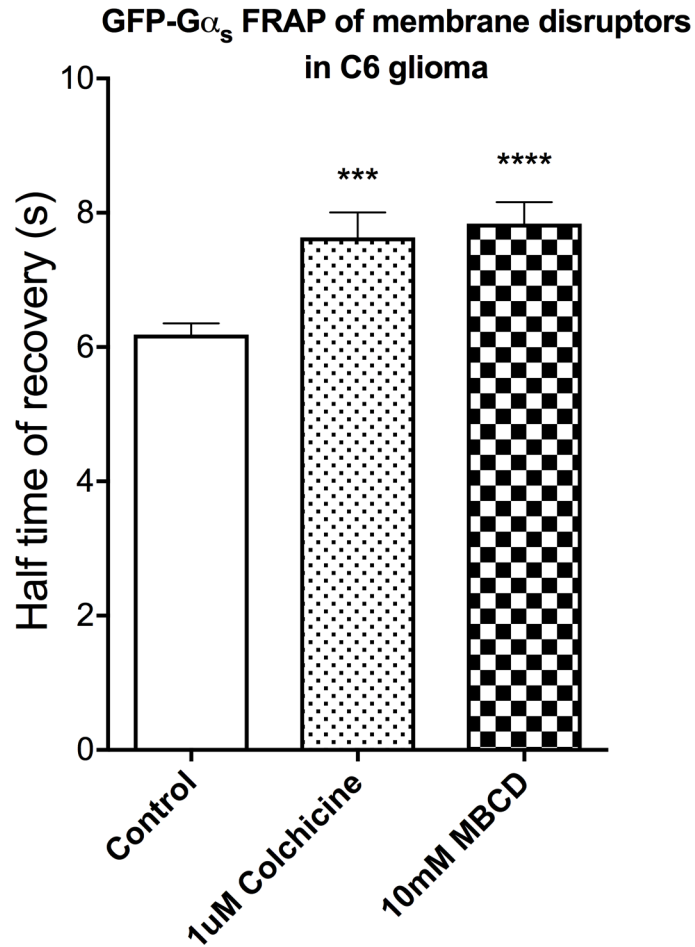
### **3.2.3 FRAP results of membrane disruption in C6 glioma with colchicine and methyl- $\beta$ -cyclodextrin**

Figure 17 shows a FRAP correlate to Figure 12 in C6 glioma, examining the FRAP response of GFP-  $G\alpha_s$  to membrane disrupting treatment. Immediately prior to microscopy, cells were treated as before with colchicine (1 $\mu$ M, 30 min treatment) or methyl- $\beta$ -cyclodextrin (MBCD) (10mM, 30 min treatment). Both microtubule disruption with colchicine and cholesterol sequestration with MBCD promote increased GFP-  $G\alpha_s$  half-time of recovery (as does antidepressant treatment, seen in previous sets of figures) and are consistent with results of membrane fractionation showing redistribution of GFP-  $G\alpha_s$  out of lipid rafts.



**Figure 16: Effect of escitalopram treatment duration on GFP-G $\alpha_s$  FRAP in C6 glioma**

C6 glioma stably expressing GFP-G $\alpha_s$  were grown in glass bottom microscope dishes and treated for the indicated durations with escitalopram. Effect on FRAP recovery is observed within 24 hours. Data were obtained from 37-140 data points depending on condition and were analyzed by one-way ANOVA (control versus treatment, \*  $p < 0.05$ , \*\*  $p < 0.01$ , \*\*\*  $p < 0.001$ , \*\*\*\*  $p < 0.0001$ ) followed by Tukey test for post hoc multiple comparisons of means and are presented as mean  $\pm$  SEM.



**Figure 17: Effect on FRAP of GFP-  $G_{\alpha_s}$  in C6 glioma by membrane disruptors**

C6 glioma stably expressing GFP- $G_{\alpha_s}$  were grown in glass bottom microscope dishes. Immediately prior to FRAP procedure, cells were treated with colchicine (1 $\mu$ M, 30 min treatment) or methyl- $\beta$ -cyclodextrin (MBCD) (10mM, 30 min treatment). Half-time to FRAP recovery is increased by both membrane disruptors. Data were obtained from 30-70 data points depending on drug and were analyzed by one-way ANOVA (control versus treatment, \*\*\*  $p < 0.001$ , \*\*\*\*  $p < 0.0001$ ) followed by Tukey test for post hoc multiple comparisons of means and are presented as mean  $\pm$  SEM.

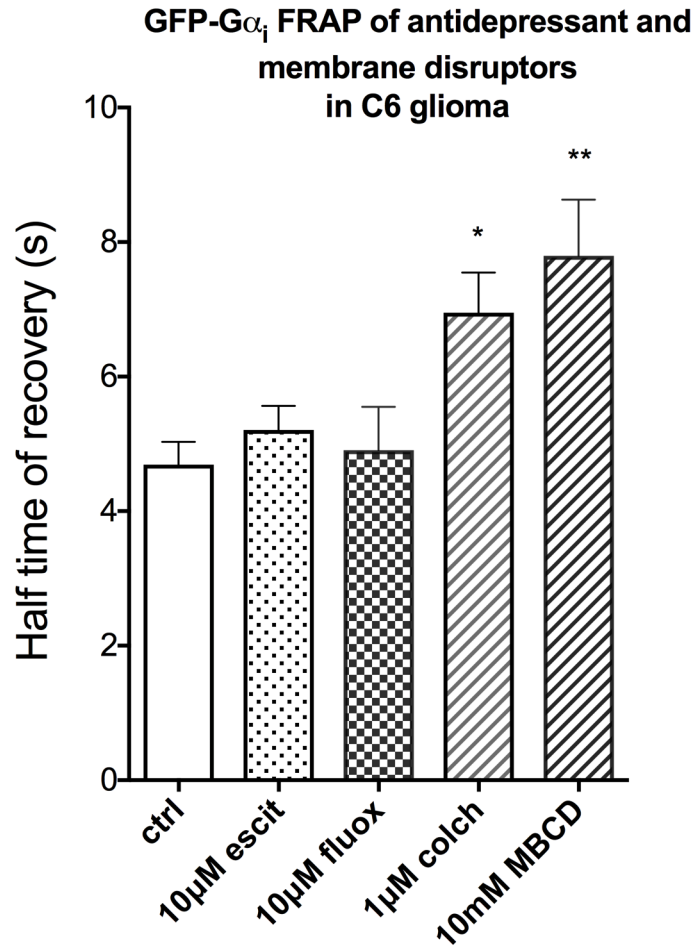
### **3.2.4 FRAP results of GFP- $G\alpha_i$ in C6 glioma contrasting antidepressant treatment and membrane disruption with colchicine and methyl- $\beta$ -cyclodextrin**

Figure 18 evaluates the response of GFP-  $G\alpha_i$  to the same conditions as in Figure 17, plus 3 day antidepressant treatment, in C6 glioma. While half-time of GFP-  $G\alpha_i$  recovery is unaffected by both escitalopram and fluoxetine treatments, colchicine and MBCD treatments both slow GFP-  $G\alpha_i$  recovery. Again, this is consistent with membrane fractionation experiments showing  $G\alpha_i$  mobilization by membrane disruption, but not by antidepressant treatment (Figure 12). Nonspecific membrane raft disruption mobilizes all G proteins, but antidepressants specifically target  $G\alpha_s$ . (Please note: In these FRAP experiments, GFP-  $G\alpha_q$  was not tested due to poor expression of the construct.)

### **3.2.5 FRAP results in C6 glioma of fluorescent proteins of varied size and membrane anchoring**

In the course of developing this assay, we sought to determine what factors might be responsible for the change in GFP-  $G\alpha_s$  mobility with antidepressant treatment. The lateral mobility of a membrane protein is dependent on a variety of factors; of particular importance are protein size and membrane attachments. To this end, the mobility of selected proteins known to interact with GFP-  $G\alpha_s$  was examined via transfection of fluorescent protein constructs into C6 glioma via electroporation.

Figure 19 compares the recovery of  $G\alpha_s$ -associated proteins. GFP-  $G\alpha_s$  and GFP-  $G\alpha_i$  are of similar size (40-45 kDa) but differ in their lipid anchoring to the membrane. While



**Figure 18: Effect on FRAP of GFP-  $G\alpha_i$  in C6 glioma by antidepressants and membrane disruptors**

C6 glioma stably expressing GFP- $G\alpha_i$  were grown in glass bottom microscope dishes. Antidepressants were 10μM and treatments lasted 3 days. For membrane disruptors, immediately prior to FRAP procedure, cells were treated with colchicine (1μM, 30 min treatment) or methyl-β-cyclodextrin (MBCD) (10mM, 30 min treatment). Half-time to FRAP recovery is increased by both membrane disruptors. Data were obtained from 11-17 data points depending on drug and were analyzed by one-way ANOVA (control versus treatment, \*  $p < 0.05$ , \*\*  $p < 0.01$ ) followed by Tukey test for post hoc multiple comparisons of means and are presented as mean  $\pm$  SEM.



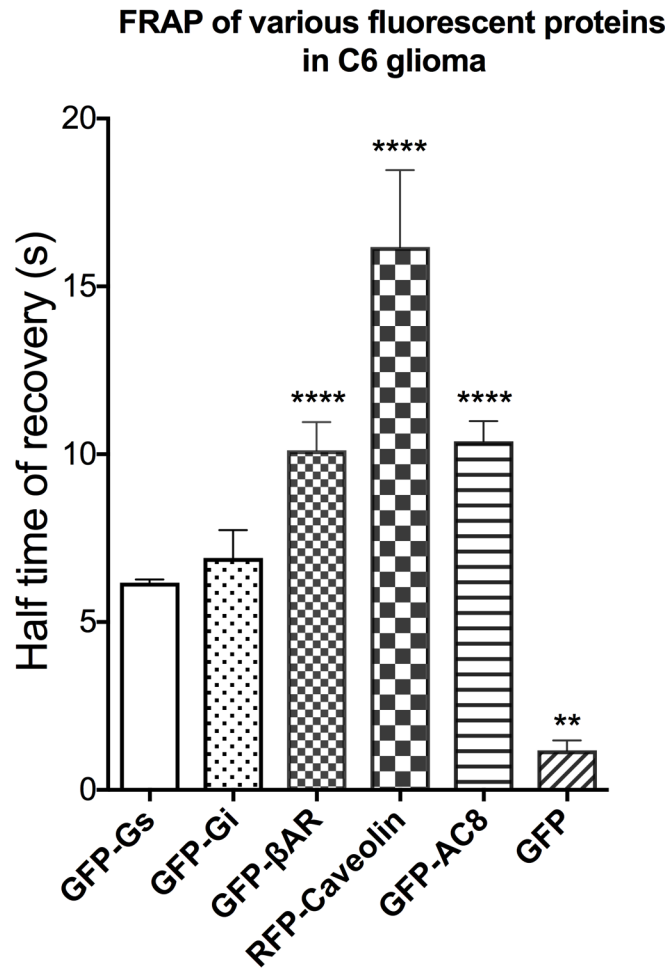


**Figure 19: Effect of size and membrane anchoring on FRAP of fluorescent proteins in C6 glioma**

C6 glioma were transfected with the listed constructs via electroporation and were grown in glass bottom microscope dishes. No drug treatments were done. FRAP recovery is dependent on size and anchoring of examined protein. Larger and more extensively anchored proteins display slower recovery. Data were obtained from 5-60 data points depending on drug and were analyzed by one-way ANOVA (control versus treatment, \*\*  $p < 0.01$ , \*\*\*\*  $p < 0.0001$ ) followed by Tukey test for post hoc multiple comparisons of means and are presented as mean  $\pm$  SEM.

$G\alpha_s$  is palmitoylated, a reversible modification, GFP-  $G\alpha_i$  is both palmitoylated and myristoylated, a nonreversible modification. Despite their different anchoring, both have similar membrane mobility.  $\beta AR_2$  and AC8 are large proteins spanning the membrane multiple times (7 and 12 membrane passes, respectively) and show a significantly slower mobility than GFP-  $G\alpha_s$ . Caveolin-1, though at 20kD less than half the molecular weight of  $G\alpha_s$ , is extensively oligomerized (200-400kD complexes) and multiply palmitoylated<sup>210</sup> and similarly has relatively slow mobility. Finally, GFP alone shows nearly instantaneous recovery. Though a small selection of proteins, these illustrate a fundamental principle of FRAP: larger, heavier proteins, or those with extensive protein or membrane associations, show slower membrane mobility than smaller or less associated proteins. Therefore, it is likely that the observed slowing of GFP-  $G\alpha_s$  subsequent to antidepressant treatment is due to its known increased association with adenylyl cyclase, a larger heavier protein. The complex of GFP-  $G\alpha_s$  with adenylyl cyclase is heavier than GFP-  $G\alpha_s$  alone, and is therefore slower moving.

In summary, the FRAP assay is entirely consistent with past data from “traditional” techniques, and boasts higher sensitivity in terms of antidepressant dose and treatment duration, as well as increased throughput. For these reasons, FRAP is the primary technique employed throughout the rest of this study, though FRAP data are supplemented with other techniques when appropriate.

### **3.2.6 FRAP of GFP- $G_{\alpha s}$ in C6 glioma demonstrating effect of ketamine and HDAC6 inhibitor tubastatin-A**

Two additional antidepressant compounds/drug classes of current clinical interest, ketamine and tubastatin-A (HDAC6 inhibitor) were also evaluated via FRAP. Currently unpublished membrane fractionation data from other members of the Rasenick laboratory demonstrate the characteristic movement of G proteins from lipid rafts with drug treatment. The case of ketamine is particularly interesting, since ketamine's clinical antidepressant efficacy is accelerated disproportionately to its effect on G protein localization. Ketamine treatment for depression, when effective, is essentially instantaneous, underlying clinical interest in the drug. Effects on G protein are observed within 24 hours by sucrose gradient/western blot analysis. This contrasts the timing seen with more traditional antidepressants in humans, whose G protein effect on various blood cells can be detected within 1 week, but whose antidepressant effects are further delayed by weeks. Data corroborating western blot data in ketamine are shown in Figure 20, with FRAP detection of effect at 15 minutes and at the lowest tested concentration of ketamine, 1 $\mu$ M. Effect of HDAC6 inhibitor tubastatin-A at 10 $\mu$ M is shown in Figure 21, showing tubastatin-A produces the characteristic increase in FRAP recovery time at 3 days, as does escitalopram. Tubastatin-A is further considered in the discussion section.

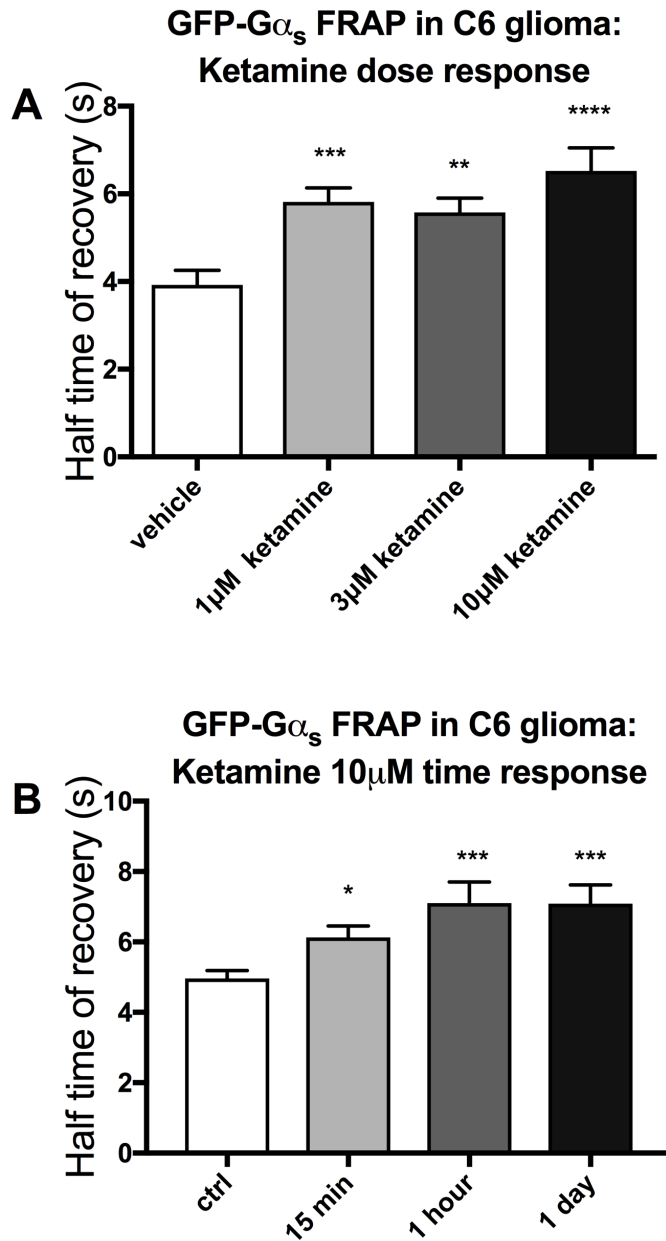


**Figure 20: Dose and time dependence of response of GFP- $G\alpha_s$  FRAP in C6 glioma**

C6 glioma stably expressing GFP- $G\alpha_s$  were grown in glass bottom microscope dishes and treated (A) for 24 hours at the indicated concentrations of ketamine or (B) with 10 $\mu$ M ketamine for the indicated time periods. Effects are both dose and time dependent, with detection at 15 minutes treatment time and at the lowest 24 hour treatment concentration, 1 $\mu$ M. Data were obtained from 24-68 data points depending on drug and were analyzed by one-way ANOVA (control versus treatment, \*  $p < 0.05$ , \*\*  $p < 0.01$ , \*\*\*  $p < 0.001$ , \*\*\*\*  $p < 0.0001$ ) followed by Tukey test for post hoc multiple comparisons of means and are presented as mean  $\pm$  SEM.

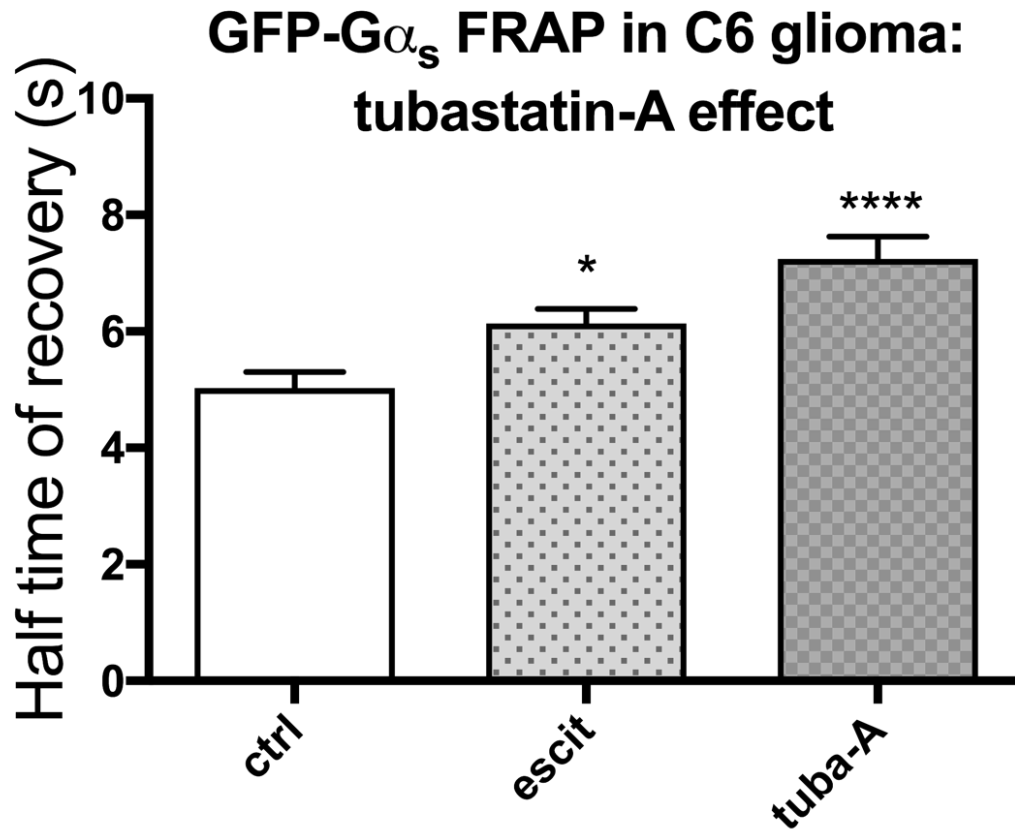


**Figure 21: GFP- $G\alpha_s$  FRAP in C6 glioma comparing tubastatin-A and escitalopram**

C6 glioma stably expressing GFP- $G\alpha_s$  were grown in glass bottom microscope dishes and treated for 3 days with either escitalopram (escit, 10 $\mu$ M) or tubastatin-A (tuba-A, 10 $\mu$ M) at the indicated concentrations. Effect on FRAP recovery is observed for both drugs. Data were obtained from 54-60 data points depending on drug and were analyzed by one-way ANOVA (control versus treatment, \*  $p < 0.05$ , \*\*\*\*  $p < 0.0001$ ) followed by Tukey test for post hoc multiple comparisons of means and are presented as mean  $\pm$  SEM.

### 3.3 Lack of SERT influence in antidepressant response

Because the cell lines chosen for this study lack reuptake transporters, notably SERT, the target of highly SERT-selective escitalopram, the effect of SERT expression in these cells on their response to antidepressant treatment was examined. C6 glioma and HEK293 stably expressing functional hSERT (human SERT) were obtained from the laboratory of Susan Amara (University of Pittsburgh, currently NIMH).

SERT and other reuptake transporters act at the synapse to recycle released neurotransmitter back into the presynaptic cell for reuse. However, C6 glioma and HEK293 are not neurons, are not known to release neurotransmitters, and do not form synapses. By expressing SERT in these cells, it is not suggested that a synapse-like arrangement or function is established, although active SERT function of reuptake may occur. Rather, these experiments were performed to examine the *sufficiency* of SERT expression to cause the antidepressant-responsive phenotype of G protein redistribution in these cells. The previous sets of experiments have established, in the case of the antidepressant-responsive C6 glioma, that SERT expression is not *necessary* for this effect. A known binding target of escitalopram (actually, at the present time, the only known target), SERT may have non-canonical actions beyond neurotransmitter reuptake and such experiments may reveal a contribution of SERT beyond its neurotransmitter reuptake function. For example, binding of escitalopram to SERT could affect SERT's interaction with another hypothetical protein involved in the characteristic response to

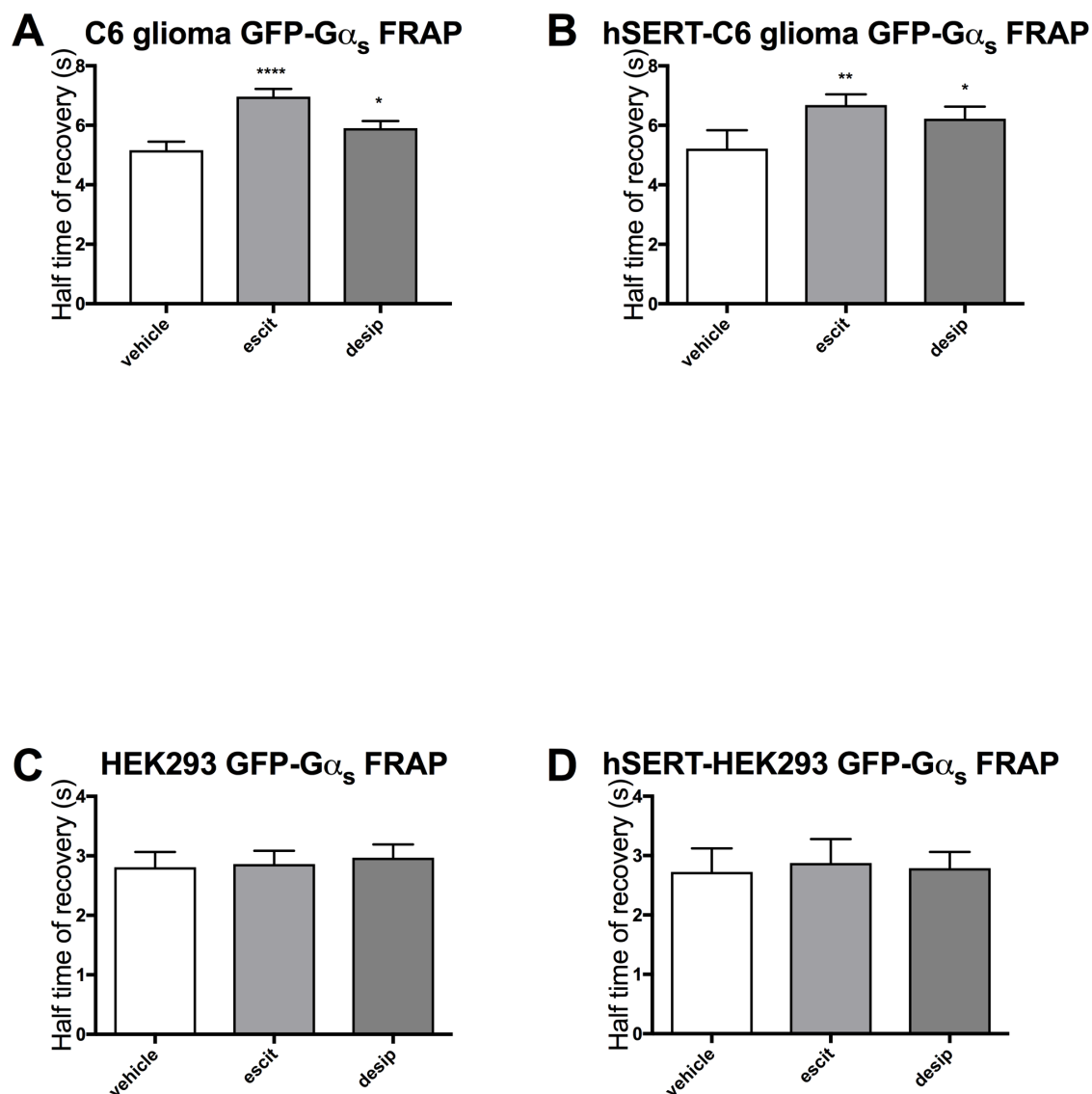
antidepressants. To this end, FRAP on wild type and hSERT- C6 glioma and HEK293 was performed.

Figure 22 compares the results of GFP-  $G\alpha_s$  FRAP in C6-hSERT and HEK293-hSERT compared to wild type after three days of antidepressant treatment. In both cases, expression of hSERT does not alter the response of the wild type cells; C6 glioma still show the characteristic increase of comparable magnitude in GFP-  $G\alpha_s$  recovery half-time, but no change is seen in HEK293-hSERT with antidepressant treatment.

Based on the results of these experiments, the expression of SERT is neither necessary nor sufficient to produce the membrane redistribution of  $G\alpha_s$  observed in antidepressant responsive cells, and this phenomenon is truly reuptake transporter-independent, or at least SERT-independent. Possible mechanisms of action are considered in the discussion section. To further examine this, two animal models, one nearly ideal, exist. SERT knockout mice exist and could be treated with escitalopram, sacrificed, and appropriate brain regions analyzed via membrane fractionation for  $G\alpha_s$  redistribution. A collaboration based on these models unfortunately failed to materialize. Based on the results of this study, one would expect to find redistribution of  $G\alpha_s$  out of lipid rafts despite the lack of SERT expression in these mice. As previously described, SERT knockout mice are not phenotypically normal and differ from their wild type relatives in a variety of ways complicating their use in the context of depression.

To ameliorate these concerns, one particularly clever manipulation of SERT has been used experimentally. The laboratory of Randy Blakely (discovery and initial characterization of SERT) has created a knock-in mouse expressing I172M SERT, a variant insensitive to





**Figure 22: Evaluation of hSERT expression on GFP-G $\alpha_s$  FRAP in C6 glioma and HEK293**

C6 glioma (A) and (B) and HEK293 (C) and (D) stably expressing hSERT were transfected with GFP-G $\alpha_s$ , grown in glass bottom microscope dishes and treated for 3 days with either 10 $\mu$ M escitalopram or desipramine. Expression of SERT in C6 glioma (B) and HEK293 (D) does not alter FRAP response compared to wild type. HEK293 do not show significant changes in recover in either wild type or hSERT-HEK293. Data were obtained from 55-75 data points depending on condition and were analyzed by one-way ANOVA (control versus treatment, \*  $p < 0.05$ , \*\*  $p < 0.01$ , \*\*\*  $p < 0.001$ , \*\*\*\*  $p < 0.0001$ ) followed by Tukey test for post hoc multiple comparisons of means and are presented as mean  $\pm$  SEM.

several antidepressants including escitalopram. The affinity of the transporter for serotonin, as well as its kinetics, are unchanged from the wild type SERT, and the mice are phenotypically normal<sup>211</sup>. As with the knockout model, one would expect these mice to retain the characteristic redistribution of  $G\alpha_s$  after treatment with antidepressants. Use of either of these models would enhance the understanding of SERT's contribution to antidepressant G protein response.

Studies of this SERT variant also illustrate a dichotomy, though not a contradiction, in the spectrum of behavioral and biochemical changes promoted by antidepressant treatment. The Blakeley studies<sup>152,211</sup> show in wild type mice a nearly immediate effect (30 minutes post injection) of antidepressants in certain behavioral tests (forced swim test, tail suspension test, novelty induced hypophagia), and this is consistent with many past studies showing rapid behavioral effects of antidepressants as well as rapid elevation of synaptic neurotransmitter content<sup>141-143</sup>. Furthermore, these behaviors were abolished in the mice expressing the antidepressant-insensitive SERT variant. This suggests an important role of reuptake inhibition in antidepressant response.

However, other behaviors in rodents such as sucrose preference have required much longer antidepressant treatment periods to manifest. Human subjects, in contrast, do not demonstrate any immediate behavioral response to antidepressants. The goal of the current study is not to claim a lack of involvement of neurotransmitter reuptake in antidepressant response; rather, that the spectrum of observed antidepressant effects is incompletely explained by neurotransmitter reuptake inhibition. The particular case of  $G\alpha_s$

redistribution appears to occur independent of this system, as seen in the C6 glioma model, and suggests the existence of additional target(s) mediating effects on G protein signaling.

### **3.4 Influence of adenylyl cyclase isoform expression on antidepressant response**

This final section of data deals with the role of adenylyl cyclase isoform expression and addresses the question: does  $G\alpha_s$  liberated from lipid raft domains in responsive cells couple selectively with certain adenylyl cyclase isoforms? Furthermore, is the “antidepressant  $G\alpha_s$  response” dependent upon the expression of these isoforms? Can “antidepressant responsiveness” be conferred to antidepressant nonresponsive cell lines and conversely, ablated in responsive cell lines by isotopic expression or knockdown of these isoforms?

Past studies <sup>212</sup> of C6 glioma have identified adenylyl cyclase type 6 (AC6) as the predominant isoform of C6 glioma, with lower expression of AC isoforms 1, 3, and 4. For this reason, AC6 was suspected as a potentially important contributor to the  $G\alpha_s$  antidepressant response.

#### **3.4.1 NKY80 and calcium ion inhibition of adenylyl cyclase 5 and 6**

First, inhibition of AC6 in C6 glioma was attempted with small molecule adenylyl cyclase inhibitor NKY80. At the time (circa 2011), NKY80 was described as a specific inhibitor of AC5, but with very few, if any, appearances in the literature at the time. Structurally,

NKY80 has similarity to adenine and presumably acts at the cyclase ATP binding site, also known as P-site.

Because of the similarity of AC5 and AC6 catalytic regions<sup>213</sup>, as well their overall similar structure, distribution, and regulation, we predicted that NKY80 would inhibit AC6. As such, it could be useful in dissecting the role of AC6 in cellular antidepressant response. If AC6 is specifically or preferentially activated by  $G\alpha_s$  subsequent to antidepressant treatment, then specific inhibition of AC6 should abolish this response. For this reason, I decided to use NKY80 in conjunction with the Salomon (membrane cyclase) assay to determine whether NKY80 would inhibit the antidepressant-induced increase in adenylyl cyclase.

Cells were grown in flasks and treated for three days with vehicle (water) or 10 $\mu$ M escitalopram, and membranes were prepared and cyclase assay run as described in Materials & Methods, both in the absence and presence of NKY80. Membranes were assayed at baseline (vehicle) or with agonist (10 $\mu$ M isoproterenol, 10mM NaF+20 $\mu$ M AlCl<sub>3</sub> (active as aluminum tetrafluoride anion [AlF<sub>4</sub>]<sup>-1</sup>), or 100 $\mu$ M forskolin). The NKY80 was used as a component of the assay reaction mixture; the cells were not co-treated with NKY80 during the antidepressant treatment period. Based on the AC5 IC<sub>50</sub> of 8.3 $\mu$ M{Pierre:2009ic}, a concentration of 10 $\mu$ M NKY80 was chosen for testing. The results are shown in Figure 20A.

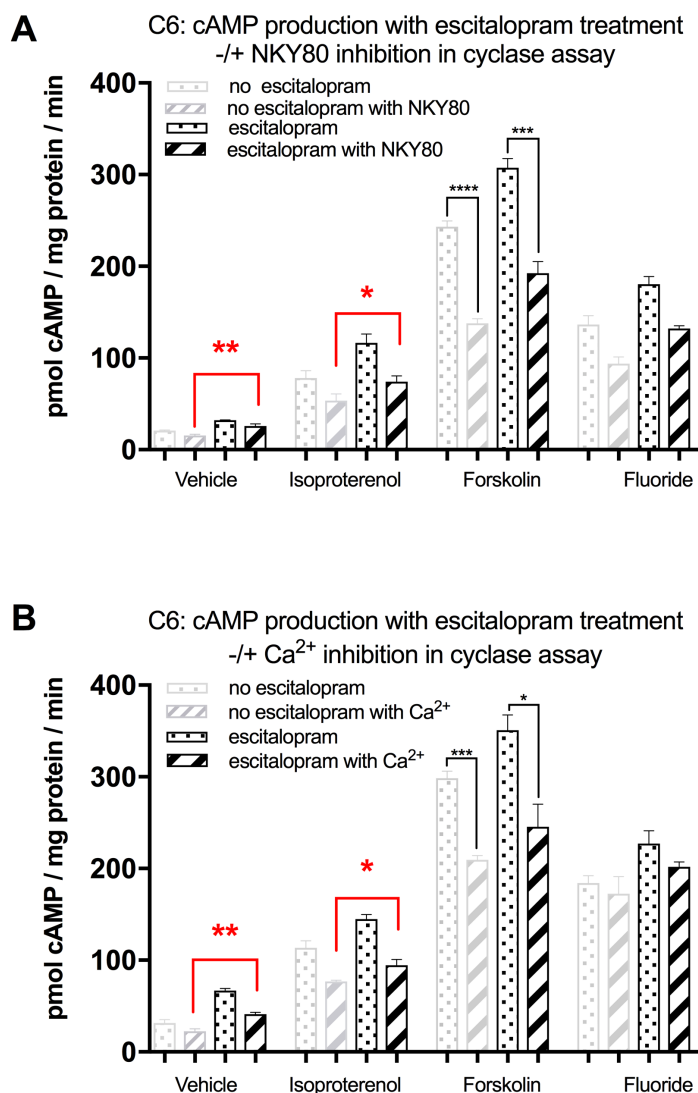


**Figure 23: C6 glioma membrane cAMP production with AC5/6 inhibitors**

C6 glioma were treated in flasks for 3 days with vehicle (water) or 10 $\mu\text{M}$  escitalopram. Membranes were prepared and assayed for cAMP production as described in Materials & Methods. Membranes were assayed in the presence and absence of (A) 10 $\mu\text{M}$  NKY80 or (B) 0.2 $\mu\text{M}$   $\text{Ca}^{2+}$  ion. Agonists used were 10 $\mu\text{M}$  isoproterenol, 100 $\mu\text{M}$  forskolin or 10mM NaF+20 $\mu\text{M}$   $\text{AlCl}_3$  (active as aluminum tetrafluoride anion  $[\text{AlF}_4]^{-1}$ ). Data show significant inhibition of cAMP for both NKY80 and  $\text{Ca}^{2+}$  while antidepressant response is maintained (red comparisons). Data from 3 similar experiments were analyzed by Student's T test (\* $p < 0.05$ , \*\*\*  $p < 0.001$ ) and are presented as mean  $\pm$  SEM. Selected comparisons shown.

NKY80 depressed the production of cAMP in both control and antidepressant-treated cells to a varying extent depending on the agonist used. NKY80 did not, however, abolish the antidepressant response per se. Note that for each agonist, the antidepressant-treated sample shows increased cAMP production compared to the untreated sample. The antidepressant effect was maintained, but total cAMP generated was reduced by NKY80.

This result was difficult to interpret at the time, with numerous possibilities: the drug may not actually act on AC6, the concentration may be inappropriate, or perhaps there is even a chemical incompatibility in the reaction mixture. The limited published data available at the time did not suggest any explanation. Perhaps somehow the activity of AC6 over the course of antidepressant treatment is required to evolve the membrane redistribution of  $G\alpha_s$  and co-treatment with antidepressant and NKY80 would be required to see an effect. Finally, AC6 may not be at all involved in the process. Since then, NKY80 has been somewhat more fully characterized. It does act as a P-site inhibitor, it does selectively inhibit both AC5 and AC6 isoforms, and does produce approximately 50% inhibition of both AC5 and AC6 at 10 $\mu$ M concentration (slightly more effective for AC5)<sup>214</sup>; this level of inhibition was evidenced in the forskolin groups, where nearly 50% inhibition of cAMP was achieved, though other groups showed less inhibition. This may indicate that NKY80 requires a more active cyclase, such as seen with forskolin stimulation, for fuller inhibitory activity.

The next set of experiments is similar to the above, but instead utilizing calcium ( $Ca^{2+}$ ) ion.  $Ca^{2+}$  is a well-characterized inhibitor of AC5 and AC6 in submicromolar concentrations, and

participates in the physiologic regulation of these isoforms<sup>213,215</sup>. Here, cyclase assays were done as above, with the same agonists, with  $\text{Ca}^{2+}$  in place of NKY80. While the assay reaction mixture includes  $\text{Ca}^{2+}$  chelator EGTA, starting  $\text{Ca}^{2+}$  concentration of 0.8mM was used to account for EGTA-  $\text{Ca}^{2+}$  binding as described in Materials & Methods. The  $\text{Ca}^{2+}$   $\text{IC}_{50}$  of both AC5 and AC6 is approximately 0.2 $\mu\text{M}$ ; in these experiments, a final  $\text{Ca}^{2+}$  concentration of 0.2 $\mu\text{M}$  was used. Figure 23B shows the results of these experiments in C6 glioma.

The results of  $\text{Ca}^{2+}$  inhibition and interpretation thereof are similar to that with NKY80. In each case,  $\text{Ca}^{2+}$  depressed the production of cAMP but did not abolish the antidepressant response. From these results, the role of AC6 in the antidepressant response cannot be confirmed nor ruled out. These results do, however, functionally confirm calcium-inhibited (AC5/6) cyclase as the predominant cyclase isoforms in C6 glioma: with both inhibitors, inhibition at  $\text{IC}_{50}$  caused a significant reduction of cAMP production, approaching 50% in some cases. If AC5/6 were expressed at lower levels, specific inhibition of these isoforms would not lower overall cAMP production to the extent observed.

The findings in C6 glioma strongly contrast the results of  $\text{Ca}^{2+}$  cyclase inhibition in HEK293. These results are shown in Figure 21 and are consistent with previously discussed data regarding cyclase activity in HEK293 (Figure 9). No increase in cAMP production is seen in HEK293 membranes in response to antidepressant treatment. Importantly, no decrease in cAMP production is observed in response to adenylyl cyclase 5/6 inhibitor  $\text{Ca}^{2+}$ . This suggests that, in contrast to C6 glioma, calcium-inhibited cyclase isoforms AC5/6 are not a

significantly functionally expressed in HEK293, a significant phenotypic difference between the two cell types.

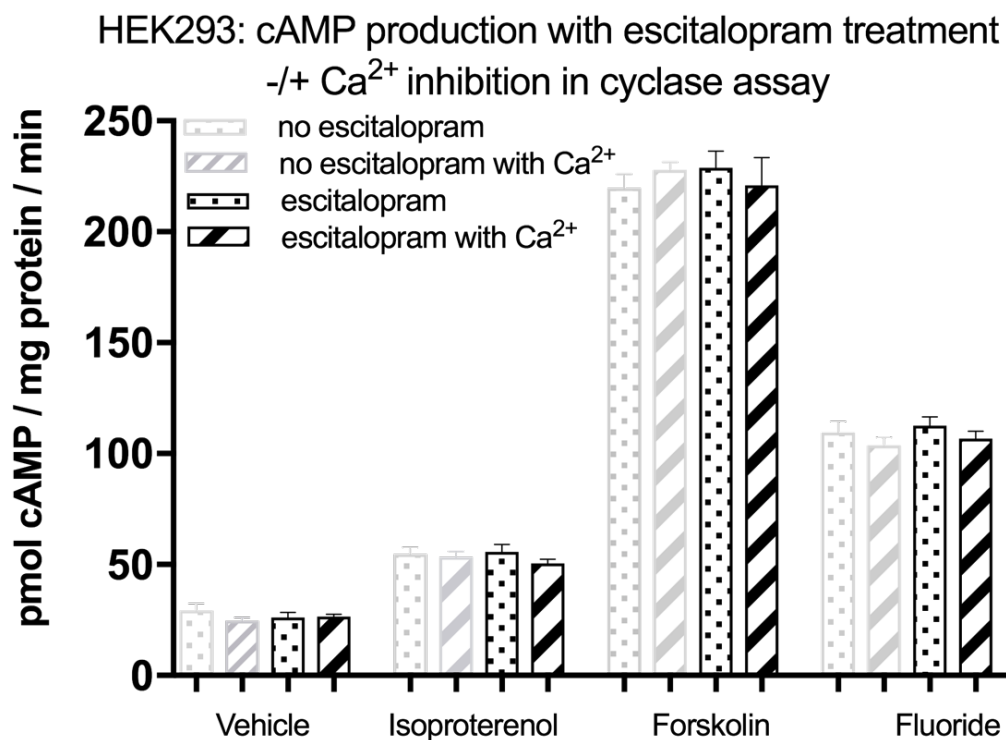


**Figure 24: HEK293 membrane cAMP production with AC5/6 inhibitor  $\text{Ca}^{2+}$**

HEK293 were treated in flasks for 3 days with vehicle (water) or 10 $\mu\text{M}$  escitalopram. Membranes were prepared and assayed for cAMP production as described in Materials & Methods. Membranes were assayed in the presence and absence of 0.2 $\mu\text{M}$   $\text{Ca}^{2+}$  ion. Agonists used were 10 $\mu\text{M}$  isoproterenol, 100 $\mu\text{M}$  forskolin or 10mM NaF+20 $\mu\text{M}$   $\text{AlCl}_3$  (active as aluminum tetrafluoride anion  $[\text{AlF}_4]^{-1}$ ). Data show no inhibition by  $\text{Ca}^{2+}$  and no response to escitalopram. Data from 6 similar experiments were analyzed by one-way ANOVA followed by Tukey test for post hoc multiple comparisons of means and are presented as mean +/- SEM



### **3.4.2 Effect of adenylyl cyclase isoform expression on HEK293 antidepressant response**

Having identified AC6 expression as a key difference between the two cell lines, I next sought to determine the effect of AC6 expression in HEK293 on antidepressant response. This was done two ways. In one set of experiments, AC6 was transfected into HEK293 via electroporation. These cells received a three-day drug treatment with escitalopram or desipramine at 10 $\mu$ M followed by sucrose density membrane fractionation to isolate lipid raft fractions for subsequent western blot. In the second approach, HEK293 were co-transfected with selected AC isoforms (2,3, and 6) and GFP-  $G\alpha_s$  for analysis via FRAP as previously described. These represent three functional classes of cyclase isoforms: calcium stimulated (AC3), calcium inhibited (AC6), and non-calcium regulated (AC2). The FRAP data are presented first, in Figure 25.

FRAP of antidepressant-treated wild type HEK293, HEK293-AC2, and HEK293-AC3 do not show an increase in half-time of recovery of GFP-  $G\alpha_s$ , which signifies a lack of response to antidepressant treatment. In contrast, HEK293 transfected with AC6 now show an antidepressant responsive FRAP phenotype, with a significant increase in half-time to recovery of GFP-  $G\alpha_s$ . Note also the increased baseline recovery halftime in AC2 and AC6-transfected cells, but not AC3. This slowing of GFP-  $G\alpha_s$  mobility could be attributed to the increased cyclase content of these cells, binding and retarding the movement of a larger fraction of  $G\alpha_s$ . AC3 expression, however, does not result in this change. This could be

explained by restriction of AC3 expression to the cell's primary cilium; AC3 is considered a marker of primary cilium in a variety of cell types <sup>216</sup>. If localized to the primary cilium,

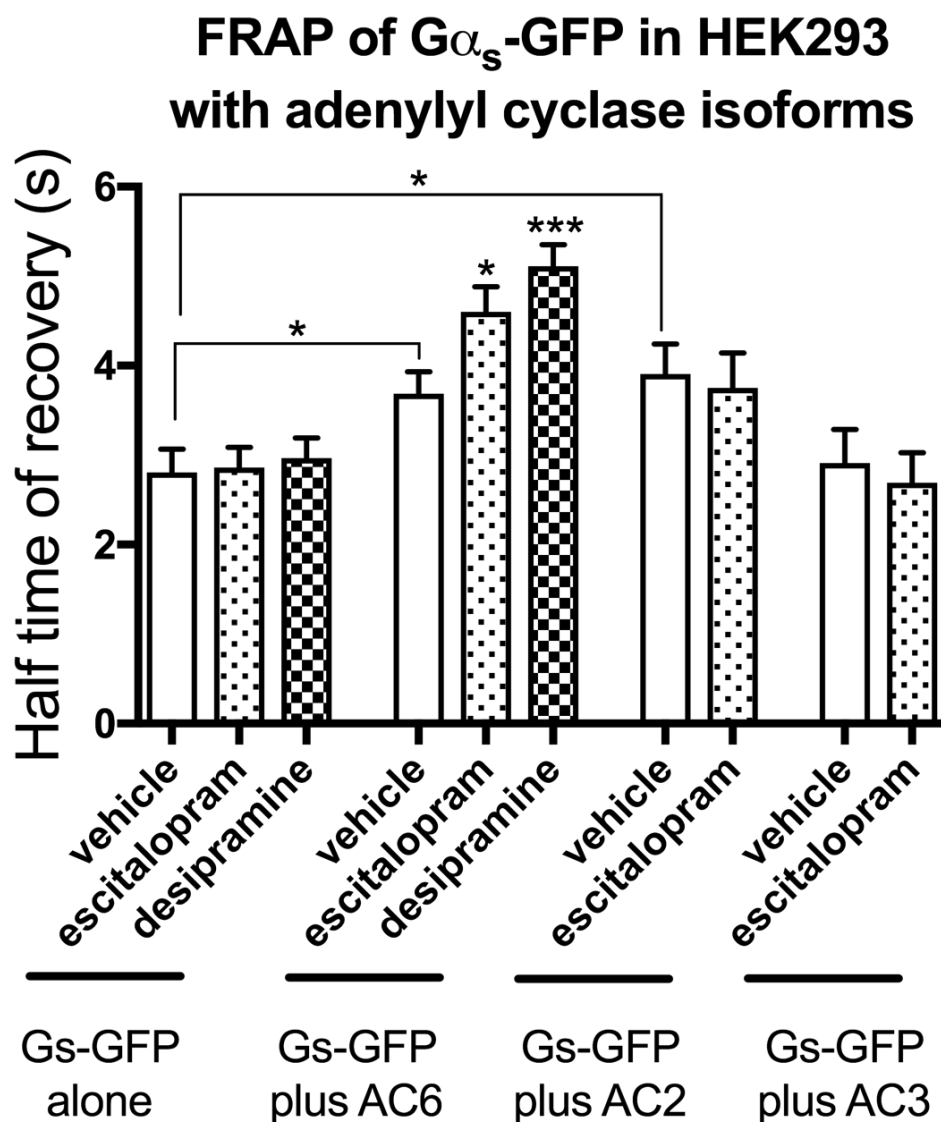


**Figure 25: Effect of adenylyl cyclase isoform expression on FRAP of GFP- $G\alpha_s$  in HEK293**

HEK293 were cotransfected with GFP- $G\alpha_s$  and the indicated adenylyl cyclase isoform, and cells stably expressing the constructs were selected with G418. Cells were grown in glass bottom microscope dishes and treated for 3 days with either 10 $\mu$ M escitalopram or desipramine. Only the cells in the HEK293-AC6 group show the characteristic increase in recovery time signifying a response to antidepressant drug. Additionally, baseline recovery was elevated in HEK293-AC6 and HEK293-AC2 compared to control, perhaps signifying a generally increased association of  $G\alpha_s$  with adenylyl cyclase. HEK293-AC3 do not show this elevation, perhaps due to targeting to primary cilia. Data were obtained from 21-58 data points depending on condition and were analyzed by one-way ANOVA (control versus treatment, \*  $p < 0.05$ , \*\*\*  $p < 0.001$ ) followed by Tukey test for post hoc multiple comparisons of means and are presented as mean  $\pm$  SEM.

AC3 expression would likely not affect FRAP results because the chance of capturing the primary cilium as a region of interest is low; I have never personally seen a structure identifiable as a primary cilium. Others have occasionally reported other isoforms such as AC6 as localized specifically to primary cilia as well<sup>217</sup>, but this this does not agree with the findings in this study which showed YFP-AC6 expression broadly over the cell membrane (Figure 26). This increase in baseline recovery half-time may also suggest adenylyl cyclase expression itself as a regulator of signaling. Since adenylyl cyclase binds active GTP-bound  $G\alpha_s$ , but not inactive GDP-bound  $G\alpha_s$ , the increased binding of  $G\alpha_s$  to cyclase could suggest that there is a pool of active  $G\alpha_s$  available to interact with cyclase, but limited by the amount of cyclase present. This notion, however, is not currently represented in the literature.

Figure 27 shows the results of membrane fractionation of HEK293-AC6 after drug treatment, which is consistent with data obtained via FRAP. As in the antidepressant-responsive C6 glioma, HEK293 expressing AC6 now show a redistribution of  $G\alpha_s$  out of lipid rafts after drug treatment. In combination with the FRAP data, this demonstrates that HEK293 expressing AC6 become antidepressant responsive with respect to  $G\alpha_s$  membrane localization. Fractionations of HEK293-AC2 and -AC3 were not performed due to the lack of response seen in the FRAP assay.

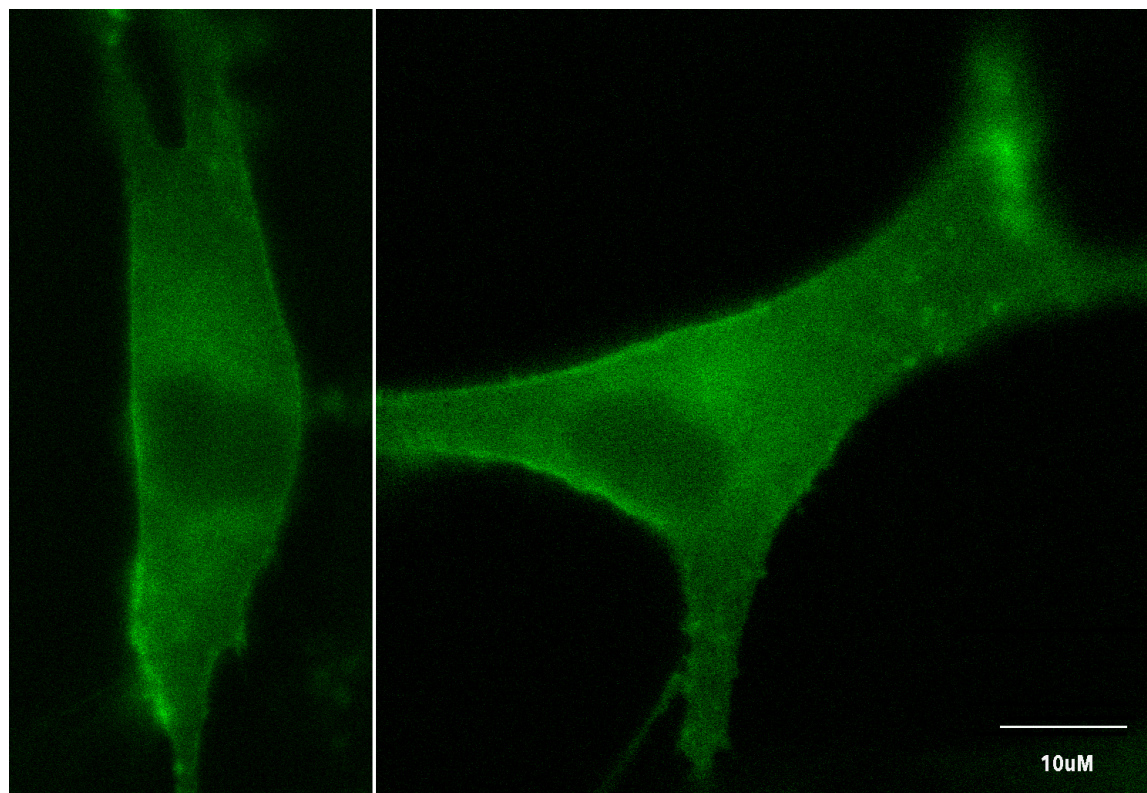


**Figure 26: Membrane expression of YFP-AC6 in C6 glioma**

C6 glioma were transfected with YFP-AC6 via electroporation and selected with G418. YFP-AC6 expression is detected over the entire membrane surface. Note: this is a false color image set to display as green.

## HEK293-AC6: $G\alpha_s$ in raft relative to control

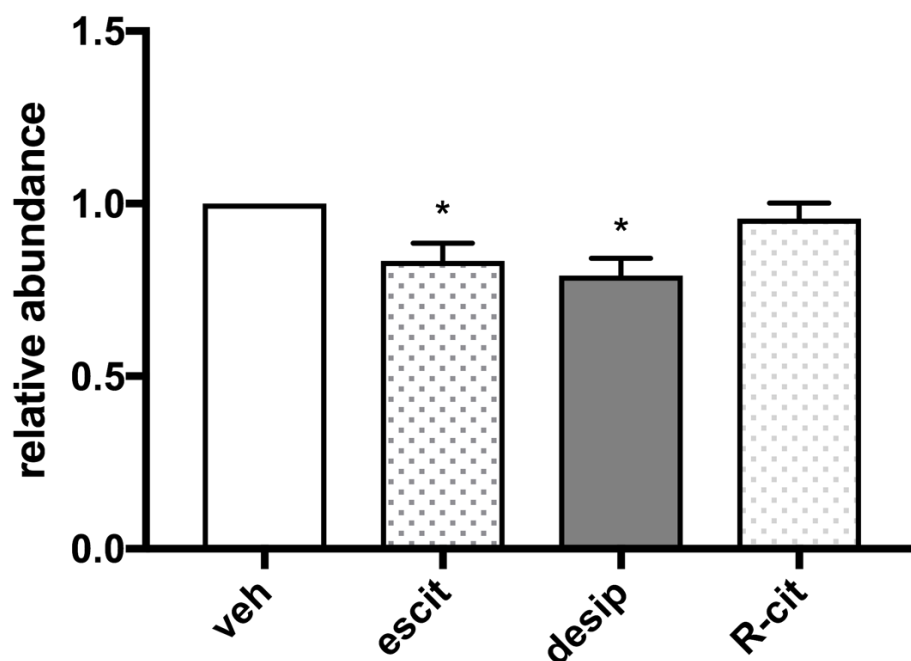


**Figure 27: Effect of AC6 expression in HEK293 on antidepressant response**

HEK293 stably expressing AC6 were grown in flasks. Membrane lipid rafts were prepared as described in Methods & Materials from cells treated with 10 $\mu$ M escitalopram, 10 $\mu$ M *R*-citalopram, or vehicle (water) and western blotted to determine G protein content. A significant reduction in lipid raft is seen in cells treated with escitalopram and desipramine, but not with non-antidepressant *R*-citalopram. Data from 4 similar experiments were analyzed by one-way ANOVA (control versus treatment, \*  $p < 0.05$ ) followed by Tukey test for post hoc multiple comparisons of means and are presented as mean  $\pm$  SEM.

### 3.4.3 FRAP of fluorescent adenylyl cyclase isoforms in C6 glioma

In the final set of experiments, fluorescent-tagged adenylyl cyclase isoforms (YFP-AC2, YFP-AC6, and GFP-AC8) were expressed in C6 glioma via electroporation. AC8 was used in place of AC3 because I did not have fluorescent AC3 with proper membrane localization. Again, these represent three classes of cyclase isoforms,  $\text{Ca}^{2+}$  stimulated (AC8),  $\text{Ca}^{2+}$  inhibited (AC6), and non-  $\text{Ca}^{2+}$  regulated (AC2). Thus far, only cyclase's effect on  $\text{G}\alpha_s$  mobility has been examined. Here, the "flip side of the coin" is studied, and the effect of  $\text{G}\alpha_s$  on cyclase mobility is measured. Figure 28 shows the results of these experiments.

Here, the following differential effect was observed: YFP-AC6 FRAP was slowed, as is observed with  $\text{G}\alpha_s$ . However, FRAP of YFP-AC2 and GFP-AC8 were unaffected. This suggests that  $\text{G}\alpha_s$  liberated from lipid raft subsequent to antidepressant treatment selectively couples with AC6 and not other isoforms. The nature of this selectivity is uncertain. One possibility is that the target(s) of antidepressants (aside from SERT) are colocalized in membrane domains or perhaps even scaffolded complexes containing AC6. These findings are more fully considered in the Discussion section. An attempt to evaluate the effect of AC6 knockdown via siRNA on antidepressant effect in C6 glioma is underway.

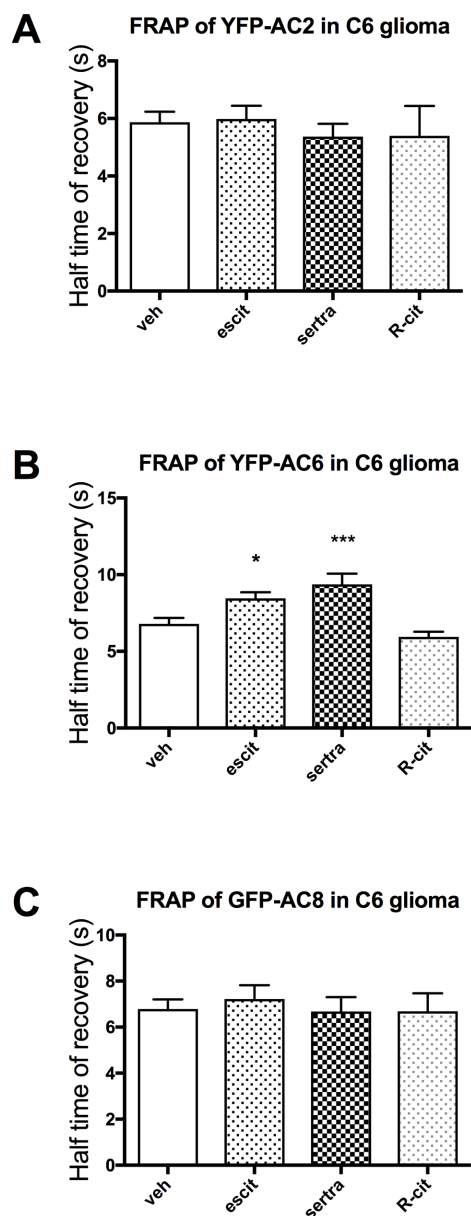


**Figure 28: FRAP of varied fluorescent adenylyl cyclase isoforms in C6 glioma**

C6 glioma were transfected via electroporation with (A) YFP-AC2, (B) YFP-AC6, or (C) GFP-AC8 and selected with G418. Cells were grown in glass bottom microscope dishes and treated for 3 days with 10 $\mu$ M escitalopram, sertraline, or *R*-citalopram. In contrast to other FRAP data presented, here fluorescent cyclase isoforms are subjected to FRAP; only native  $G\alpha_s$  is present. Only in the case of C6 glioma expressing YFP-AC6 (B) was a change in mobility observed after antidepressant treatment, suggesting that  $G\alpha_s$  liberated from lipid rafts subsequent to antidepressant treatment selectively couples with AC6 and not other AC isoforms tested. *R*-citalopram did not affect mobility in any condition. Data were obtained from 21-73 data points depending on condition and were analyzed by one-way ANOVA (control versus treatment, \*  $p < 0.05$ , \*\*\*  $p < 0.001$ ) followed by Tukey test for post hoc multiple comparisons of means and are presented as mean  $\pm$  SEM.



### 3.5 Accumulation of antidepressants in lipid rafts of C6 glioma and HEK293

In order to determine whether antidepressant compounds selectively accumulate in lipid rafts, suggesting a specific target or site of action in rafts, cells were grown in flasks and treated with drug for three days. After this, lipid rafts were harvested via sucrose gradient and examined for drug content with mass spectroscopy. Drug lipophilicity was assessed via octanol/water partitioning (Figure 29A). These studies showed the antidepressant compounds tested were relatively amphiphilic, with greater lipophilicity of antipsychotics aripiprazole and olanzapine. In contrast to the above, less lipophilic antidepressants of several classes showed significant accumulation in lipid rafts, while the more lipophilic antipsychotics did not accumulate. This includes antidepressants of the MAOI class, (phenelzine), and SSRIs (fluoxetine and escitalopram). Accumulation of tricyclics (desipramine, imipramine, amitriptyline) was minimal or absent. This demonstrates that accumulation of antidepressants in lipid rafts occurs independent of the drugs' lipid solubility and suggests a specific binding target or targets for these drugs in lipid raft (Figure 29B). Notably, escitalopram accumulates while *R*-citalopram does not; both isomers are of equal lipophilicity and should accumulate equally on the basis of their lipid solubilities. Figure 29C contrasts significant accumulation of escitalopram in lipid rafts from C6 glioma, with minimal accumulation in HEK293. Also shown is the lack of accumulation of *R*-citalopram in C6 glioma rafts.

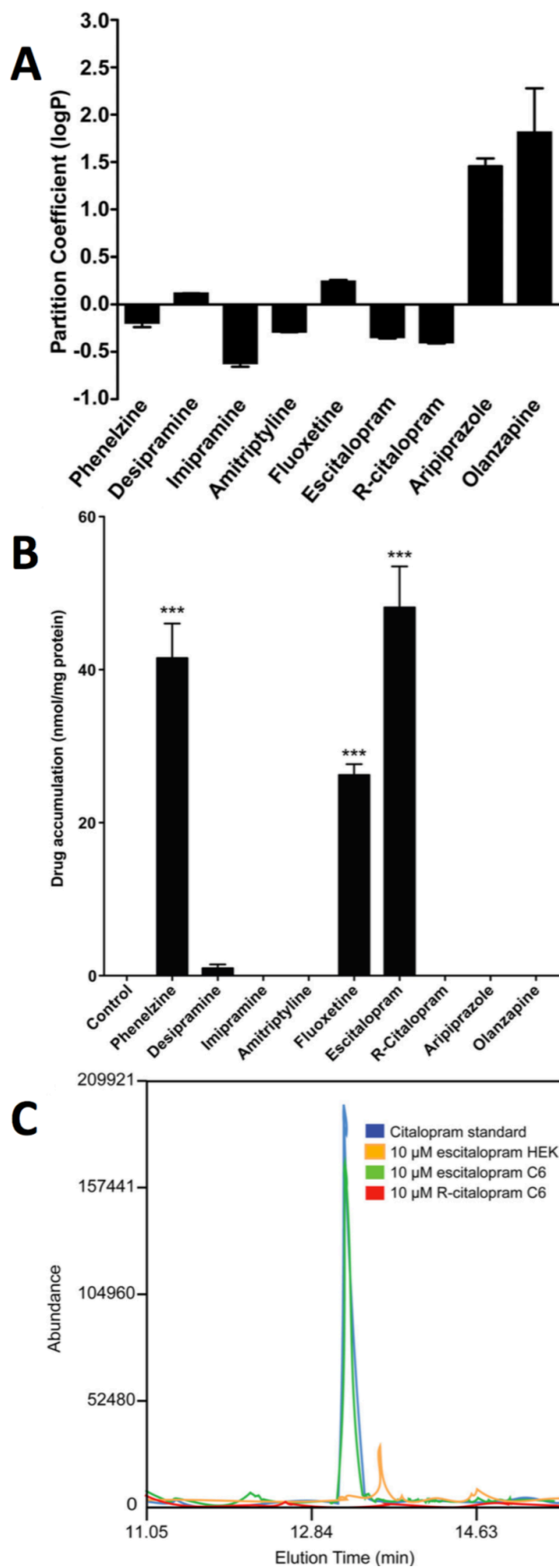


**Figure 29: Accumulation of antidepressant in lipid rafts of C6 glioma and HEK293**

Cells were treated for 3 days with the indicated compound (10 $\mu$ M), and lipid raft fractions were prepared from membranes. (A) UV absorbance was used to determine partition coefficient ( $\log P$ ) for psychoactive compounds. Partitioning between octanol and water shows that each is relatively amphiphilic, with the exception of aripiprazole and olanzapine. (B) Drug accumulation was determined and quantified by comparing peak intensities from the total ion chromatograph (TIC) of GC-MS analyses on accumulated drug with standard curves generated from methanol standards. Calculated moles of drug were normalized to protein content and reported as nmol/mg of protein. Phenelzine, fluoxetine, escitalopram, and to a lesser extent desipramine were observed to accumulate in lipid rafts, whereas the inactive stereoisomer *R*-citalopram and the antipsychotic olanzapine did not. Data were analyzed by Student's *t* test, and data are represented as mean S.E. (*n* 3; \*\*\*, *p* < 0.0001). (C) TIC chromatogram overlay of drug accumulation in lipid rafts of C6 cells treated with 10 $\mu$ M escitalopram *versus* *R*-citalopram as compared with lipid rafts isolated from escitalopram-treated HEK cells.



## Chapter 4: Discussion and Future Directions

A reasonable question at this juncture might be: How is all of this happening? A variety of drug classes -- including monoamine oxidase inhibitors, tricyclics, SSRIs, and assorted newer, non-canonical antidepressants (HDAC6 inhibitor, ketamine) -- with no known shared mechanism of action, somehow converge upon and enhance  $G\alpha_s$  signaling, but not that of other G proteins. It is challenging to imagine a unified explanation for the preceding collection of observations, and perhaps no single model is large enough to contain all of the extant data. During the preparation of this manuscript, several new findings of potential relevance were made by other members of the Rasenick lab and are unpublished, but inform the discussion and must be included.

While the use of glial cells in a depression/antidepressant study may raise an occasional eyebrow, neither glia nor neurons are singly implicated in depression, and glia have in recent years been more explicitly considered for a role in depression as well as the general functioning of the synapse itself<sup>218-220</sup>. Glial content of the brain has been variously estimated from 100 glia: 1 neuron, down more recently to a possible 1:1 ratio<sup>221</sup>. Whether glia dramatically exceed neurons or equal their number, they are a critical cell type in the brain, and debating the significance of glia vs. neurons in brain function is as strange as physiologists arguing about which organ system is most important in the body.

In an approach similar to that of Donati et al.<sup>48</sup>, which examined lipid raft from brains of suicide victims for G protein content, Rasenick lab colleague Harinder Singh found dramatic differences in tubulin acetylation in lipid rafts from brains of depressed suicide subjects compared to controls. While controls showed a varying degree of  $\alpha$ -tubulin acetylation in lipid rafts, suicide victims were nearly and consistently devoid of this acetylation. The overall amount of tubulin acetylation, as measured in homogenates, was equivalent in the 2 groups. This finding relates to the potential involvement of lipid raft tubulin acetylation and the use of HDAC inhibitors in depression. Dr. Singh has also found C6 glioma treatment with HDAC6 inhibitor tubastatin-A to produce increased  $\alpha$ -tubulin acetylation in rafts as well as the characteristic shift in  $G\alpha_s$  from lipid raft into non-raft domains, which is corroborated by FRAP data. Interactions between tubulin and  $G\alpha_s$  are well established<sup>222</sup>, but the mechanism of tubastatin-A with respect to  $G\alpha_s$  displacement from lipid rafts is not. Treatment with tricyclic imipramine and SSRI escitalopram, however, produced no changes in raft  $\alpha$ -tubulin acetylation in lipid rafts. Therefore, although extremely intuitively attractive, decreased tubulin acetylation appears **not** to be the mechanism of action of traditional antidepressants.

One particularly difficult question in antidepressants' shared G protein mechanism is the drugs' target or targets: Do these myriad drugs bind the same site? If different drugs or drug classes act at different sites, this phenomenon is actually multiple independent phenomena (yet leading to the same G protein endpoint) and increasingly difficult to interpret without more information. It is similarly difficult to fathom how these drugs

could be acting at the same shared site, given their diverse structures and the lack of an identified signature antidepressant structural motif.

One molecule known to bind multiple antidepressant structures is, of course, SERT.

Crystallization studies in bacterial SERT homolog LeuT and recently in SERT itself have identified at least two sites, a primary site known to recognize citalopram and tricyclic antidepressants, and a secondary allosteric site known to bind citalopram (enhancing citalopram affinity at the primary site)<sup>223,224</sup>. These particular antidepressants share a projecting aminopropyl moiety (three carbon chain terminating in an amino group). Other antidepressants such as sertraline lack this group, yet are known to inhibit SERT, leaving the possibility of additional binding sites. Though not widely studied, it has been noted that the structure of adenylyl cyclase shares similarities with the topological arrangement of a range of channels and transporters, and that the cyclase structure (12 transmembrane spans with two large intracellular segments forming the catalytic unit) is somewhat unusual for an enzyme synthesizing a cytosolic second messenger<sup>225</sup>. It could be, then, that adenylyl cyclases (AC6 in particular?), like reuptake transporters, are able to bind antidepressants directly.

In this model, the AC6 molecule, or perhaps a novel site created by AC6 and proteins it scaffolds, binds antidepressants. This interaction could be tested by a number of techniques such as surface plasmon resonance (SPR) or *in silico* modeling of potential antidepressant binding sites on adenylyl cyclase. Additionally, an experiment similar to Erb et al.<sup>67</sup> could be done in which plasma membranes and lipid rafts from antidepressant

treated HEK293 are compared to transfected HEK293-AC6 in terms of antidepressant accumulation. If AC6 indeed promotes the accumulation of antidepressant drugs, then HEK293-AC6 membranes should show a significant accumulation of a variety of antidepressant molecules compared to the wild type. Likewise, antidepressant accumulation in C6 glioma with AC6 knocked down should show a decreased accumulation of a variety of antidepressants corresponding to the extent of the knockdown, as well as a loss of effect on  $G\alpha_s$  localization.

How, though, could the accumulation of antidepressants through such a mechanism lead to the observed effects on G proteins,  $G\alpha_s$  in particular? To address this point, a second recent finding from the Rasenick lab will be introduced. We had considered in the past evaluating transcriptional or proteomic changes secondary to antidepressant treatment, and this study was finally undertaken by Rasenick lab colleague Nathan Wray through RNA-seq. This technique quantifies the various RNA species present in a sample. The strongest and most significant “hits” detected were for  $\Delta$ -5, -6, and -9 fatty acid desaturases FADS1, FADS2 and stearoyl-CoA desaturase-1 (SCD1), demonstrating increased transcription with antidepressant treatment. Fatty acid desaturases catalyze the introduction of double bonds, converting straighter, more saturated acyl chains (such as those associated with lipid raft domains) into more kinked, less saturated acyl chains (such as those associated with non-raft domains)<sup>226</sup>. Though these enzymes are understood in terms of their biochemical actions and localization (primarily endoplasmic reticulum<sup>227-229</sup>), their regulation is poorly understood. Transcription factor SREBP1 (sterol regulatory element binding protein 1) regulates desaturase transcription and contains a sterol-sensing domain



(SSD), which is believed to respond to physical steric changes in the membrane, in addition to membrane sterol content, though the precise signals are unclear<sup>230</sup>. To test the involvement of desaturases, one could quantify the effect of antidepressant treatment on membrane lipid species, and such experiments are planned.

Chen et al. have demonstrated in a yeast model, accumulation of SSRI sertraline (cells treated with nanomolar sertraline concentrations, within human therapeutic range) in membrane causing a steric distortion of the membrane, detection of this effect by the cell, and triggering of a cellular response (autophagy in this case)<sup>231</sup>. Notwithstanding the exhortations of yeast geneticists, mammals are not yeast, but this study demonstrates the ability of an antidepressant to accumulate in membranes, and cause a physical effect in the membrane which is both detected and responded to by the cell. Note that in this model, the authors attribute membrane binding solely to sertraline's amphipathic character at physiologic pH due to the lack of SERT expression in these cells. In defense of a model potentially lacking a specific target of antidepressant binding, this raises the notion of natural accumulation of some, but not all, antidepressants in membranes based solely on their lipid solubility. Accumulation of antidepressants could trigger a steric effect independent of a specific target. Additionally, the finding in Erb et al.<sup>67</sup> that while SSRIs fluoxetine and escitalopram and MAOI phenelzine accumulated in lipid rafts, little or none of three tested tricyclics (desipramine, imipramine, amitriptyline), which share a similar structure, accumulated, is curious. This finding cannot be reasoned away if one assumes a common antidepressant site of action, nor can it necessarily be explained with the existing data. It could be that tricyclic antidepressant binding to rafts is particularly labile due to

their structure or perhaps does not survive the raft preparation procedure due to an incompatibility with a particular reagent or condition; Recall that in Eisensamer et al., direct application of tricyclic desipramine to extracted lipid rafts fractions resulted in accumulation of the drug<sup>66</sup>. Finally, if one considers a model of nonspecific accumulation of antidepressants based on lipid solubility, how is the lack of accumulation of escitalopram stereoisomer *R*-citalopram in Erb et al., which has identical chemical characteristics, explained? Perhaps in this case, *R*-citalopram binds a molecule *outside* of rafts with higher affinity than its attraction to lipids. Certainly, the entire rest of the cell provides a greater range of targets than do tiny lipid rafts. This could be similarly tested and quantified.

To summarize thus far, we have considered mechanisms allowing binding of antidepressants to lipid rafts in the presence or absence of a specific target, and activation of desaturase enzymes. These proposed mechanisms are testable at multiple points, as described above. In the case of specific binding to AC6, perhaps a local steric effect occurs, which is somehow detected, promoting the activation of desaturases, which either target the sterically deformed membrane region directly or in a more generalized pattern. This would occur in the endoplasmic reticulum before transport to the plasma membrane and would suggest intracellular binding of antidepressants, though similar reasoning could be made for such a phenomenon occurring at the plasma membrane. The antidepressant-deformed AC6 microdomain, having triggered a response, becomes more desaturated and non-raftlike. The differential response of G proteins to the remodeled, less saturated membrane could be due to the way in which G proteins are anchored to the membrane. Recall that while  $G\alpha_s$  is singly acylated,  $G\alpha_i$  and  $G\alpha_q$  are dually acylated. This dual lipid

anchoring provides increased hydrophobic interactions with the longer acyl chains constituting lipid rafts and anchors  $G\alpha_i$  and  $G\alpha_q$  more strongly in rafts. Thus, as the membrane becomes more desaturated, either in a targeted or a general fashion, the reduced lipid raft content of the cell would “force”  $G\alpha_s$  out of rafts first due to its weaker anchoring. The enhanced interaction observed between  $G\alpha_s$  and adenylyl cyclase with antidepressant treatment could be due to regulatory properties of membrane lipids themselves<sup>232</sup>, as lipid regulation of signaling is not limited to physical segregation of partners by lipid rafts, and the desaturated lipid species may regulate the relevant enzymes differently. Affinity between  $G\alpha_s$  and adenylyl cyclase could be enhanced, or perhaps the GTPase activity of  $G\alpha_s$  could be negatively regulated by the desaturated lipid environment, promoting longer and more fruitful  $G\alpha_s$  – adenylyl cyclase interactions.

Thus, in the hypothesis of direct binding of antidepressants to AC6, and desaturation targeted to these domains, the conceptualization of the antidepressant-  $G\alpha_s$  phenomenon as “ $G\alpha_s$  moves out of lipid rafts” becomes instead, “lipid rafts become nonrafts” and  $G\alpha_s$  and adenylyl cyclase are caught up in the middle of it, enhancing their interaction. This is depicted in Figure 30. This also addresses the lingering question: if AC6 is primarily a raft-associated protein, how does exodus of  $G\alpha_s$  from rafts enhance  $G\alpha_s$  specifically with AC6 but not other isoforms tested? In the case of a model in which antidepressants are not binding specifically to AC6, or desaturation is not targeted directly to AC6 microdomains, the above concepts still apply and suggest a desaturation of the membrane, loss of rafts,

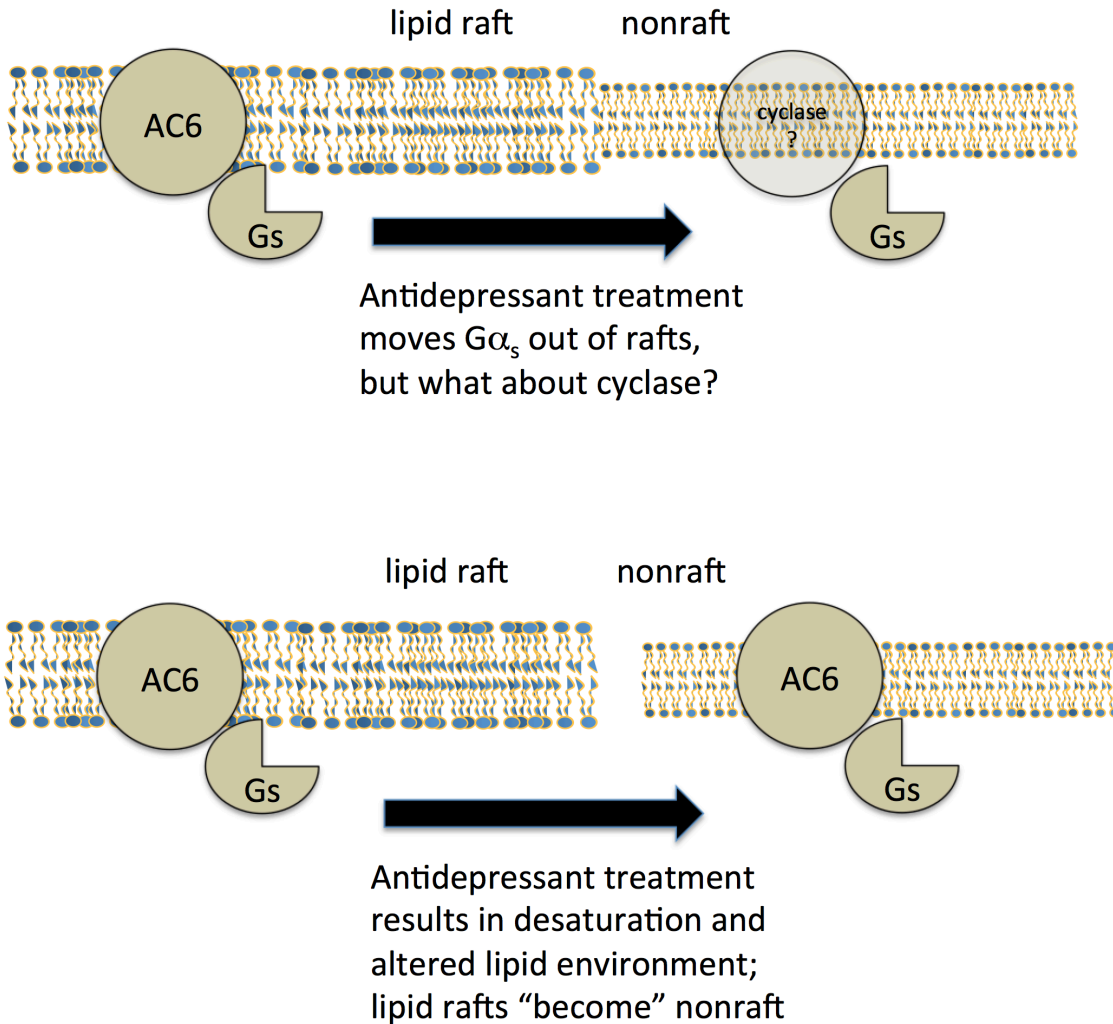


**Figure 30: Reconceptualization of G protein antidepressant effect**

The Rasenick laboratory has traditionally described the antidepressant effect as  $G\alpha_s$  "moving out of lipid rafts." However, the cyclase implicated in this thesis, AC6, is typically considered a raft-localized cyclase. Alterations in AC6 localization in response to antidepressant treatment have not been determined due to the poor quality of available antibodies.

With the benefit of recent desaturase findings, a better description of the phenomenon of antidepressant response may be "AC6 microdomains experience a desaturation of their lipid environment" or more simply, "rafts become nonrafts."

and specific loss of  $G\alpha_s$  due to its weaker membrane anchoring. The irony that a phenomenon assumed and demonstrated to be a specific, targeted effect, rather than a general membrane disruptive phenomenon, may actually be a general membrane disruptive phenomenon, is not lost on the author. Furthermore, this proposed mechanism of action may place a limit on the potential efficacy of antidepressants, at least on the component of their mechanism that depends on G protein changes. This study demonstrated a mass exodus of  $G\alpha_s$ ,  $G\alpha_i$  and  $G\alpha_q$  from lipid rafts with membrane disrupting colchicine and methyl- $\beta$ -cyclodextrin treatments. In contrast, the apparently milder membrane disruption mediated by antidepressant specific or nonspecific binding and activation of desaturases causes the loss of only  $G\alpha_s$  from lipid raft (and only certain cell lines such as wild type C6 glioma). If antidepressants had a stronger effect upon the membrane, additional G protein classes could be displaced; one could envision the dual liberation of  $G\alpha_s$  and  $G\alpha_i$  and potential conflicts on regulation of adenylyl cyclase. The particular involvement of AC6 in this phenomenon would be particularly concerning if  $G\alpha_i$  were liberated from rafts, as AC6 is one of the cyclase isoforms negatively regulated by  $G\alpha_i$ .

The issue of G protein anchoring in the antidepressant response could be evaluated directly by the use of G protein chimeras with altered N-terminal acylation sites. Suggested experiments are illustrated in Figure 31. Thus,  $G\alpha_i$  and  $G\alpha_q$  could be created carrying the single palmitoylation of  $G\alpha_s$ , while  $G\alpha_s$  could be festooned with the dual acylations of either  $G\alpha_i$  and  $G\alpha_q$ . In this case, one would expect a loss of  $G\alpha_i$  and  $G\alpha_q$  from lipid raft after antidepressant treatment, but the retention of  $G\alpha_s$ . Unpublished data from colleague Sam Erb suggested such a result, as chimeric  $G\alpha_s$  carrying the dual  $G\alpha_i$ -type acylation did not

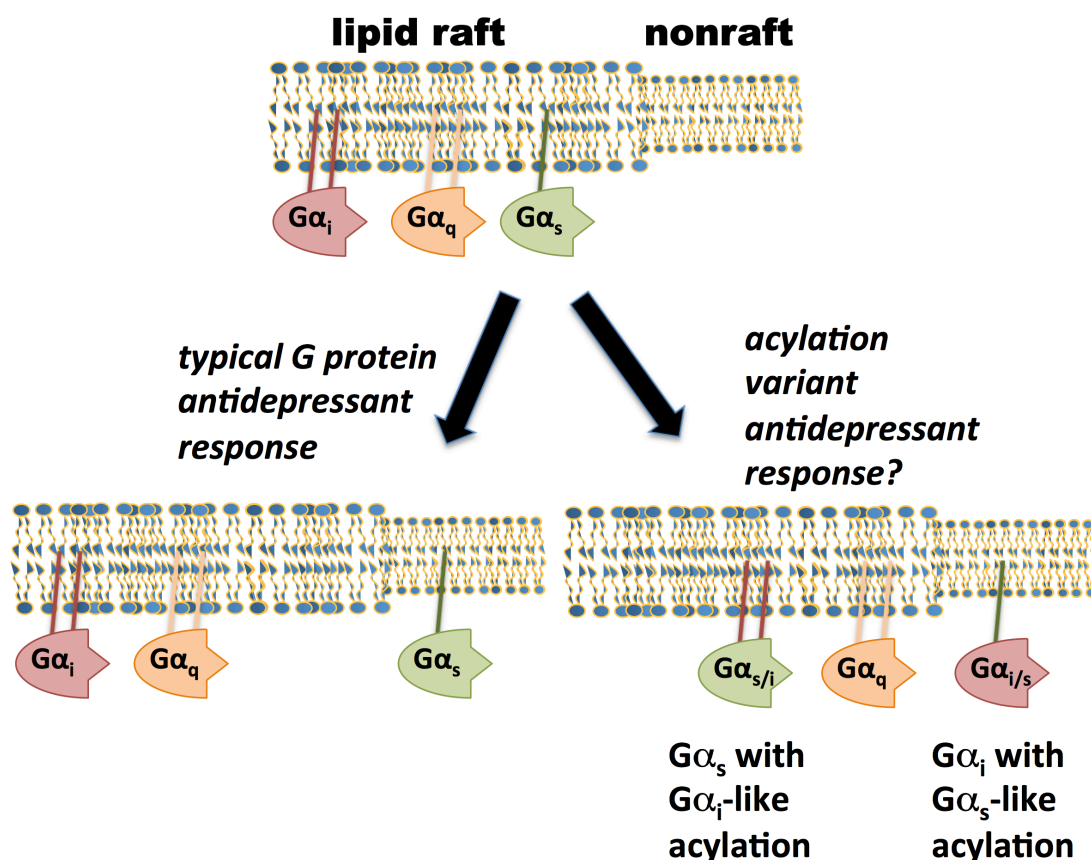


**Figure 31: Use of G protein acylation variants to evaluate the role of acylation in the antidepressant response.**

If preferential  $G\alpha_s$  movement from lipid rafts is dependent on the comparatively weaker  $G\alpha_s$  lipid raft anchoring, manipulation of G proteins' lipid anchors could alter the G protein response to antidepressant treatment.  $G\alpha_s$  expressing the N-terminal region of  $G\alpha_i$  carries the  $G\alpha_i$ -type acylation of palmitoylation/myristoylation and may be retained in lipid rafts as is  $G\alpha_i$ . Likewise, modifying  $G\alpha_i$  with a  $G\alpha_s$ -type single palmitoylation may result in loss of the modified  $G\alpha_i$  from lipid rafts, subsequent to antidepressant treatment.  $G\alpha_q$  could be similarly tested. These experiments will be performed in the future.

appear to be altered by antidepressant treatment, while wild type  $G\alpha_s$  in the same cell did redistribute from lipid rafts. This finding was not followed up because attempts to replicate this finding via FRAP of chimeric GFP-  $G\alpha_s$ /  $G\alpha_i$  were unsuccessful due to poor expression and localization of the construct. This could possibly be addressed through use of a transient rather than stable transfection, or a different cellular system (such as PC12 pheochromocytoma).

Prior to the recent desaturase finding, a related model of antidepressant action was developed and is presented as an alternative. This model also clarifies how a particular adenylyl cyclase isoform could establish an antidepressant responsive G protein phenotype in nonresponsive cells such as HEK293. HEK293 appear to lack or express low levels of  $Ca^{2+}$  - inhibited adenylyl cyclase isoforms AC5 and AC6. Unpublished northern blot data by colleague Sam Erb show very limited AC5 and no AC6 RNA in HEK293 cells. Unfortunately, the best available antibodies are targeted jointly to AC5 and AC6 and are, frankly, woefully non-specific and have been of limited use. The present study contains functional assays of adenylyl cyclase in the context of  $Ca^{2+}$  or NKY80 (specific AC5/6 inhibitor) inhibition which demonstrate a clear difference between the main cell lines examined. In C6 glioma membranes, cAMP production was profoundly diminished by these inhibitors (in response to some agonists, nearly 50% inhibition at the  $IC_{50}$  of either inhibitor, suggesting a predominance of these isoforms). In contrast, cAMP production from HEK293 membranes was unaffected by either inhibitor, suggesting a lack of AC5/6 isoforms.

In the case of adenylyl cyclase as a specific target of antidepressant binding, the lack of AC6 (or potentially AC5; no data rule out this possibility) would mean no binding of antidepressant and no antidepressant effect. If antidepressants instead accumulate in lipid rafts nonspecifically due to their lipid solubility, their presence could disturb the more ordered acyl chains of the raft domain and constitute a type of membrane disruption (or activate desaturases) and lead to the selective effects on  $G\alpha_s$  as described above. In the case of HEK293, AC6 (or potentially AC5) and the  $G\alpha_s$  it would scaffold are simply not present to “take advantage” of these effects upon lipid rafts. Why then, is signaling not enhanced through other lipid raft cyclases in HEK293 with antidepressant treatment? Other raft cyclases include  $Ca^{2+}$ -stimulated isoforms AC1, AC3 and AC8. AC3 may be limited to primary cilia and would not contribute meaningfully to total cellular cAMP production. In the case of AC1 and AC8, these isoforms are closely associated with capacitative  $Ca^{2+}$  entry, to the extent that their activity is not stimulated through evoked  $Ca^{2+}$  release from the endoplasmic reticulum, nor via plasma membrane influx through ionophores, but only by capacitative  $Ca^{2+}$  entry<sup>233,234</sup>. This is likely achieved through close physical anchoring of the AC1 or AC8 microdomains and their contents to capacitative  $Ca^{2+}$  channels. Perhaps this increased anchoring renders these microdomains and their contents less sensitive to any membrane disrupting effects of antidepressants. This hypothesis is depicted in Figure 32. Thus, HEK293 may accumulate antidepressant as do C6, but lacks the proper cyclase to capitalize on the lipid raft disruption created. For this reason, quantification of antidepressant accumulation in HEK293 and HEK293-AC6 should be performed.



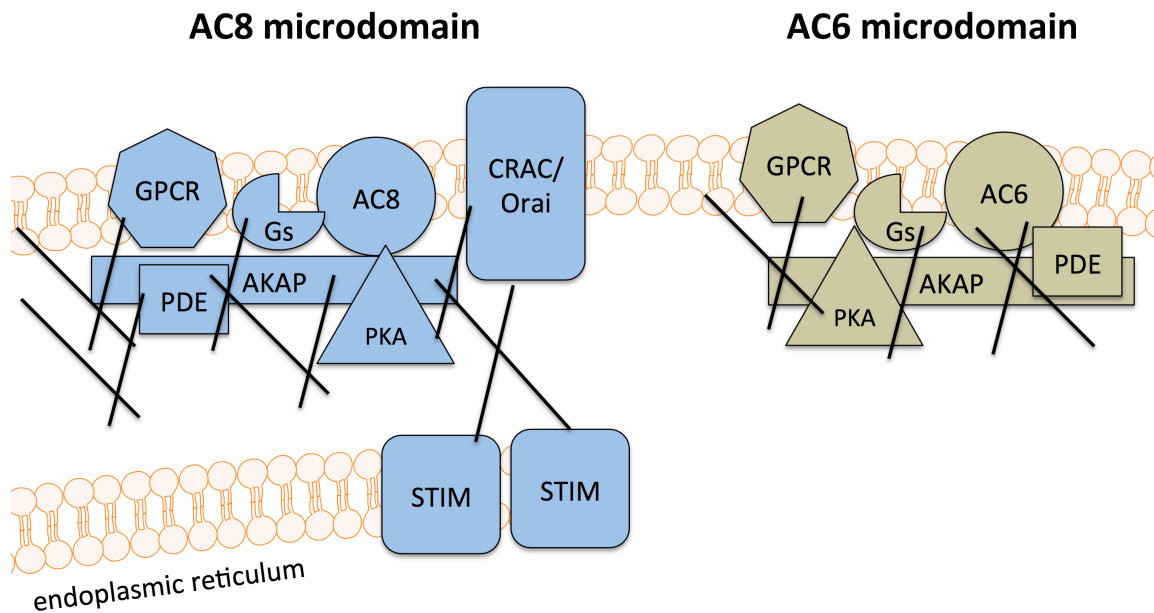


**Figure 32: Cyclase specificity in the G protein antidepressant response. Why AC6?**

FRAP experiments on fluorescent cyclase isoforms in C6 glioma cells showed selective involvement of AC6, but not AC2 or AC8, in response to antidepressant treatment. Like AC6, AC8 (and AC1) is typically localized to lipid rafts and would also be subject to a desaturated membrane environment subsequent to antidepressant treatment. Unlike AC6, AC8 is closely linked with capacitative  $\text{Ca}^{2+}$  entry and incorporates additional proteins spanning both plasma and endoplasmic reticulum membranes, and would constitute a larger protein complex with increased cytoskeletal anchoring. Such a complex could be more resistant to the desaturating effects of antidepressant treatment and retain and scaffold a more saturated, lipid raft environment, compared to AC6. A cell line lacking AC6, such as HEK293, could experience desaturation after antidepressant treatment, but lack cyclase microdomains sensitive to desaturation effects, and fail to demonstrate enhanced Figure  $\text{G}\alpha_s$ –AC coupling.

The previous requirement of three days' treatment for detection of antidepressant effect via sucrose gradient fractionation was consistent with an accumulation model of action. Detection of antidepressant effect at one day of treatment using the newer FRAP technique is surprising in that context, unless the threshold for accumulation related changes is very low. This is perhaps the case, as detection of effect was also made at 50 nM escitalopram using FRAP, although this experiment utilized a three day treatment period. A time series at 50 nM was not done and perhaps would reveal the effect at an earlier time point. Additionally, the ability to detect effect at this low concentration is key to the potential use of this effect in circulating cells as a clinical biomarker of antidepressant response, because this effect occurs far sooner than the 4-12 weeks one must wait to find out if the antidepressant is going to work.

Finally, if antidepressant binding triggers a steric effect that either activates desaturases or is inherently disruptive to the membrane, why does expression of SERT in HEK293 not confer antidepressant responsiveness? If, in fact, a specific target is required, AC6 could bind more antidepressant molecules than SERT, or perhaps SERT binds antidepressants in a way that is less disruptive to the membrane. The experiments in this paper dealing with SERT contribution to the antidepressant effect show that expression of SERT, a protein known to bind antidepressants<sup>223</sup>, in C6 glioma does not enhance the antidepressant response. It appears that increased binding of antidepressant due to SERT either does not create a disruptive effect or does not further signal desaturase activity, suggesting again that binding of antidepressant to SERT does not participate in the phenomenon of  $G\alpha_s$  redistribution.



## Chapter 5: Conclusion

This study has examined a long-noted component of antidepressant response that does not involve antidepressants' canonical mechanism of action via reuptake inhibition, and identified a cellular contributor to the effect -- adenylyl cyclase 6, which may bind antidepressants directly -- present in responsive cells, absent in nonresponsive cells, and whose expression is able to confer antidepressant responsiveness.

The selective effect of antidepressants on  $G\alpha_s$  redistribution from lipid raft may, in fact, be a general membrane disruption or alteration whose "selectivity" is a function of antidepressants' limited ability to alter the membrane, compared to other treatments such as colchicine or methyl- $\beta$ -cyclodextrin. This disruption may be caused directly by antidepressant binding to the membrane or mediated through the activation of desaturase enzymes.

It is hoped that further clarification of these mechanisms of antidepressant drugs will lead to the development of drugs more consistently effective in the treatment of depression. Perhaps, for example, one could look for milder direct disruptors of raft structure or stronger activators of desaturase enzymes, an avenue of inquiry otherwise unlikely.

The following additional experiments are proposed:

- 1) evaluation of antidepressant response in AC6 knockdowns in C6 glioma
- 2) assessment of AC6 antidepressant binding (such as via SPR)

- 3) quantification of membrane accumulation for a wider variety of antidepressants including ketamine, and perhaps a re-examination of tricyclics' failure to accumulate in the membrane.
- 4) quantification of antidepressant in HEK293 wild type and HEK293-AC6; also quantification in C6 glioma AC6 knockdowns
- 5) identification/quantification of membrane lipid species in the presence and absence of selected antidepressants in C6 glioma
- 6) revisit chimeric studies; perhaps existing constructs can be modified or better versions can be obtained; perhaps they would work in another cell line

Ideally, all of these conditions would be tried. Agreement among these various approaches will lend stronger support to the overall hypothesis, which some might argue is weakened by the lack of a definite target. If AC6 turns out not to directly bind antidepressants or create a binding site, finding another target could be quite difficult, a molecular needle in a haystack. A proteomic comparison study of antidepressant effects, either whole cell or focused on lipid rafts, to look for further proteins (potential drug targets) implicated in the process could be useful in this regard.

Progress in the study of depression itself, like antidepressant action, has been frustrating, and still lacks an overall model of the pathology. Depression may be similar to the disease of yore, dropsy. In the early 20<sup>th</sup> century, sufferers of edema (such as swollen legs) were said to have "dropsy." Today it is known that such edema could be caused by a variety of causes. Kidney failure could reduce fluid excretion. Hepatic disease could cause

hypoalbuminemia, resulting in decreased osmotic pull in the vasculature and loss of fluid to interstitial compartments. Heart failure also results in edema. Approaching dropsy as a monolithic entity, or even as a disease itself, would stymie efforts to understand it.

Depression itself may be phenotype like dropsy, not a disease.



### Works Cited

1. Kessler, R. C. *et al.* The epidemiology of major depressive disorder: results from the National Comorbidity Survey Replication (NCS-R). *JAMA* **289**, 3095–3105 (2003).
2. DeRubeis, R. J. *et al.* Cognitive therapy vs medications in the treatment of moderate to severe depression. *Arch. Gen. Psychiatry* **62**, 409–416 (2005).
3. Greenberg, P. E., Fournier, A.-A., Sisitsky, T., Pike, C. T. & Kessler, R. C. The economic burden of adults with major depressive disorder in the United States (2005 and 2010). *J. Clin. Psychiatry* **76**, 155–162 (2015).
4. Lépine, J.-P. & Briley, M. The increasing burden of depression. *Neuropsychiatr Dis Treat* **7**, 3–7 (2011).
5. Schildkraut, J. J. The catecholamine hypothesis of affective disorders. A review of supporting evidence. *Int J Psychiatry* **4**, 203–217 (1967).
6. McEwen, B. S. Glucocorticoids, depression, and mood disorders: structural remodeling in the brain. *Metab. Clin. Exp.* **54**, 20–23 (2005).
7. Pittenger, C. & Duman, R. S. Stress, depression, and neuroplasticity: a convergence of mechanisms. *Neuropsychopharmacology* **33**, 88–109 (2008).
8. Huang, G.-J., Bannerman, D. & Flint, J. Chronic fluoxetine treatment alters behavior, but not adult hippocampal neurogenesis, in BALB/c mice. *Molecular Psychiatry* **13**, 119–121 (2008).
9. Andrade, C. & Rao, N. S. K. How antidepressant drugs act: A primer on neuroplasticity as the eventual mediator of antidepressant efficacy. *Indian J Psychiatry* **52**, 378–386 (2010).
10. Hollon, S. D. *et al.* Effect of cognitive therapy with antidepressant medications vs antidepressants alone on the rate of recovery in major depressive disorder: a randomized clinical trial. *JAMA Psychiatry* **71**, 1157–1164 (2014).
11. Trivedi, M. H. *et al.* Evaluation of outcomes with citalopram for depression using measurement-based care in STAR\*D: implications for clinical practice. *Am J Psychiatry* **163**, 28–40 (2006).
12. López-Ibor, J. J., López-Ibor, M.-I. & Pastrana, J. I. Transcranial magnetic stimulation. *Current Opinion in Psychiatry* **21**, 640–644 (2008).
13. Pagnin, D., de Queiroz, V., Pini, S. & Cassano, G. B. Efficacy of ECT in Depression: A Meta-Analytic Review. *FOC* **6**, 155–162 (2008).
14. Prudic, J. *et al.* Resistance to antidepressant medications and short-term clinical response to ECT. *Am J Psychiatry* **153**, 985–992 (1996).
15. Hammond, D. C. Neurofeedback Treatment of Depression with the Roshi. *Journal of Neurotherapy* **4**, 45–56 (2008).
16. Malone, D. A. *et al.* Deep brain stimulation of the ventral capsule/ventral striatum for treatment-resistant depression. *Biological Psychiatry* **65**, 267–275 (2009).
17. O'Reardon, J. P. *et al.* Efficacy and safety of transcranial magnetic stimulation in the acute treatment of major depression: a multisite randomized controlled trial. *Biological Psychiatry* **62**, 1208–1216 (2007).



18. Krishnan, V. & Nestler, E. J. in *Current Topics in Behavioral Neurosciences* **7**, 121–147 (Springer Berlin Heidelberg, 2011).
19. Willner, P. The chronic mild stress (CMS) model of depression: History, evaluation and usage. *Neurobiol Stress* **6**, 78–93 (2017).
20. Heurteaux, C. *et al.* Deletion of the background potassium channel TREK-1 results in a depression-resistant phenotype. *Nat Neurosci* **9**, 1134–1141 (2006).
21. Lira, A. *et al.* Altered depression-related behaviors and functional changes in the dorsal raphe nucleus of serotonin transporter-deficient mice. *Biological Psychiatry* **54**, 960–971 (2003).
22. Holmes, A., Yang, R. J., Murphy, D. L. & Crawley, J. N. Evaluation of antidepressant-related behavioral responses in mice lacking the serotonin transporter. *Neuropsychopharmacology* **27**, 914–923 (2002).
23. Petit-Demouliere, B., Chenu, F. & Bourin, M. Forced swimming test in mice: a review of antidepressant activity. *Psychopharmacology (Berl.)* **177**, 245–255 (2005).
24. Rodgers, R. J. & Dalvi, A. Anxiety, defence and the elevated plus-maze. *Neuroscience & Biobehavioral Reviews* **21**, 801–810 (1997).
25. Willner, P., Towell, A., Sampson, D., Sophokleous, S. & Muscat, R. Reduction of sucrose preference by chronic unpredictable mild stress, and its restoration by a tricyclic antidepressant. *Psychopharmacology (Berl.)* **93**, 358–364 (1987).
26. Xu, F. *et al.* Macaques exhibit a naturally-occurring depression similar to humans. *Sci Rep* **5**, 9220 (2015).
27. Fredriksson, R., Lagerström, M. C., Lundin, L.-G. & Schiöth, H. B. The G-Protein-Coupled Receptors in the Human Genome Form Five Main Families. Phylogenetic Analysis, Paralogon Groups, and Fingerprints. *Molecular Pharmacology* **63**, 1256–1272 (2003).
28. Keller, A. & Vosshall, L. B. Better smelling through genetics: mammalian odor perception. *Current Opinion in Neurobiology* **18**, 364–369 (2008).
29. Hillenbrand, M., Schori, C., Schöppe, J. & Plückthun, A. Comprehensive analysis of heterotrimeric G-protein complex diversity and their interactions with GPCRs in solution. *Proc. Natl. Acad. Sci. U.S.A.* **112**, E1181–E1190 (2015).
30. Flower, D. R. Modelling G-protein-coupled receptors for drug design. *Biochim. Biophys. Acta* **1422**, 207–234 (1999).
31. Prossnitz, E. R., Arterburn, J. B. & Sklar, L. A. GPR30: A G protein-coupled receptor for estrogen. *Molecular and Cellular Endocrinology* **265-266**, 138–142 (2007).
32. Logothetis, D. E., Kurachi, Y., Galper, J., Neer, E. J. & Clapham, D. E. The  $\beta\gamma$  subunits of GTP-binding proteins activate the muscarinic  $K^+$  channel in heart. *Nature* **325**, 321–326 (1987).
33. Oldham, W. M. & Hamm, H. E. Heterotrimeric G protein activation by G-protein-coupled receptors. *Nat Rev Mol Cell Biol* **9**, 60–71 (2008).
34. Moffett, S., Brown, D. A. & Linder, M. E. Lipid-dependent Targeting of G Proteins into Rafts. *the journal of biological chemistry* **275**, 2191–2198 (2000).
35. Wedegaertner, P. B. Lipid Modifications and Membrane Targeting of Galpha. *Neurosignals* **7**, 125–135 (1998).

36. Takai, Y., Sasaki, T. & Matozaki, T. Small GTP-binding proteins. *Physiological Reviews* **81**, 153–208 (2001).
37. Hepler, J. R. & Gilman, A. G. G proteins. *Trends in Biochemical Sciences* **17**, 383–387 (1992).
38. Mangmool, S. & Kurose, H. Gi/o Protein-Dependent and -Independent Actions of Pertussis Toxin (PTX). *Toxins* **3**, 884–899 (2011).
39. Kaper, J. B., Morris, J. G. & Levine, M. M. Cholera. *Clinical Microbiology Reviews* **8**, 48–86 (1995).
40. Kilander, M. B. C. *et al.* Disheveled regulates precoupling of heterotrimeric G proteins to Frizzled 6. *The FASEB Journal* (2014). doi:10.1096/fj.13-246363
41. Levitzki, A. & Klein, S. G-Protein Subunit Dissociation Is not an Integral Part of G-Protein Action. *ChemBioChem* **3**, 815–818 (2002).
42. Frank, M. G Protein Activation without Subunit Dissociation Depends on a G i-specific Region. *Journal of biological Chemistry* **280**, 24584–24590 (2005).
43. Lambert, N. A. Dissociation of Heterotrimeric G Proteins in Cells. *Science signaling* **1**, 1–5 (2008).
44. DeWire, S. M., Ahn, S., Lefkowitz, R. J. & Shenoy, S. K.  $\beta$ -Arrestins and Cell Signaling. *Annu. Rev. Physiol.* **69**, 483–510 (2007).
45. Rankovic, Z., Brust, T. F. & Bohn, L. M. Bioorganic & Medicinal Chemistry Letters. *Bioorganic & Medicinal Chemistry Letters* **26**, 241–250 (2016).
46. Sbail, O. *et al.* Biased signaling through G-protein-coupled PROKR2 receptors harboring missense mutations. *The FASEB Journal* **28**, 3734–3744 (2014).
47. Cowburn, R. F., Marcusson, J. O., Eriksson, A., Wiehager, B. & O'Neill, C. Adenylyl cyclase activity and G-protein subunit levels in postmortem frontal cortex of suicide victims. *Brain Research* **633**, 297–304 (1994).
48. Donati, R. J. *et al.* Postmortem Brain Tissue of Depressed Suicides Reveals Increased Gs Localization in Lipid Raft Domains Where It Is Less Likely to Activate Adenylyl Cyclase. *Journal of Neuroscience* **28**, 3042–3050 (2008).
49. Menkes, D. B., Rasenick, M. M., Wheeler, M. A. & Bitensky, M. W. Guanosine triphosphate activation of brain adenylyl cyclase: enhancement by long-term antidepressant treatment. *Science* **219**, 65–67 (1983).
50. Zhang, L. & Rasenick, M. M. Chronic Treatment with Escitalopram but Not R-Citalopram Translocates G $\alpha_s$  from Lipid Raft Domains and Potentiates Adenylyl Cyclase: A 5-Hydroxytryptamine Transporter-Independent Action of This Antidepressant Compound. *Journal of Pharmacology and Experimental Therapeutics* **332**, 977–984 (2010).
51. Singer, S. J. & Nicolson, G. L. The fluid mosaic model of the structure of cell membranes. *Science* **175**, 720–731 (1972).
52. Lee, A. G., Birdsall, N. J., Metcalfe, J. C., Toon, P. A. & Warren, G. B. Clusters in lipid bilayers and the interpretation of thermal effects in biological membranes. *Biochemistry* **13**, 3699–3705 (1974).
53. Wunderlich, F., Ronai, A., Speth, V., Seelig, J. & Blume, A. Thermotropic lipid clustering in tetrahymena membranes. *Biochemistry* **14**, 3730–3735 (1975).
54. Klausner, R. D. & Wolf, D. E. Selectivity of fluorescent lipid analogs for lipid domains. *Biochemistry* **19**, 6199–6203 (1980).

55. Karnovsky, M. J., Kleinfeld, A. M. & Hoover, R. L. The concept of lipid domains in membranes. *The Journal of cell ...* (1982).
56. Pike, L. J. Rafts defined: a report on the Keystone Symposium on Lipid Rafts and Cell Function. in **47**, 1597–1598 (2006).
57. Allen, J. A., Halverson-Tamboli, R. A. & Rasenick, M. M. Lipid raft microdomains and neurotransmitter signalling. *Nat Rev Neurosci* **8**, 128–140 (2007).
58. Pucadyil, T. J. & Chattopadhyay, A. Cholesterol modulates ligand binding and G-protein coupling to serotonin<sub>1A</sub> receptors from bovine hippocampus. *Biochimica et Biophysica Acta (BBA)- ...* (2004).
59. Xu, W. *et al.* Localization of the kappa opioid receptor in lipid rafts. *J. Pharmacol. Exp. Ther.* **317**, 1295–1306 (2006).
60. Cooper, D. M. F. & Crossthwaite, A. J. Higher-order organization and regulation of adenylyl cyclases. *Trends Pharmacol. Sci.* **27**, 426–431 (2006).
61. Ramadurai, S. *et al.* Lateral Diffusion of Membrane Proteins. *J. Am. Chem. Soc.* **131**, 12650–12656 (2009).
62. Domański, J., Marrink, S. J. & Schäfer, L. V. Transmembrane helices can induce domain formation in crowded model membranes. *Biochim. Biophys. Acta* **1818**, 984–994 (2012).
63. Nyholm, T. K. Lipid-protein interplay and lateral organization in biomembranes. *Chemistry and Physics of Lipids* **189**, 48–55 (2015).
64. Pike, L. J. & Miller, J. M. Cholesterol depletion delocalizes phosphatidylinositol biphosphate and inhibits hormone-stimulated phosphatidylinositol turnover. *the journal of biological chemistry* **273**, 22298–22304 (1998).
65. Simons, K. & Toomre, D. Lipid rafts and signal transduction. *Nat Rev Mol Cell Biol* **1**, 31–39 (2001).
66. Eisensamer, B. *et al.* Antidepressants and antipsychotic drugs colocalize with 5-HT<sub>3</sub> receptors in raft-like domains. *Journal of Neuroscience* **25**, 10198–10206 (2005).
67. Erb, S. J., Schappi, J. M. & Rasenick, M. M. Antidepressants Accumulate in Lipid Rafts Independent of Monoamine Transporters to Modulate Redistribution of the G protein, Gas. *Journal of biological Chemistry* (2016). doi:10.1074/jbc.M116.727263
68. Maurice, D. H. *et al.* Advances in targeting cyclic nucleotide phosphodiesterases. *Nat Rev Drug Discov* **13**, 290–314 (2014).
69. Cheng, X., Ji, Z., Tsalkova, T. & Mei, F. Epac and PKA: a tale of two intracellular cAMP receptors. *Acta Biochim. Biophys. Sin. (Shanghai)* **40**, 651–662 (2008).
70. Ponsioen, B. *et al.* Detecting cAMP-induced Epac activation by fluorescence resonance energy transfer: Epac as a novel cAMP indicator. *EMBO Rep* **5**, 1176–1180 (2004).
71. Klarenbeek, J., Goedhart, J., van Batenburg, A., Groenewald, D. & Jalink, K. Fourth-Generation Epac-Based FRET Sensors for cAMP Feature Exceptional Brightness, Photostability and Dynamic Range: Characterization of Dedicated Sensors for FLIM, for Ratiometry and with High Affinity. *PLoS ONE* **10**, e0122513 (2015).
72. Blendy, J. A. The Role of CREB in Depression and Antidepressant Treatment. *Biological Psychiatry* **59**, 1144–1150 (2006).

73. Malberg, J. E. & Blendy, J. A. Antidepressant action: to the nucleus and beyond. *Trends Pharmacol. Sci.* **26**, 631–638 (2005).
74. Pandey, G. N., Dysken, M. W., Garver, D. L. & Davis, J. M. Beta-adrenergic receptor function in affective illness. *Am J Psychiatry* **136**, 675–678 (1979).
75. Mann, J. J. *et al.* Reduced sensitivity of lymphocyte beta-adrenergic receptors in patients with endogenous depression and psychomotor agitation. *N. Engl. J. Med.* **313**, 715–720 (1985).
76. Jeanningros, R., Mazzola, P., Azorin, J. M., Samuelian-Massa, C. & Tissot, R. Beta-adrenoceptor density of intact mononuclear leukocytes in subgroups of depressive disorders. *Biological Psychiatry* **29**, 789–798 (1991).
77. Mooney, J. J., Schatzberg, A. F., Cole, J. O., Kizuka, P. P. & Schildkraut, J. J. Enhanced signal transduction by adenylate cyclase in platelet membranes of patients showing antidepressant responses to alprazolam: preliminary data. *J Psychiatr Res* **19**, 65–75 (1985).
78. Pandey, G. N., Sudershan, P. & Davis, J. M. Beta adrenergic receptor function in depression and the effect of antidepressant drugs. *Acta Pharmacol Toxicol (Copenh)* **56 Suppl 1**, 66–79 (1985).
79. Fujita, M. *et al.* Downregulation of Brain Phosphodiesterase Type IV Measured with <sup>11</sup>C-(R)-Rolipram Positron Emission Tomography in Major Depressive Disorder. *Biological Psychiatry* **72**, 548–554 (2012).
80. Fujita, M., Richards, E. M., Niciu, M. J. & Ionescu, D. F. cAMP signaling in brain is decreased in unmedicated depressed patients and increased by treatment with a selective serotonin reuptake inhibitor. *Molecular ...* (2016).
81. Rasmusson, A. M., Shi, L. & Duman, R. Downregulation of BDNF mRNA in the Hippocampal Dentate Gyrus after Re-exposure to Cues Previously Associated with Footshock. *Neuropsychopharmacology* **27**, 133–142 (2002).
82. Ueyama, T., Kawai, Y., Nemoto, K. & Sekimoto, M. Immobilization stress reduced the expression of neurotrophins and their receptors in the rat brain. *Neuroscience* (1997).
83. Russo-Neustadt, A., Ha, T., Ramirez, R. & Kesslak, J. P. Physical activity–antidepressant treatment combination: impact on brain-derived neurotrophic factor and behavior in an animal model. *Behavioural Brain Research* **120**, 87–95 (2001).
84. Smith, M. A., Makino, S. & Kvetnansky, R. Stress and glucocorticoids affect the expression of brain-derived neurotrophic factor and neurotrophin-3 mRNAs in the hippocampus | Journal of Neuroscience. *Journal of ...* (1995).
85. Dwivedi, Y., Rizavi, H. S. & Pandey, G. N. Antidepressants reverse corticosterone-mediated decrease in brain-derived neurotrophic factor expression: Differential regulation of specific exons by antidepressants and corticosterone. *Neuroscience* **139**, 1017–1029 (2006).
86. Tsankova, N. M. *et al.* Sustained hippocampal chromatin regulation in a mouse model of depression and antidepressant action. *Nat Neurosci* **9**, 519–525 (2006).
87. Balu, D. T. *et al.* Differential regulation of central BDNF protein levels by antidepressant and non-antidepressant drug treatments. *Brain Research* **1211**, 37–43 (2008).

88. Altar, C. A., Laeng, P., Jurata, L. W. & Brockman, J. A. Electroconvulsive Seizures Regulate Gene Expression of Distinct Neurotrophic Signaling Pathways | Journal of Neuroscience. *The Journal of neuroscience* **24**, 2667–2677 (2004).
89. Monteggia, L. M., Barrot, M. & Powell, C. M. Essential role of brain-derived neurotrophic factor in adult hippocampal function. in (2004).
90. Tang, W.-J. & Guo, Q. The adenylyl cyclase activity of anthrax edema factor. *Molecular Aspects of Medicine* **30**, 423–430 (2009).
91. Shen, Y., Zhukovskaya, N. L., Guo, Q., Florián, J. & Tang, W.-J. Calcium-independent calmodulin binding and two-metal-ion catalytic mechanism of anthrax edema factor. *EMBO J* **24**, 929–941 (2005).
92. Linder, J. U. Class III adenylyl cyclases: molecular mechanisms of catalysis and regulation. *Cell. Mol. Life Sci.* **63**, 1736–1751 (2006).
93. Hess, K. C. *et al.* The ‘Soluble’ Adenylyl Cyclase in Sperm Mediates Multiple Signaling Events Required for Fertilization. *Developmental Cell* **9**, 249–259 (2005).
94. Gehring, C. Adenyl cyclases and cAMP in plant signaling - past and present. *Cell Communication and Signaling* 2010 8:1 **8**, 15 (2010).
95. Moutinho, A., Hussey, P. J., Trewavas, A. J. & Malho, R. cAMP acts as a second messenger in pollen tube growth and reorientation. *Proc. Natl. Acad. Sci. U.S.A.* **98**, 10481–10486 (2001).
96. Sadana, R. & Dessauer, C. W. Physiological Roles for G Protein-Regulated Adenylyl Cyclase Isoforms: Insights from Knockout and Overexpression Studies. *Neurosignals* **17**, 5–22 (2009).
97. Sadana, R. & Dessauer, C. W. Physiological Roles for G Protein-Regulated Adenylyl Cyclase Isoforms: Insights from Knockout and Overexpression Studies. *Neurosignals* **17**, 5–22 (2009).
98. Ludwig, M.-G. & Seuwen, K. Characterization of the human adenylyl cyclase gene family: cDNA, gene structure, and tissue distribution of the nine isoforms. *Journal of Receptors and Signal Transduction* **22**, 79–110 (2002).
99. Halls, M. L. & Cooper, D. M. F. Regulation by Ca<sup>2+</sup>-Signaling Pathways of Adenylyl Cyclases. *Cold Spring Harbor Perspectives in Biology* **3**, a004143–a004143 (2011).
100. Beazely, M. A. & Watts, V. J. Regulatory properties of adenylate cyclases type 5 and 6: A progress report. *European Journal of Pharmacology* **535**, 1–12 (2006).
101. Dessauer, C. W. & Gilman, A. G. The Catalytic Mechanism of Mammalian Adenylyl Cyclase. EQUILIBRIUM BINDING AND KINETIC ANALYSIS OF P-SITE INHIBITION. *Journal of biological Chemistry* **272**, 27787–27795 (1997).
102. Fagan, K. A. Regulation of the Ca<sup>2+</sup>-inhibitable Adenylyl Cyclase Type VI by Capacitative Ca<sup>2+</sup> Entry Requires Localization in Cholesterol-rich Domains. *Journal of biological Chemistry* **275**, 26530–26537 (2000).
103. Pagano, M. *et al.* Insights into the residence in lipid rafts of adenylyl cyclase AC8 and its regulation by capacitative calcium entry. *AJP: Cell Physiology* **296**, C607–C619 (2008).
104. Smith, K. E. Residence of Adenylyl Cyclase Type 8 in Caveolae Is Necessary but Not Sufficient for Regulation by Capacitative Ca<sup>2+</sup> Entry. *Journal of biological Chemistry* **277**, 6025–6031 (2001).

105. Buxton, I. L. & Brunton, L. L. Compartments of cyclic AMP and protein kinase in mammalian cardiomyocytes. *Journal of biological Chemistry* (1983).
106. Theurkauf, W. E. & Vallee, R. B. Molecular characterization of the cAMP-dependent protein kinase bound to microtubule-associated protein 2. (1982).
107. Smith, F. D., Langeberg, L. K. & Scott, J. D. The where's and when's of kinase anchoring. *Trends in Biochemical Sciences* **31**, 316–323 (2006).
108. Bauman, A. L. *et al.* Dynamic regulation of cAMP synthesis through anchored PKA-adenylyl cyclase V/VI complexes. *Mol. Cell* **23**, 925–931 (2006).
109. Delint-Martinez, I., Willoughby, D., Hammond, G. V. R., Ayling, L. J. & Cooper, D. M. F. Palmitoylation targets AKAP79 to lipid rafts and promotes its regulation of the calcium sensitive adenylyl cyclase type 8. *Journal of biological Chemistry* (2011). doi:10.1074/jbc.M111.243899
110. Guinzberg, R. *et al.* Newly synthesized cAMP is integrated at a membrane protein complex signalosome to ensure receptor response specificity. *FEBS J.* **284**, 258–276 (2016).
111. Krishnan, V. *et al.* Calcium-Sensitive Adenylyl Cyclases in Depression and Anxiety: Behavioral and Biochemical Consequences of Isoform Targeting. *Biological Psychiatry* **64**, 336–343 (2008).
112. Chen, X. *et al.* Ablation of Type III Adenylyl Cyclase in Mice Causes Reduced Neuronal Activity, Altered Sleep Pattern, and Depression-like Phenotypes. *Biological Psychiatry* (2015). doi:10.1016/j.biopsych.2015.12.012
113. Palagini, L., Baglioni, C., Ciapparelli, A., Gemignani, A. & Riemann, D. Sleep Medicine Reviews. *Sleep Medicine Reviews* **17**, 377–390 (2013).
114. Bishop, G. A., Berbari, N. F., Lewis, J. & Mykityn, K. Type III adenylyl cyclase localizes to primary cilia throughout the adult mouse brain. *J. Comp. Neurol.* **505**, 562–571 (2007).
115. Wang, Z. *et al.* Adult Type 3 Adenylyl Cyclase-Deficient Mice Are Obese. *PLoS ONE* **4**, 1–11 (2009).
116. Satir, P., Pedersen, L. B. & Christensen, S. T. The primary cilium at a glance | Journal of Cell Science. *J Cell Sci* (2010).
117. Wray, N. R., Pergadia, M. L. & Blackwood, D. Molecular Psychiatry - Abstract of article: Genome-wide association study of major depressive disorder: new results, meta-analysis, and lessons learned. *Molecular ...* (2012).
118. Rasenick, M. M. Depression and Adenylyl Cyclase - Sorting Out the Signals. *Biological Psychiatry* **80**, 812–814 (2016).
119. Reiach, J. S., Li, P. P., Warsh, J. J., Kish, S. J. & Young, L. T. Reduced adenylyl cyclase immunolabeling and activity in postmortem temporal cortex of depressed suicide victims. *J Affect Disord* **56**, 141–151 (1999).
120. Joeyen-Waldorf, J. *et al.* Adenylate cyclase 7 is implicated in the biology of depression and modulation of affective neural circuitry. *Biological Psychiatry* **71**, 627–632 (2012).
121. Hines, L. M. *et al.* A sex-specific role of type VII adenylyl cyclase in depression. *Journal of Neuroscience* **26**, 12609–12619 (2006).
122. Torres, G. E., Gainetdinov, R. R. & Caron, M. G. Plasma membrane monoamine transporters: structure, regulation and function. *Nat Rev Neurosci* **4**, 13–25 (2003).

123. Owens, M. J. & Nemeroff, C. B. The serotonin transporter and depression. *Depression and anxiety* (1998).
124. Schloss, P. & Williams, D. C. The serotonin transporter: a primary target for antidepressant drugs. *J. Psychopharmacol. (Oxford)* **12**, 115–121 (1998).
125. Cameron, K. N., Solis, E., Ruchala, I., De Felice, L. J. & Eltit, J. M. Amphetamine activates calcium channels through dopamine transporter-mediated depolarization. *Cell Calcium* **58**, 457–466 (2015).
126. Nyola, A. *et al.* Substrate and drug binding sites in LeuT. *Current Opinion in Structural Biology* **20**, 415–422 (2010).
127. Sánchez, C., Reines, E. H. & Montgomery, S. A. A comparative review of escitalopram, paroxetine, and sertraline. *International Clinical Psychopharmacology* **29**, 185–196 (2014).
128. Sánchez, C. The Pharmacology of Citalopram Enantiomers: The Antagonism by R-Citalopram on the Effect of S-Citalopram\*. *Basic Clin Pharmacol Toxicol* **99**, 91–95 (2006).
129. Zhou, Z. *et al.* LeuT-desipramine structure reveals how antidepressants block neurotransmitter reuptake. *Science* **317**, 1390–1393 (2007).
130. Perona, M. T. G. *et al.* Animal models of depression in dopamine, serotonin, and norepinephrine transporter knockout mice: prominent effects of dopamine transporter deletions. *Behavioural Pharmacology* **19**, 566–574 (2008).
131. Olivier, J., Van Der Hart, M. & Van Swelm, R. A study in male and female 5-HT transporter knockout rats: An animal model for anxiety and depression disorders. *Neuroscience* (2008).
132. Weber, T. Inducible gene manipulations in serotonergic neurons. *Front. Mol. Neurosci.* (2009). doi:10.3389/neuro.02.024.2009
133. Karg, K. & Burmeister, M. The Serotonin Transporter Promoter Variant (5-HTTLPR), Stress, and Depression Meta-analysis Revisited: Evidence of Genetic Moderation | May 02, 2011 | JAMA Psychiatry | JAMA Network. *Archives of general ...* (2011).
134. Lesch, K.-P. & Gutknecht, L. Pharmacogenetics of the serotonin transporter. *Progress in Neuro-Psychopharmacology and Biological Psychiatry* **29**, 1062–1073 (2005).
135. Juhasz, G. *et al.* Variability in the effect of 5-HTTLPR on depression in a large European population: the role of age, symptom profile, type and intensity of life stressors. *PLoS ONE* **10**, e0116316 (2015).
136. Long, H. *et al.* The long rather than the short allele of 5-HTTLPR predisposes Han Chinese to anxiety and reduced connectivity between prefrontal cortex and amygdala. *Neurosci. Bull.* **29**, 4–15 (2013).
137. Nakamura, M., Ueno, S., Sano, A. & Tanabe, H. The human serotonin transporter gene linked polymorphism (5-HTTLPR) shows ten novel allelic variants. *Molecular Psychiatry* **5**, 32–38 (2000).
138. Robitzek, E. H., Selikoff, I. J., Mamlok, E. & Tendlaw, A. Isoniazid and Its Isopropyl Derivative in the Therapy of Tuberculosis in Humans: Comparative Therapeutic and Toxicologic Properties. *CHEST* **23**, 1 (1953).
139. Selikoff, I. J. & Robitzek, E. H. Tuberculosis Chemotherapy with Hydrazine Derivatives of Isonicotinic Acid. *CHEST* **21**, 385 (1952).

140. López-Muñoz, F., Álamo, C., Juckel, G. & Assion, H.-J. Half a Century of Antidepressant Drugs. *Journal of Clinical Psychopharmacology* **27**, 555–559 (2007).
141. Engleman, E. A., Perry, K. W., Mayle, D. A. & Wong, D. T. Simultaneous increases of extracellular monoamines in microdialysates from hypothalamus of conscious rats by duloxetine, a dual serotonin and norepinephrine uptake inhibitor. *Neuropharmacology* **12**, 287–295 (1995).
142. Koch, S. Comparison of effects of dual transporter inhibitors on monoamine transporters and extracellular levels in rats. *Neuropharmacology* **45**, 935–944 (2003).
143. Felton, T. M., Kang, T. B., Hjorth, S. & Auerbach, S. B. Effects of selective serotonin and serotonin/noradrenaline reuptake inhibitors on extracellular serotonin in rat diencephalon and frontal cortex. *Naunyn-Schmied Arch Pharmacol* **367**, 297–305 (2003).
144. Amsterdam, J. D. & Chopra, M. Monoamine Oxidase Inhibitors Revisited. *Psychiatric Annals* **31**, 361–370 (2001).
145. Fangmann, P., Assion, H.-J., Juckel, G., González, C. Á. & López-Muñoz, F. Half a Century of Antidepressant Drugs. *Journal of Clinical Psychopharmacology* **28**, 1–4 (2008).
146. Carlsson, A., Corrodi, H., Fuxe, K. & Hökfelt, T. Effect of antidepressant drugs on the depletion of intraneuronal brain 5-hydroxytryptamine stores caused by 4-methyl- $\alpha$ -ethyl-meta-tyramine - ScienceDirect. *European Journal of Pharmacology* **5**, 357–366 (1969).
147. Carlsson, A., Corrodi, H., Fuxe, K. & Hökfelt, T. Effects of some antidepressant drugs on the depletion of intraneuronal brain catecholamine stores caused by 4, $\alpha$ -dimethyl-meta-tyramine - ScienceDirect. *European journal of ...* **5**, 367–373 (1969).
148. Carlsson, A., Fuxe, K., Hamberger, B. & Lindqvist, M. Biochemical and Histochemical Studies on the Effects of Imipramine-like Drugs and (+)-Amphetamine on Central and Peripheral Catecholamine Neurons. *Acta Physiologica* **67**, 481–497 (1966).
149. Wong, D. T., Horng, J. S., Bymaster, F. P. & Hauser, K. L. A selective inhibitor of serotonin uptake: Lilly 110140, 3-(p-Trifluoromethylphenoxy)-n-methyl-3-phenylpropylamine - ScienceDirect. *Life Sciences* **15**, 471–479 (1974).
150. Wong, D. T., Bymaster, F. P., Horng, J. S. & Molloy, B. B. A new selective inhibitor for uptake of serotonin into synaptosomes of rat brain: 3-(p-trifluoromethylphenoxy). N-methyl-3-phenylpropylamine. *J. Pharmacol. Exp. Ther.* **193**, 804–811 (1975).
151. Owens, J. The Discovery of Fluoxetine Hydrochloride (Prozac). *Nat Rev Drug Discov* **4**, 764–774 (2005).
152. Nackenoff, A. G., Moussa-Tooks, A. B., McMeekin, A. M., Veenstra-VanderWeele, J. & Blakely, R. D. Essential Contributions of Serotonin Transporter Inhibition to the Acute and Chronic Actions of Fluoxetine and Citalopram in the SERT Met172 Mouse. *Neuropsychopharmacology* **41**, 1733–1741 (2016).
153. Hjorth, S. *et al.* Serotonin autoreceptor function and antidepressant drug action. *J. Psychopharmacol. (Oxford)* **14**, 177–185 (2000).



154. Garcia, A. S. *et al.* Autoreceptor-mediated inhibition of norepinephrine release in rat medial prefrontal cortex is maintained after chronic desipramine treatment. *Journal of Neurochemistry* **91**, 683–693 (2004).
155. Tsuruda, P. R. *et al.* Influence of ligand binding kinetics on functional inhibition of human recombinant serotonin and norepinephrine transporters. *Journal of Pharmacological and Toxicological Methods* **61**, 192–204 (2010).
156. Chen, J. & Rasenick, M. Chronic antidepressant treatment facilitates G protein activation of adenylyl cyclase without altering G protein content. *J Pharmacol Exp Ther* 1995-Chen-509-17. *Journal of Pharmacology and Experimental Therapeutics* **275**, 509–517 (1995).
157. Chen, J. & Rasenick, M. M. Chronic Treatment of C6 Glioma Cells with Antidepressant Drugs Increases Functional Coupling Between a G Protein ( $G_s$ ) and Adenylyl Cyclase. *Journal of Neurochemistry* **64**, 724–732 (1995).
158. Bradner, J. E. *et al.* chemical phylogenetics of histone deacetylases. *Nat Meth* **6**, 238–243 (2010).
159. Jochems, J. *et al.* Antidepressant-Like Properties of Novel HDAC6-Selective Inhibitors with Improved Brain Bioavailability. *Neuropsychopharmacology* **39**, 389–400 (2013).
160. Hobara, T. *et al.* Journal of Psychiatric Research. *J Psychiatr Res* **44**, 263–270 (2010).
161. Covington, H. E. *et al.* Antidepressant Actions of Histone Deacetylase Inhibitors. *Journal of Neuroscience* **29**, 11451–11460 (2009).
162. Verdel, A. *et al.* Active maintenance of mHDA2/mHDAC6 histone-deacetylase in the cytoplasm. *Curr.Biol.* **10**, 747–749 (2000).
163. Zhang, Y. *et al.* HDAC-6 interacts with and deacetylates tubulin and microtubules in vivo. *EMBO J* **22**, 1168–1179 (2003).
164. Schappi, J. M., Krbanjevic, A. & Rasenick, M. M. Biochimica et Biophysica Acta. *BBA - Biomembranes* **1838**, 674–681 (2014).
165. Machado-Vieira, R., Salvadore, G., DiazGranados, N. & Zarate, C. A., Jr. Ketamine and the next generation of antidepressants with a rapid onset of action. *Pharmacology and Therapeutics* **123**, 143–150 (2009).
166. Hillhouse, T. M. & Porter, J. H. A brief history of the development of antidepressant drugs: From monoamines to glutamate. *Experimental and Clinical Psychopharmacology* **23**, 1–21 (2015).
167. Autry, A. E. *et al.* NMDA receptor blockade at rest triggers rapid behavioural antidepressant responses. *Nature* **475**, 91–95 (2011).
168. Lepack, A. E., Bang, E., Lee, B., Dwyer, J. M. & Duman, R. S. Fast-acting antidepressants rapidly stimulate ERK signaling and BDNF release in primary neuronal cultures. *Neuropharmacology* **111**, 242–252 (2016).
169. Zanos, P. *et al.* NMDAR inhibition-independent antidepressant actions of ketaminemetabolites. *Nature* 1–18 (2016). doi:10.1038/nature17998
170. Lorén, N. *et al.* Fluorescence recovery after photobleaching in material and life sciences: putting theory into practice. *Quart. Rev. Biophys.* **48**, 323–387 (2015).
171. Axelrod, D. *et al.* Lateral motion of fluorescently labeled acetylcholine receptors in membranes of developing muscle fibers. *Proc. Natl. Acad. Sci. U.S.A.* **73**, 4594–

- 4598 (1976).
172. Axelrod, D., Koppel, D. E., Schlessinger, J. & Elson, E. Mobility measurement by analysis of fluorescence photobleaching recovery kinetics - ScienceDirect. *Biophysical Journal* (1976).
  173. Peters, R., Peters, J., Tews, K. H. & Bähr, W. A microfluorimetric study of translational diffusion in erythrocyte membranes. *Biochim. Biophys. Acta* **367**, 282–294 (1974).
  174. Reits, E. A. J. & Neefjes, J. J. From fixed to FRAP: measuring protein mobility and activity in living cells. *Nat Cell Biol* **3**, E145–E147 (2001).
  175. Mueller, F., Morisaki, T., Mazza, D. & McNally, J. G. Minimizing the impact of photoswitching of fluorescent proteins on FRAP analysis. *Biophysical Journal* **102**, 1656–1665 (2012).
  176. Yu, J.-Z. & Rasenick, M. M. Real-Time Visualization of a Fluorescent  $G\alpha_s$ : Dissociation of the Activated G Protein from Plasma Membrane. *Molecular Pharmacology* **61**, 352–359 (2002).
  177. Zacharias, D. A., Violin, J. D., Newton, A. C. & Tsien, R. Y. Partitioning of Lipid-Modified Monomeric GFPs into Membrane Microdomains of Live Cells. *Science* **296**, 913–916 (2002).
  178. Benda, P., Lightbody, J., Sato, G., Levine, L. & Sweet, W. Differentiated Rat Glial Cell Strain in Tissue Culture. *Science* **161**, 370–371 (1968).
  179. Schmidek, H. H., Nielsen, S. L., Schiller, A. L. & Messer, J. Morphological studies of rat brain tumors induced by N-nitrosomethylurea. *J. Neurosurg.* **34**, 335–340 (1971).
  180. KAPLAN, N. Histopathology, invasion, migration and tumorigenicity in the C6 rat glioma model. *Turkish Neurosurgery* (2005).
  181. Davidoff, M. S. *et al.* Leydig cells of the human testis possess astrocyte and oligodendrocyte marker molecules. *Acta Histochem.* **104**, 39–49 (2002).
  182. Buniatian, G. *et al.* The immunoreactivity of glial fibrillary acidic protein in mesangial cells and podocytes of the glomeruli of rat kidney in vivo and in culture. *Biol. Cell* **90**, 53–61 (1998).
  183. Dunn, R. *et al.* Reduction in S100 protein beta subunit mRNA in C6 rat glioma cells following treatment with anti-microtubular drugs. *the journal of biological chemistry* **262**, 3562–3566 (1987).
  184. Chao, C.-C., Kan, D., Lo, T.-H., Lu, K.-S. & Chien, C.-L. Induction of neural differentiation in rat C6 glioma cells with taxol. *Brain Behav* **5**, e00414 (2015).
  185. Takanaga, H., Yoshitake, T., Hara, S., Yamasaki, C. & Kunitomo, M. cAMP-induced astrocytic differentiation of C6 glioma cells is mediated by autocrine interleukin-6. *the journal of biological chemistry* **279**, 15441–15447 (2004).
  186. Trentin, A. G. & Alvarez-Silva, M. Thyroid hormone regulates protein expression in C6 glioma cells. *Braz. J. Med. Biol. Res.* **31**, 1281–1284 (1998).
  187. Boone, M. *et al.* Genome dynamics of the human embryonic kidney 293 lineage in response to cell biology manipulations. *Nature Communications* **5**, 1–12 (2014).
  188. Graham, F. L. & Smiley, J. Characteristics of a Human Cell Line Transformed by DNA from Human Adenovirus Type 5. *Journal of General ...* 1–14 (1977).

189. Frisch, S. M. & Mymryk, J. S. Adenovirus-5 E1A: paradox and paradigm. *Nat Rev Mol Cell Biol* **3**, 441–452 (2002).
190. Shaw, G., Morse, S., Ararat, M. & Graham, F. L. Preferential transformation of human neuronal cells by human adenoviruses and the origin of HEK 293 cells. *The FASEB Journal* (2002). doi:10.1096/fj.01-0995fje
191. Adler, E. M. Differentiation of PC12 Cells. *Sci. STKE* **2006**, tr9–tr9 (2006).
192. Greene, L. A. & Tischler, A. S. Establishment of a noradrenergic clonal line of rat adrenal pheochromocytoma cells which respond to nerve growth factor. *Proceedings of the National ...* (1976).
193. Williams, N. G., Zhong, H. & Minneman, K. P. Differential coupling of alpha1-, alpha2-, and beta-adrenergic receptors to mitogen-activated protein kinase pathways and differentiation in transfected PC12 cells. *the journal of biological chemistry* **273**, 24624–24632 (1998).
194. Jensen, F. C., Girardi, A. J., Gilden, R. V. & Koprowski, H. INFECTION OF HUMAN AND SIMIAN TISSUE CULTURES WITH ROUS SARCOMA VIRUS. *Proc. Natl. Acad. Sci. U.S.A.* **52**, 53 (1964).
195. Gluzman, Y. SV40-transformed simian cells support the replication of early SV40 mutants. *Cell* **23**, 175–182 (1981).
196. Daugherty, R. L. *et al.*  $\alpha$ -Catenin is an inhibitor of transcription. *Proceedings of the National Academy of Sciences* **111**, 5260–5265 (2014).
197. Lin, Y.-H., Swanson, E. R., Li, J., Mkrtchjan, M. A. & Russell, B. Cyclic mechanical strain of myocytes modifies CapZb1 post translationally via PKCe. *Journal of Muscle Research and Cell Motility* 1–9 (2015). doi:10.1007/s10974-015-9420-6
198. Salomon, Y. Adenylate Cyclase Assay. *Advances in Cyclis Nucleotide Research* **10**, 35–55 (1979).
199. Sorci, G., Agneletti, A. L. & Donato, R. Effects of S100A1 and S100B on microtubule stability. An in vitro study using triton-cytoskeletons from astrocyte and myoblast cell lines. *NSC* **99**, 773–783 (2000).
200. Gasper, R., Meyer, S., Gotthardt, K., Sirajuddin, M. & Wittinghofer, A. It takes two to tango: regulation of G proteins by dimerization. *Nat Rev Mol Cell Biol* **10**, 423–429 (2009).
201. Donati, R., Thukral, C. & Rasenick, M. Chronic Treatment of C6 Glioma Cells with Antidepressant Drugs Results in a Redistribution of Gs $\alpha$  Mol Pharmacol-2001-Donati-1426-32. *Molecular Pharmacology* **59**, 1–7 (2001).
202. Lamichhane, R. *et al.* Single-molecule view of basal activity and activation mechanisms of the G protein-coupled receptor  $\beta$  2AR. *Proc. Natl. Acad. Sci. U.S.A.* **112**, 14254–14259 (2015).
203. Insel, P. A. Forskolin as a Tool for Examining Adenylyl Cyclase Expression, Regulation, and G Protein Signaling. *Embryonic origin of the adult hematopoietic system: advances and questions* **23**, 305–314 (2003).
204. Medvinsky, A., Rybtsov, S. & Taoudi, S. Embryonic origin of the adult hematopoietic system: advances and questions. *Development* **138**, 1017–1031 (2011).
205. Sunahara, R. K., Dessauer, C. W. & Gilman, A. G. Complexity and Diversity of Mammalian Adenylyl Cyclases. *Annu. Rev. Pharmacol. Toxicol.* 461–480 (1996).
206. Head, B. P. *et al.* Microtubules and Actin Microfilaments Regulate Lipid

- Raft/Caveolae Localization of Adenylyl Cyclase Signaling Components. *Journal of biological Chemistry* **281**, 26391–26399 (2006).
207. Kabouridis, P. S., Janzen, J., Magee, A. L. & Ley, S. C. Cholesterol depletion disrupts lipid rafts and modulates the activity of multiple signaling pathways in T lymphocytes. *European Journal of Immunology* 954–963 (2000).
208. Czysz, A. H., Schappi, J. M. & Rasenick, M. M. Lateral diffusion of G $\alpha$ s in the plasma membrane is decreased after chronic but not acute antidepressant treatment: role of lipid raft and non-raft membrane microdomains. *Neuropsychopharmacology* **40**, 766–773 (2015).
209. Sogaard, B., Mengel, H., Rao, N. & Larsen, F. The Pharmacokinetics of Escitalopram After Oral and Intravenous Administration of Single and Multiple Doses to Healthy Subjects. *The Journal of Clinical Pharmacology* **45**, 1400–1406 (2013).
210. Williams, T. M. & Lisanti, M. P. The caveolin proteins. *Genome Biol* 214.1–214.8 (2004).
211. Thompson, B. J. *et al.* Transgenic elimination of high-affinity antidepressant and cocaine sensitivity in the presynaptic serotonin transporter. *Proc. Natl. Acad. Sci. U.S.A.* **108**, 3785–3790 (2011).
212. DeBernardi, M. A., Munshi, R., Yoshimura, M., Cooper, D. M. & Brooker, G. Predominant expression of type-VI adenylate cyclase in C6-2B rat glioma cells may account for inhibition of cyclic AMP accumulation by calcium. *Biochem. J.* **293 ( Pt 2)**, 325–328 (1993).
213. Hanoune, J. Regulation and role of adenylyl cyclase isoforms. *Annual review of pharmacology and ...* (2001).
214. Brand, C. S., Hocker, H. J., Gorfe, A. A., Cavasotto, C. N. & Dessauer, C. W. Isoform Selectivity of Adenylyl Cyclase Inhibitors: Characterization of Known and Novel Compounds. *Journal of Pharmacology and Experimental Therapeutics* **347**, 265–275 (2013).
215. Guillou, J.-L., Nakata, H. & Cooper, D. M. F. Inhibition by Calcium of Mammalian Adenylyl Cyclases. *the journal of biological chemistry* **274**, 35539–35549 (1999).
216. Ma, X., Peterson, R. & Turnbull, J. Adenylyl Cyclase type 3, a marker of primary cilia, is reduced in primary cell culture and in lumbar spinal cord in situ in G93A SOD1 mice. *BMC Neuroscience* **12**, 71 (2011).
217. Vuolo, L., Herrera, A., Torroba, B., Menendez, A. & Pons, S. Ciliary adenylyl cyclases control the Hedgehog pathway. *Journal of Cell Science* **128**, 2928–2937 (2015).
218. Rajkowska, G. & Miguel-Hidalgo, J. Gliogenesis and Glial Pathology in Depression. *CNSDDT* **6**, 219–233 (2007).
219. Rial, D. *et al.* Depression as a Glial-Based Synaptic Dysfunction. *Front Cell Neurosci* **9**, 521 (2015).
220. Schafer, D. P., Lehrman, E. K. & Stevens, B. The ‘quad-partite’ synapse: microglia-synapse interactions in the developing and mature CNS. *Glia* **61**, 24–36 (2013).
221. Azevedo, F. A. C. *et al.* Equal numbers of neuronal and nonneuronal cells make the human brain an isometrically scaled-up primate brain. *J. Comp. Neurol.* **513**,

- 532–541 (2009).
222. Dave, R. H. *et al.* A molecular and structural mechanism for G protein-mediated microtubule destabilization. *Journal of biological Chemistry* **286**, 4319–4328 (2011).
  223. Andersen, J. *et al.* Location of the antidepressant binding site in the serotonin transporter: importance of Ser-438 in recognition of citalopram and tricyclic antidepressants. *the journal of biological chemistry* **284**, 10276–10284 (2009).
  224. Coleman, J. A., Green, E. M. & Gouaux, E. X-ray structures and mechanism of the human serotonin transporter. *Nature* **532**, 334–339 (2016).
  225. Krupinski, J. *et al.* Adenylyl cyclase amino acid sequence: possible channel- or transporter-like structure. *Science* **244**, 1558–1564 (1989).
  226. Glaser, C., Heinrich, J. & Koletzko, B. Role of FADS1 and FADS2 polymorphisms in polyunsaturated fatty acid metabolism. *Metab. Clin. Exp.* **59**, 993–999 (2010).
  227. Park, W. J. *et al.* A novel FADS1 isoform potentiates FADS2-mediated production of eicosanoid precursor fatty acids. *J. Lipid Res.* **53**, 1502–1512 (2012).
  228. Heinemann, F. S. & Ozols, J. Stearoyl-CoA desaturase, a short-lived protein of endoplasmic reticulum with multiple control mechanisms. *Prostaglandins, Leukotrienes and Essential Fatty Acids* **68**, 123–133 (2003).
  229. Park, H. G., Park, W. J., Kothapalli, K. S. D. & Brenna, J. T. The fatty acid desaturase 2 (FADS2) gene product catalyzes  $\Delta^4$  desaturation to yield n-3 docosahexaenoic acid and n-6 docosapentaenoic acid in human cells. *The FASEB Journal* **29**, 3911–3919 (2015).
  230. Hagen, R. M., Rodriguez-Cuenca, S. & Vidal-Puig, A. An allostatic control of membrane lipid composition by SREBP1. *FEBS Letters* **584**, 2689–2698 (2010).
  231. Chen, J., Korostyshevsky, D., Lee, S. & Perlstein, E. O. Accumulation of an antidepressant in vesiculogenic membranes of yeast cells triggers autophagy. *PLoS ONE* **7**, e34024 (2012).
  232. Janmey, P. A. Protein regulation by phosphatidylinositol lipids. *Chemistry & Biology* **2**, 61–65 (1995).
  233. Everett, K. L. & Cooper, D. M. F. An improved targeted cAMP sensor to study the regulation of adenylyl cyclase 8 by  $\text{Ca}^{2+}$  entry through voltage-gated channels. *PLoS ONE* **8**, e75942 (2013).
  234. Fagan, K. A., Mahey, R. & Cooper, D. M. Functional co-localization of transfected  $\text{Ca}^{2+}$ -stimulable adenylyl cyclases with capacitative  $\text{Ca}^{2+}$  entry sites. *the journal of biological chemistry* **271**, 12438–12444 (1996).

## Vita

Name: Jeffrey Michael Schappi

Education: University of Illinois at Chicago, Department of Physiology & Biophysics, PhD student. Laboratory of Dr. Mark Rasenick. 2010-present

University of Illinois at Chicago, Non-degree graduate studies, 2008-2010

University of Illinois at Urbana-Champaign, B.S. Biology 1992

Teaching: University of Illinois at Chicago, Urban Health Program Summer Pre-Matriculation Program. Designed and taught neurophysiology component of program, 2011-2015

Professional Membership: Society for Neuroscience

Publications: Erb SJ, Schappi JM, Rasenick MM. Antidepressants Accumulate in Lipid Rafts Independent of Monoamine Transporters to Modulate Redistribution of the G Protein,  $G\alpha_s$ . J Biol Chem. 2016 Sep 16;291(38):19725-33.

Donati RJ, Schappi J, Czysz AH, Jackson A, Rasenick MM. Differential effects of antidepressants escitalopram versus lithium on  $G_s$  alpha membrane relocalization. BMC Neurosci. 2015 Jul 11;16:40.

Czysz AH, Schappi JM, Rasenick MM. Lateral Diffusion of  $G\alpha_s$  in the Plasma Membrane Is Decreased after Chronic but not Acute Antidepressant Treatment: Role of Lipid Raft and Non-Raft Membrane Microdomains. Neuropsychopharmacology. 2015 Feb; 40(3): 766–773.

Schappi JM, Krbanjevic A, Rasenick MM. Tubulin, actin and heterotrimeric G proteins: coordination of signaling and structure. Biochim Biophys Acta. 2014 Feb;1838(2):674-81.

## Copyright

Data in this thesis were published in:

Czysz AH, Schappi JM, Rasenick MM. Lateral Diffusion of  $G\alpha_s$  in the Plasma Membrane Is Decreased after Chronic but not Acute Antidepressant Treatment: Role of Lipid Raft and Non-Raft Membrane Microdomains. *Neuropsychopharmacology*. 2015 Feb; 40(3): 766–773.

Donati RJ, Schappi J, Czysz AH, Jackson A, Rasenick MM. Differential effects of antidepressants escitalopram versus lithium on  $G_s$  alpha membrane relocation. *BMC Neurosci*. 2015 Jul 11;16:40.

Erb SJ, Schappi JM, Rasenick MM. Antidepressants Accumulate in Lipid Rafts Independent of Monoamine Transporters to Modulate Redistribution of the G Protein,  $G\alpha_s$ . *J Biol Chem*. 2016 Sep 16;291(38):19725-33

### Publisher Permissions:

#### Nature journals (Neuropsychopharmacology)

If you are the author of this content (or his/her designated agent) please read the following. Since 2003, ownership of copyright in original research articles remains with the Authors\*, and provided that, when reproducing the Contribution or extracts from it, the Authors acknowledge first and reference publication in the Journal, the Authors retain the following non-exclusive rights:

- a. To reproduce the Contribution in whole or in part in any printed volume (book or thesis) of which they are the author(s).
- b. They and any academic institution where they work at the time may reproduce the Contribution for the purpose of course teaching.
- c. To reuse figures or tables created by them and contained in the Contribution in other works created by them.
- d. To post a copy of the Contribution as accepted for publication after peer review (in Word or Tex format) on the Author's own web site, or the Author's institutional repository, or the Author's funding body's archive, six months after publication of the printed or online edition of the Journal, provided that they also link to the Journal article on Nature Research's web site (eg through the DOI).

#### BMC journals (BMC Neuroscience)

Copyright on any open access article in a journal published by BioMed Central is retained by the author(s). Authors grant BioMed Central a license to publish the article and identify itself as the original publisher. Authors also grant any third party the right to use the article freely as long as its integrity is maintained and its original authors, citation details and publisher are identified. The Creative Commons Attribution License 4.0 formalizes these and other terms and conditions of publishing articles.

In accordance with our Open Data policy, the Creative Commons CC0 1.0 Public Domain Dedication waiver applies to all published data in BioMed Central open access articles.

### **ASBMB journals (The Journal of Biological Chemistry)**

Authors need **NOT** contact the journal to obtain rights to reuse their own material. They are automatically granted permission to do the following:

- Reuse the article in print collections of their own writing.
- Present a work orally in its entirety.
- Use an article in a thesis and/or dissertation.
- Reproduce an article for use in the author's courses. (If the author is employed by an academic institution, that institution also may reproduce the article for teaching purposes.)
- Reuse a figure, photo and/or table in future commercial and noncommercial works.
- Post a copy of the paper in PDF that you submitted via BenchPress.
- Link to the journal site containing the final edited PDFs created by the publisher.
- Authors who published their papers under the "Author's Choice" option may post the final edited PDFs created by the publisher to their own/departamental/university Web sites immediately upon publication. All other authors may do so 12 months after publication.